PERFORMANCE OF A PULSATING HEAT PIPE USING MULTIMODE HEAT TRANSFER INSERT

Md. Sojib Kaisar

Student ID: 1015102006

A Thesis Submitted in Partial Fulfillment of the Requirements for the Degree of

MASTER OF SCIENCE IN MECHANICAL ENGINEERING

Department of Mechanical Engineering

BANGLADESH UNIVERSITY OF ENGINEERING & TECHNOLOGY

April 2022

PERFORMANCE OF A PULSATING HEAT PIPE USING MULTIMODE HEAT TRANSFER INSERT

Md. Sojib Kaisar

Student ID: 1015102006P

A Thesis Submitted in Partial Fulfillment of the Requirements for the Degree of

MASTER OF SCIENCE IN MECHANICAL ENGINEERING

Department of Mechanical Engineering

BANGLADESH UNIVERSITY OF ENGINEERING & TECHNOLOGY

April 2022

The thesis titled "**PERFORMANCE OF A PULSATING HEAT PIPE USING MULTIMODE HEAT TRANSFER INSERT**" submitted by Md. Sojib Kaisar (Roll No: 1015102006P, session: October 2015) has been accepted as satisfactory in partial fulfillment of the requirement for the degree of **Master of Science in Mechanical Engineering** on April 17, 2022.

BOARD OF EXAMINERS

1. _____

Dr. Aloke Kumar Mozumder   Chairman
Professor   (Supervisor)
Department of ME, BUET, Dhaka

2. _____

Head   Member
                                                                              (Ex-Officio)
Department of ME, BUET, Dhaka

3. _____

Dr. Md. Ashraful Islam
Professor   Member
Department of ME, BUET, Dhaka

4. _____

Dr. Hasan Mohammad Mostofa Afroz   Member (External)
Professor
Department of ME, DUET, Gazipur

CERTIFICATE OF RESEARCH

This is to certify that the work presented in this thesis is carried out by the author under the supervision of Dr. Aloke Kumar Mozumder, Professor of the Department of Mechanical Engineering, Bangladesh University of Engineering and Technology, Dhaka, Bangladesh.

Md. Sojib Kaisar

_____   _____
Dr. Aloke Kumar Mozumder   Md. Sojib Kaisar

DECLARATION

It is hereby declared that this thesis/project or any part of it has not been submitted elsewhere for the award of any degree or diploma.

Date: 17-04-2022

Md. Sojib Kaisar

_____

Md. Sojib Kaisar

Author

ACKNOWLEDGMENT

I am very grateful and indebted to my supervisor Dr. Aloke Kumar Mozumder, Professor of the Department of Mechanical Engineering, Bangladesh University of Engineering and Technology, for his kind supervision, constant guidance, encouragement, support and thoughtful discussion throughout the entire research work.

I am also grateful to the Department of Mechanical Engineering, BUET for providing necessary lab facilities for the research.

I would also like to thank my parents for their help and mental support during my research.

Author

ABSTRACT

Closed Loop Pulsating Heat pipe (CLPHP) is one of the most popular passive heat transfer systems used mostly in electronic cooling. The subtle complexity of internal thermo-fluidic transport phenomena of this device is quite unique. In the present experimental study, a CLPHP is made from a long capillary copper tube with an inner diameter of 2.1mm and an outer diameter of 3.1mm. The tube is bent into eight number of U-turns and divided into three regions; evaporator region (50mm), adiabatic region (100mm) and condenser region (50mm). A rosette like wire fin structure is inserted at the center of the CLPHP to compare the performance with no wire insert (plain tube) and a wire insert. The thermal performance is studied with water, methanol, ethanol and acetone for different fill ratios (20% to 80% with 20% increment) and different heat input (4W to 35W). This experimental study reveals that the thermal resistance of rosette inserts CLPHP perform better compared to a wire insert and no wire insert CLPHPs. Acetone performs better than the other working fluids due to its low latent heat and specific heat. Less quantity of heat is required for acetone which provides early start of nucleation boiling in the evaporator region of the CLPHP. Thermal resistance drops quickly at low heat input range (up to 10-15W) and becomes almost uniform at high heat input. It is observed that the thermal performance also depends on different fill ratios. It has been found from this experimental study that 60% fill ratio of various fluids showed better result compared to other fill ratios. It happens due to the presence of optimum amount of fluid in liquid phase which transfers more heat by nucleation boiling. A comparative study on thermal performance has been carried out for rosette insert CLPHP with respect to no wire insert (Plain tube) and a plain wire insert CLPHPs. Convection and boiling heat transfer are the usual modes of heat transfer in heat pipe. The shape, size and structure of the rosette wire inserts are like that they always conform a solid contact between the fin of the rosette and inner surface of the tube. This solid contact introduces a new mode (conduction) of heat transfer, which ultimately enhances the overall heat transfer in heat pipe. Actually, the introduction of conduction heat transfer in heat pipe technology is the main objective of the present study. An overall decrement of the thermal resistance is approximately 10% for rosette insert compared to plain tube heat pipe and 7% reduction with compared to plain wire insert heat pipe among all the experimental conditions. Acetone with 60% fill ratio shows the best thermal

performance in rosette insert CLPHP among all experimental conditions. Thermo-physical properties like latent heat and specific heat of working fluids have an effect on thermal performance of CLPHP. Rosette insert CLPHP performs better for all working fluids than plain tube and plain wire insert CLPHPs.

NOMENCLATURE

AC	=	Alternating current
σ	=	Surface tension (N/m)
Bo	=	Bond Number
$\cos\Theta$	=	Electrical Power factor
C_{pl}	=	Specific Heat of Liquid
Eö	=	Eotvos number
D_f	=	Fin diameter of rosette
D_t	=	Inner diameter of tube
D, D_i	=	Inner diameter of the tube (mm)
D_w	=	Diameter of the main wire of rosette
D_{crit}	=	Critical diameter (mm)
h_{fg}	=	Latent heat of liquid
I	=	Electrical current (A)
k_l	=	Thermal conductivity of liquids (W/m˚C)
Leff	=	Effective length of pulsating heat pipe
ρ_{liq}, ρ_l	=	Density of liquid of a working fluid (kg/m^3)
ρ_{vap}, ρ_v	=	Density of Vapor a working fluid (kg/m^3)
$(\Delta P)_{sat}$	=	Pressure difference between evaporator and condenser
g	=	Gravitational acceleration (m/s^2)
Q/Q_{input}	=	Heat input at evaporator region (W)
q_c	=	Heat flux (W/m^2)
R_{th}	=	Thermal resistance (˚C/W)
R_a	=	Thermal resistance of evaporator and adiabatic region (˚C/W)
Rc	=	Thermal resistance of adiabatic and condenser region (˚C/W)
T_e	=	Average temperature of evaporator region (˚C)
T_a	=	Average temperature of adiabatic region (˚C)
T_c	=	Average temperature of condenser region (˚C)
$(\Delta T)_{sat}$	=	Temperature difference between evaporator and condenser
μ_l	=	Viscosity of liquid (Nsm^{-2})
V	=	Electrical voltage (V)

LIST OF ABBREVIATIONS AND ACRONYMS

CLPHP	=	Closed Loop Pulsating Heat Pipe
FR	=	Filling ratio
OLPHP	=	Open Loop Pulsating Heat Pipe
PHP	=	Pulsating Heat Pipe
PT	=	Plain tube
RI	=	Rosette inserts
WI	=	Wire inserts
WF	=	Working fluid

TABLE OF CONTENTS

LISTS OF FIGURES:

xv

LISTS OF TABLES:

CHAPTER 1: INTRODUCTION

Thermal management is a challenging task for every heat-producing system still it is necessary. As heat transfer is concerned, electronic devices produce excess heat during operation. As a result, the performance of electronic components may drop severely due to excess heat. Thus, proper thermal management is necessary for their optimum and smooth operation. Modern electronic devices are designed to achieve better performance from compact packages. Therefore, effective heat dissipation is critical for the design. Forced convection and heat sinks are not suitable solutions for this. Therefore, a proper cooling device is necessary to achieve a high rate of heat removal and can conserve uniform temperature technological improvement. One solution is to extract heat by using heat pipes to remove the excess heat by directly attaching it to the heat source.

1.1: Overview of Heat pipe

The heat pipe was introduced nearly about seven decades ago, patented by Gaugler [1]. The conventional heat pipe consists of a porous wick material lining inside a small diameter straight tube. The straight tube has two ends, one is an evaporator with heat input to the system, and the other is a condenser with a heat sink. In the evaporator section, fluid changes its phase to vapor from the liquid by gaining heat, and the other end causes condensation. The wick structure helps to liquid to travel back to the evaporation section. Though the heat pipe is an effective way to transfer heat, it is difficult to design the wicked structure inside the heat pipe [2]. Heat pipes are high-effective thermal conductivity two-phase flow heat transfer devices that move the liquid to vapor and vice versa between the evaporator and condenser. Heat exchangers with heat pipes can handle substantially higher heat fluxes than standard heat exchangers because of their excellent heat transport capacity. Heat pipe technology is increasingly being used to improve heat exchangers' thermal performance in microelectronics, saving energy in traditional heating, ventilating, and air conditioning (HVAC) systems. Besides, Heat pipes are used in operating rooms, surgery centers, hotels, clean rooms, and other industrial sectors, such as spacecraft and various types of nuclear reactor technologies, as an entirely inherent cooling apparatus. It regulates the temperature in the human body. The heat pipe is a self-

contained construction that uses a two-phase fluid flow with capillary circulation to obtain high thermal energy conductivity. A heat pipe is evaporation–condensation device for transmitting heat that uses the latent heat of vaporization to transport heat over large distances with a minimal temperature difference. It operates in a two-phase flow regime.

Heat added to the evaporator is transferred to the working fluid by conduction and causes vaporization of the active liquid at the surface of the capillary structure. Vaporization causes the local vapor pressure in the evaporator to increase and vapor to flow toward the condenser, thereby transporting the latent heat of vaporization. Since energy is extracted at the condenser, the vapor transported through the vapor space is condensed at the surface of the capillary structure, releasing the latent heat. Closed circulation of the working fluid is maintained by capillary action and bulk forces. An advantage of a heat pipe over other conventional methods to transfer heat, such as a finned heat sink, is that a heat pipe can have an extremely high thermal conductance in steady-state operation. Hence, a heat pipe can transfer high heat over a relatively long length with a comparatively small temperature differential. Heat pipes with liquid-metal working fluids can have a thermal conductivity of a thousand or tens of thousands of folds better than the best solid metallic conductors, such as silver or copper. In a heat pipe, energy is transported by utilizing the phase change of the working substance instead of a large temperature gradient and without external power. Also, the amount of energy transferred through a small cross-section is much larger than that by conduction or convection. Heat pipes may be operated over a broad range of temperatures by choosing an appropriate working fluid in Fig. 1.1.
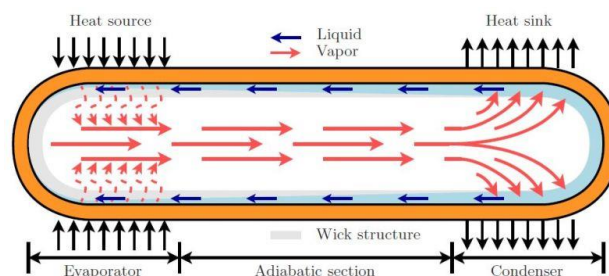
Figure 1.1: Operation process of standard heat pipe structure [2]

To increase the effectiveness to design consideration, another device Pulsating Heat Pipe (PHP) is first invented by Smyrnov G. F. and Savchenkov G. A. [3]. Pulsating

heat pipe (PHP) is a passive heat transfer device which has potential applications in many fields, like fuel cell, solar cell, space and electronic cooling, heat recovery, hybrid vehicles and so on. Following that, Akachi [5] suggested a new kind of Pulsating Heat Pipe. PHP consists of a capillary tube of several U-bend turns to form a parallel path passage. It has three sections, an evaporator, condenser, and adiabatic section in the middle. Heat is collected at the evaporator section, and vapor plugs are generated by this section of liquid and force the liquid slugs towards the condensation section where vapor bubbles permit to dissipate heat to the environment and recall more fluid from the evaporator. Flow oscillations are caused by this liquid slug motion that conducts device operation without any assistance of gravity. As a result, this is more effective concerning other wickless passive heat transfer devices such as Thermosiphons (TS). PHP can be classified into three configurations: Closed Loop Pulsating Heat Pipe (CLPHP), Open Loop Pulsating Heat Pipe (OLPHP), and Closed Loop PHP with check valves. In open-loop configuration, both the ends are welded and pinched off. On the other hand, both the ends are connected to each other for a closed-loop.

Though it is a very recent invention, many scientists conducted a significant amount of research study to know the behavior of the PHP. Many studies are conducted by the researchers on these three types of PHP significantly, and closed-loop PHP without check valves shows better performance due to fluid circulation advantage and cost benefits.

It is difficult to describe the exact thermodynamic phenomena of the PHP, Groll and Khandekar [4] tried to explain using pressure enthalpy concept. It has been proposed that heat addition in the evaporator is done at constant pressure combined with isentropic pressure increase due to bubble formation. Bubbles are travels through the adiabatic section pressure decreases at constant temperature. Since the phenomena within the condenser are complicated but considered constant pressure condensation with negative isentropic work. A constant temperature pressure drop in the adiabatic section completes the cycle. Lots of assumptions was considered during these studies makes difficult to study PHPs.

PHPs are dependent on different parameter. Cross-sectional area of tube, turn number, Heat flux, filling ratio and properties of working fluid have major effects on PHPs.

Rough surface inside the tube may affect the fluid oscillation that results poor performance. It also shown that an optimum filling for different geometry and working fluid is desirable for better performance of the PHP. The cross-section diameter of tube has a great influence on PHP performance. Designing of any PHPs, bond number is a major constrain that limits the diameter of the capillary tube. Since the fluid flow is mainly continued by the surface tension opposed by the gravity force, the following relation allows a minimum internal diameter to be considered for design parameter [7].

$$D \leq D_{cr} = 2\sqrt{\frac{\sigma}{g(\rho_f - \rho_g)}} \tag{1}$$

Here, D is the allowable diameter of the PHP. If the allowable diameter is larger than the critical diameter, the surface tension will not the dominant over gravity thus no flow or very little flow inside the capillary tube. If the diameter becomes equal or little smaller than the critical diameter, surface tension becomes dominant factor and oscillation of the working fluid occurs and results better performance. Heat flux in the evaporator turns creates a pressure gradient that pushes working fluid to move along the capillary tube.

1.2: Characterization factors of Pulsating Heat Pipes

Pulsating heat pipes are basically specified by the following features:

i.   At least one heat receiving area known as Evaporator

ii. At least one heat-dissipating area known as Condenser

iii. No assisted structures such as wick

iv. An optional adiabatic portion that separates the evaporator and condenser zones

This tube is classified into three types: shown in Fig. 1.2

- Open Loop Pulsating Heat Pipe (OLPHP)

- Closed Loop Pulsating Heat Pipe (CLPHP)

- Closed Loop with flow check valve Pulsating Heat Pipe
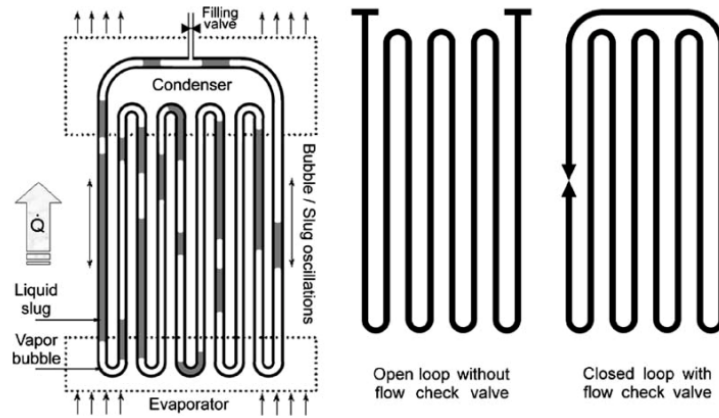
Figure 1.2: Schematic of a pulsating heat pipe and its design variations [4]

1.3: Operating mechanism of Pulsating Heat Pipe (PHP)

The tool is first evacuated and crammed in part with a working fluid, which distributes itself obviously inside the shape of liquid-vapor plugs and bubbles in the capillary tubes. There isn't any outside control over the tubes' preliminary plug/bubble distribution. One end of this tube bundle receives heat transferring it to the other end by a pulsating action of the liquid-vapor system. The performance success primarily depends on the continuous maintenance or sustenance of these non-transported because of the pressure pulsation caused inside the system. The device's construction inherently ensures that no external mechanical power source is needed for fluid transport. The driving pressure pulsations are fully thermally driven.

1.4: Operating mechanism of CLPHP

Consider a case when CLPHP is kept fully isothermal, say at room temperature. In this case, the liquid and the vapor phases inside the device must exist in equilibrium at the saturation pressure corresponding to the fixed temperature. Referring to the pressure-enthalpy diagram, the thermodynamic state of all the liquid plugs, irrespective of their size and position, can be represented by point-A. Similarly, point-B represents the thermodynamic state of all the vapor bubbles present in the PHP. Suppose the temperature of the entire CLPHP structure is now quasi-statically increased to a new constant value. The system will again come to a new equilibrium temperature, and corresponding saturation pressure points A' and B' in Fig 1.3. In doing so, there will be some evaporation mass transfer from the liquid until

equilibrium is reached again. A similar phenomenon will be observed if the system is quasi-statically cooled to new equilibrium conditions A'' and B'' [4, 7].
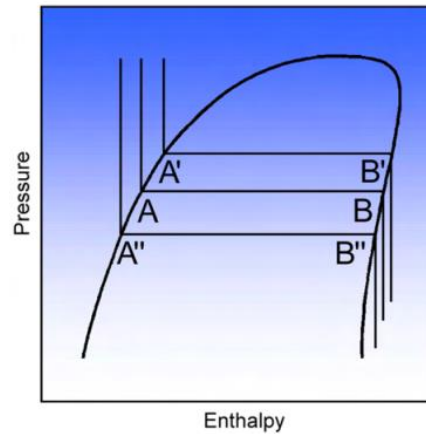
Figure 1.3: Typical pressure enthalpy diagram of a pure working fluid [7]

An actual working CLPHP is not isothermal; a temperature gradient exists between the evaporator and the condenser section. Temperature differences also exist amongst the U bends within the evaporator and the condenser due to local non-uniform heat transfer rates that is always expected in natural systems. The net effect of all these temperature gradients within the plan is to cause non-equilibrium pressure conditions that, as stated earlier, are the primary driving force for thermodynamic transport. This leads to thermally driven two-phase flow instabilities. The heating process in the evaporator continuously tries to push point-A upwards on the liquid saturation line of the pressure enthalpy diagram. Simultaneously, point B is forced to move downwards on the vapor line. In this way, a sustained non-equilibrium state exists between the driving thermal potentials and natural causality that tries to equalize the pressure in the system. Further, inherent perturbations are always present in biological systems. These present perturbations are due to:

❖ Pressure fluctuations within the evaporator and condenser tube sections due to local non-uniform heating and cooling.

❖ Unsymmetrical liquid-vapor distributions cause an uneven void fracture in the tubes

❖ The pressure of an approximately triangular or saw-tooth alternating component of pressure drop is superimposed on the average pressure gradient in a capillary slug flow due to the presence of vapor bubbles.

Thus, a self-sustained thermally driven oscillating flow is obtained in a CLPHP [8].

1.5: Design consideration parameters:

Several research studies indicated the bellow main variables affecting PHP performance:

a) **Geometrical Variables**: Total length of the PHP, number of turns of evaporator/condenser/adiabatic section, diameter/size and shape of tube.

b) **Physical Variables:** Quantity of the working liquid such as filling ratio, physical properties of the operating fluid, and tube material.

c) **Operational Variables:** Open or closed loop operation, Heating and cooling methodology and orientation of PHP during operation.

Various variables simultaneously affect the operation and performance of PHPs. So far as capillary slug flow exists inside the entire device, it has been demonstrated that latent heat will not play a significant role in the device performance. Nevertheless, bubbles are certainly needed for self-sustained thermally driven oscillations. The performance of PHP depends on the flow pattern as well as the above parameter. That makes PHP more challenging to undertake mathematical modeling using conventional techniques.

1.6: Influence Factors of PHP Performance:

There are some primary design parameters affecting the PHP system dynamics.

- Inner diameter of tube

- Input heat flux

- Filling ratio of Working fluid

- Total number of turns

- Device orientation with respect to gravity

- Thermo-physical properties of working fluid

Some secondary conditions that influence the operation:

- Use of control check valve

- Rigidity of the tube materials

- Material and tube combination

- Cross section of tube

- Pattern of flow inside the device

1.6.1: Internal diameter of PHP:

The rise of the velocity of cylindrical bubbles in liquid under adiabatic condition becomes zero when surface tension predominates and this condition is given by,

$$E\ddot{o} = (Bo)^2 = (E\ddot{o})_{crit} \approx \frac{D^2_{crit}.g.(\rho_{liq}-\rho_{vap})}{\sigma} \approx 4$$

(2)

$$D_{crit} \approx 2.\sqrt{\frac{\sigma}{g.(\rho_{liq}-\rho_{vap})}}$$

(3)

When the diameter of the PHPs is higher than the critical diameter from Eq. 3, the gravity force plays a dominant over the surface tension. Thus, vapor could not flow fluently, shown in Fig 1.4. If the diameter is lower than the critical velocity, surface tension and buoyancy forces become dominant and two-phase flow occurs inside the tube.

1.6.2: Effect on turn number and bend radius

Previously, various test experiments suggest that there is a critical number of turns to make a PHP operational under antigravity condition when the actual turn should be greater than it. In addition, this critical turn number is not a constant value at all. It depends on exact parameters and working conditions, such as inner diameter, heat flux, and the working fluid's thermos-physical properties. Besides, experimental results suggest that a higher turn number can lower the thermal resistance, thus increasing the heat pipe's thermal performance. Srikrishna [9] investigated an empirical study on bend radius on single-loop PHP and found that smooth and larger

bend radii have better performance than sharp and small radii. Besides, the loss of pressure in the bend radius can be neglected if it is below 15% of total pressure loss.
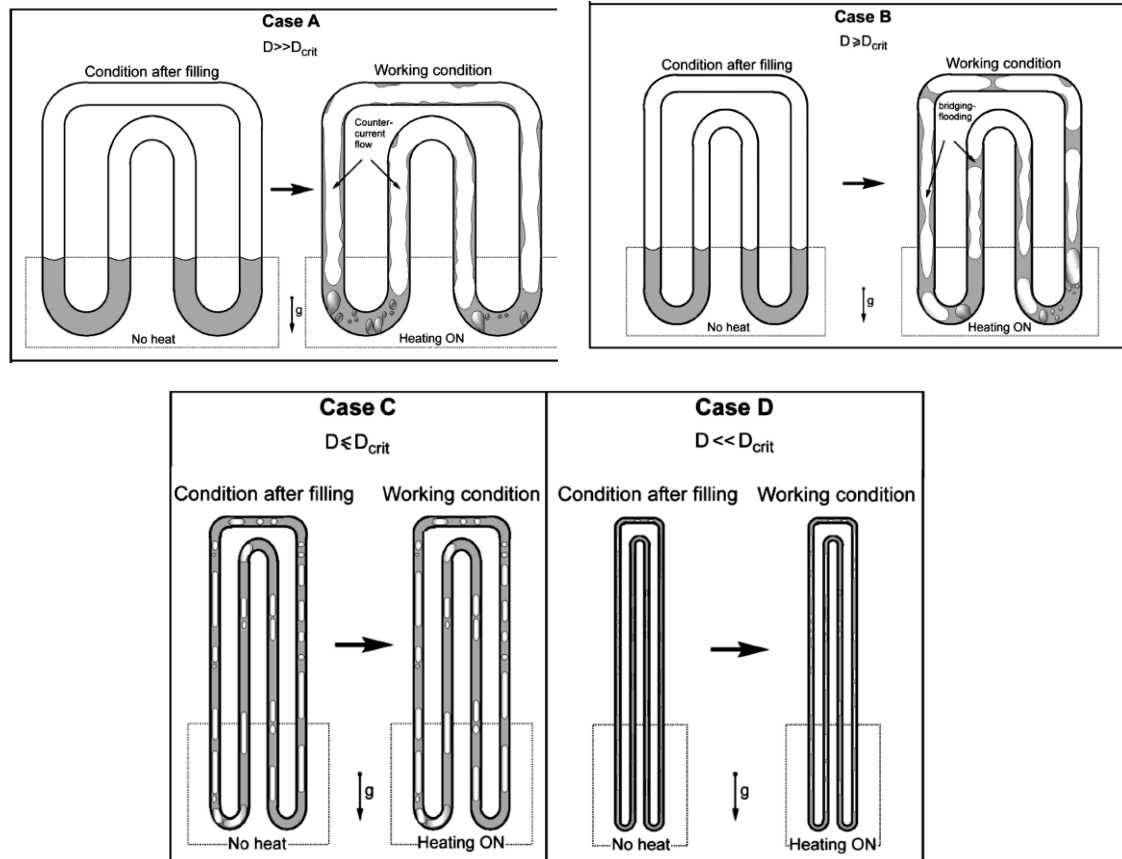
Figure 1.4: Effect of inner diameter on the fluid distribution insider the circular tube of CLPHPs: case A: D>>Dcrit, case B: D≥Dcrit , Case C: D≤Dcrit, Case D: D<<Dcrit [7]

Fig. 1.4 depicts that the flow regime of working fluid inside the CLPHP with various diameter of tubes. Diameter of the tube should be close to critical diameter of the tube. Otherwise, the flow of working fluids cannot perform the actual pulsating action.

1.6.3: Effect of PHP lengths

Zilong [6] suggests that the thermal performance is better for the lower lengths of CLPHPs, because it will require less buoyancy force and surface tension to flow the vapor plug and slug from the evaporator to condenser. Higher distances provide higher frictional pressure drop inside the tube and the temperature oscillations become

more unsteady and the startup time requires higher for it. As a result, the temperature difference between the evaporator and condenser becomes higher and less heat transfer occurs.

1.6.4: Effect of filling ratio

Fill ratio defined as the ratio of working fluid filled in to the volume of pulsating heat pipe. Various tests were conducted to find the optimum filling condition of different working fluid because it dramatically influences the performance of the CLPHPs. A wide range of investigations suggests that the optimum state of filling ratio is situated in 40% to 70% of various working fluids. A lower filling ratio cannot produce enough pressure or vapor-liquid plug to generate the bubble pumping. A higher filling ratio generates an annular liquid flow, so no oscillating action has occurred. 100% filling ratio of working fluid acts as a single-phase thermosyphon; on the other hand, 0% (dry run) of filling shows as a pure conductive heat transfer device with deficient performance.

1.6.5: Effect of heat flux

Since the PHPs are heat transfer devices, the effect of heat flux also plays an important role as it is difficult to explain. Generally, in the PHPs the heat is added to the evaporator section, so lower heat flux will produce less bubble inside the tube and little bubble pumping action will occur thus resulting in a deficient heat transfer performance. Thermal resistance will be higher. Increasing the heat flux produces a large number of bubbles, and two-phase bubble pumping will also increase. As a result, the thermal performance will be better. Although higher heat flux can produce better thermal performance, it also depends on the various conditions like turn number, working fluid, length of the adiabatic section, etc. Khandaker [8, 9] also suggests that heat flux affects the following conditions:

- Internal bubble dynamics, sizes, and agglomeration/breaking patterns

- Level of perturbations and flow instabilities, and

- Flow pattern transition from capillary slug flow to semi-annular and annular.

By increasing the heat input, the flow inside the tube transformed from oscillating slug flow to annular flow, thereby improving performance. Evaporator U-sections experiences convective boiling through the thin liquid film rather than nucleate type

boiling in slug flow regime. Further increase of heat flux will lead to some evaporator dry-out phenomenon. 'Dry out' means almost all the liquid inside the tube available is in pulsating action such as bubble form, and there is minimal liquid present that cannot compensate a large amount of heat input.

1.6.6: Effect of Geometry of PHP structure

To enhance the heat transfer performance many studies are conducted both numerically and experimentally. Different geometry and orientation are considered for studies to obtain the better performance of the PHP. Various working fluids with filling ratio in PHP have been studied to find the optimum filling ratio and fluid for lower thermal resistance. Heat enhancing geometries like fin, inserts, wavy structured insert are also studied in both OLPHP and CLPHP [11, 12]. Different insert geometries inside PHP have been studied and better result is found compare to without insert setup. Insert in PHP assists the heat transfer mode both conduction and convection (multimode) that improves the performance.

In this study, the tests will be conducted experimentally to investigate the performance of Pulsating Heat Pipe (PHP) with an insert of modified geometry aiming for heat transfer in a multimode manner (targeting for conduction heat transfer along with the usual enhancement of convective heat transfer). It is an experimental work, so the primary objectives are as follows:

i.   A rosette-like insert will be used for the augmentation of heat transfer in a multimode manner. The performance of Pulsating Heat Pipe (PHP) with a modified insert will be compared with PHP of no insert and plain wire insert.

ii. The dominating parameters like temperature, working fluid filling ratio, input power will be measured for calculation purposes.

iii. An analysis to evaluate the performance (like thermal resistance, heat transfer, temperature distribution) and getting the optimum operating conditions of the PHPs will be conducted on the basis of measured and calculated values.

CHAPTER 2: LITERATURE REVIEW

Heat pipes are new to the world of the heat transfer, they can start a new horizon toward the economic heat transfer strategies and passive cooling system as well as process identification. Although simple in construction, PHPs become complicated devices when one tries to fully understand their operation. Research on PHPs can be categorized as either experimental or theoretical. Many researchers found complex thermodynamic theories and a wide range of dependable parameters affect the performance of the PHP. Various methods were applied to enhance the heat transfer performance of PHPs.

The original concept of heat pipe was proposed in 1944 by Gaugler [11]. Although Gaugler patented a very lightweight heat transfer device, that was essentially an introductory presentation of a heat pipe. During this period, the technology did not require a sophisticated yet constructively simple two-phase and passive heat transfer device and paid little attention.

This device did not receive much attention until 1964 when Grove and his colleagues at Los Alamos National Laboratory independently reinvented the same concept for their existing space program and its application. They renamed the device as 'Heat pipe.' Grover [12] provided limited theoretical analysis and presented experiments on stainless steel heat pipes with a wire mesh wick and sodium as working fluid. Lithium and silver were also mentioned as working fluids.

Heat can be absorbed in the evaporator zone and delivered to the condenser region, where the vapor condenses. The heat is released to the cooling medium using the working fluid in a heat pipe. During the two years between mid-1964 to mid-1966 RCA Corporation made heat pipes using glass, copper, nickel, stainless steel, and molybdenum. Working fluids included water, cesium, sodium, lithium, bismuth, etc. It is the first commercial organization to work on heat pipes [13]. During 1967 and 1968, various articles were published in the United States scientific press indicating a broad application of the heat pipes for electronic cooling, air conditioning, engine cooling, and others. Heat pipe was first used in space for satellite thermal control on GEOS-B, launched from Vandenberg Air Force base in 1968. The purpose of the heat pipe was to minimize the temperature difference between various transponders in the

satellite. NASA developed a new type of heat pipe called rotating heat pipe in which the wick was omitted in 1969. These heat pipes were utilized for cooling motor rotors and turbine blade rotors.

The fundamental aspect of 'Pulsating Heat Pipe (PHP)' is contained in the patent by Smyrnov and Savchenkov [4]; the exploitation of the concept from an engineering point of view was done by Hisateru Akachi. The very first examples of the group of advanced PHPs seen in 1990 by Akachi. The experiments were done on a Loop-type heat pipe; at least one non-return flow valve is integrated into the tubes. Loop-type heat pipes were claimed to overcome some shortcomings of the traditional heat pipes. It was also described that working fluids unsuitable for standard Heat Pipes might be used in the loop-type heat pipes with comparable or even better performance.

Pulsating heat pipes, like conventional heat pipes, are closed, two-phase systems capable of transporting heat without any additional power input, but they significantly differ from traditional heat pipes in several ways. A typical PHP is a small meandering tube that is partially filled with a working fluid [13]. The tube is bent back and forth parallel to itself, and the ends of the tube may be connected in a closed-loop or pinched off and welded shut in an open loop. It is widely acknowledged that closed-loop PHP has superior heat transfer performance. For this reason, most experimental work is done with closed-loop PHPs. In addition to the oscillatory flow, the working fluid can also be circulated in the closed-loop PHP, resulting in heat transfer enhancement. Although the addition of a check valve could improve the heat transfer performance of the PHPs by making the working fluid move in a specific direction, it is difficult and expensive to install these valves.

Several studies have been conducted with both Closed Loop Pulsating Heat pipes (CLPHP) and Open Loop Pulsating Heat pipes (OLPHP). Experimental and simulation-based studies are ubiquitous in both cases. In both situations, CLPHP shows overall better performance. Since PHPs are dependent on turn number, working fluid, filling ratio, cross-section diameter, geometry, etc., most of the studies were obviously focused on these factors. Besides, different angular geometry configurations were also studied. Zilong [14] experimented with the thermal performance on CLPHP that gravity plays a significant positive role in the thermal version of PHP. A copper CLPHP is considered for the experiment, and a filling ratio

of 50% to 70% of ethanol is measured for the performance. The anti-gravity PHP experiences a longer startup process exhibits more intense steady temperature oscillations, and has a more excellent thermal resistance.

M. Arab [15] investigated extra-long PHP with conventional thermosyphon in applying solar water heaters. The effect of adiabatic length is also studied in the experimental investigation. Tests were done with a filling ratio of 30%, 50%, and 70%. It had been seen that 70% FR of PHP shows better performance against thermosyphon. The investigation also suggests that the length of an adiabatic section should be less to reduce heat loss if good insulation material is not used. Also, evaporator length should be higher for the sustainable operation of PHPs.

Consequently, closed-loop PHP without a check valve becomes the most favorable choice for PHP structures. Recently, PHPs with a sintered metal wick has been analyzed by Holley and Faghri [16]. The wicks should aid in heat transfer and liquid distribution. There has been some exploration into pulsating heat pipes where one or both ends are left open without being sealed.

Heat pipes are not a low-cost cooling solution in general, but they are the most effective and have a lot of promise as power and volume requirements grow. As a result of these factors, heat pipes have primarily been used in applications with unique operating conditions and needs, such as thermal space management, aircraft devices, traction devices, audio amplifiers, closed cabinet cooling, and extreme climatic conditions. Heat pipes provide a crucial isothermal environment with minimal temperature differences between individual components due to their high thermal conductivity.

The downsizing and effectiveness of heat pipes were a breakthrough invention in the application of heat pipe technology in recent times. Trials on the use of pulsing heat pipes with an inner diameter of roughly 3 mm for cooling electronics items have been extensively conducted by heat pipe companies in the United States and Japan. Recently, researchers conducted experimental studies of the wick and wickless designs and cooling characteristics of injection pumps with a diameter of 3- or 4-mm using water, ethanol, ammonia, etc., as working fluids. [17]

Although many experiments had been conducted to know the operating mechanism and the thermos-physical properties of the CLPHPs after introducing PHPs, recent

analysis has seen that the studies are moved to enhance the thermal performance capability to get a better result from the same structures. To improve the thermal performance, many ways are followed and studied. Using the variety working fluids, adding the heat transfer area to the geometry, changing the operation orientation and many more. Inclination angle change can enhance performance and vertical orientation has shown better results in this category. Effects of fin insert inside the tube is also experimented to improve the performance. It has been found that the thermal resistance within the fin inserted (a plain wire) PHPs are less than the standard structure. The thermal performance is better for the fin structures. Though, the experiments were done in OLPHPs. In the CLPHPs, this study can also be applied to investigate thermal performance. Different shaped inserts within the PHPs have also experimented. M. Farhadi [18] overviewed some studies on twisted tape inserts in CLPHPs. Various kind of twisted tape layouts were performed yet. Pressure drop is thwart property while using twisted tape inserts in the CLPHP. Although the performance was emphasized for utilizing the twisted tape but rise in pressure drop was also observed. But the overall performance was mentionable which means more increase of heat transfer than pressure drop.

Thermal performance enhancement could be increased by the properties of working fluids which are responsible for the heat transfer enhancement. Hybrid nanofluids with higher conductivity could increase the thermal performance of the PHPs. Numerical and experimental investigations were conducted by M. Zufar [19] to observe the performance of PHPs. Experimental evaluations were done with heating power of 10-100W and filling ratio of 50% and 60%. Weight concentration of 0.1wt% Al_2O_3-CuO and 0.1wt% of SiO_2-CuO hybrid nanofluids were used as working fluids during this test and compare it with the water. SiO_2-CuO exhibits lowest thermal resistance among the working fluids. Al_2O_3-CuO also perform better than water but not as great as SiO_2-CuO. Nevertheless, the conductivity of SiO_2-CuO is lower than the Al_2O_3-CuO but high viscosity of Al_2O_3-CuO hinders the fluid transportation in PHP. Lowest thermal resistance was attained at higher heat supply. Maximum 57% of decrement of thermal resistance was determined for SiO2-CuO from water. Meanwhile, the hybrid nanofluids were able to achieve start-up pulsation earlier than water.

A range of CLPHPs has been experimentally studied to investigate the effect of several influence parameters such as internal diameter, operating inclination angle, working fluid, and the number of bends. S. Khandekar [20] investigate a parametric study on CLPHP. It is seen that different liquids are beneficial under other operating conditions. An optimum tradeoff of various thermophysical properties has to be achieved depending on the imposed thermomechanical boundary condition. He also suggested that the performance of PHP improves with the increase in internal diameter for a given temperature differential. It also may be safely concluded that thermos-mechanical interactions and instabilities in a pulsating heat pipe in particular, and in capillary-sized tubes in general, is quite complex, and further experiments are indeed needed.

Thermo-physical properties of surfactant solution have positive impact on the thermal performance of the PHP. Thermal performance of CLPHP with various alcohols and surfactant solutions were investigated by D. Bastakoti [21]. The experiment was conducted with methanol, ethanol, Cetyltrimethyl ammonium chloride (CTAC) and compared the performance with that of deionised water. Heat load was maintained about 15W to 80W. Lower saturation pressure gradient and temperature $(dP/dT)_{sat}$ of ethanol and methanol promotes higher velocity of fluids within the PHP. CTAC yielded higher thermal resistance at lower heat supply which can be blamed upon the higher viscosity value that resists the heated solution at evaporator section. But lowest thermal resistance was attained by 2000ppm CTAC solution at higher heat supply when 35% and 50% fill ratio is maintained. Although, surfactant solution showed better performance from the other conventional working fluids but the visualization technique is recommended for further study.

Design and performance test of a PHP was carried out along with fuel cell stack. Ancillary cooling equipment can be replaced by using the pulsating heat pipes which reducing parasitic losses and increasing energy output. Heat pipe effectiveness was found to be dependent upon several factors such as energy input, types of working fluid and filling ratio. Working fluids were tested included acetone, methanol and deionized water. Methanol with fill ratio of 45% showed better thermal performance. A PHP evaporator inserted within bipolar plates of a horizontally configured stack would allow for the condenser to protrude from the stack and transfer heat to its

surroundings. Several pulsating heat pipes aligned between cells would remove heat directly from the source and act as an active fin array. [22]

Hybrid CLPHP made of aluminum partially filled with working fluid of FC-72 was experimented in space application with non-uniform heating pattern and microgravity conditions. The non-uniform heating system promote the overall circulation of fluid in a superior direction resulting the increase of thermal performance compared to homogenous heating. Sudden absence of buoyancy force activates an oscillating slug/plug flow regime allowing the device to work also without assistance of gravity. [23]

Biological nanofluids application in the PHP is cost efficient and effective to yield better thermal performance. Silver nanoparticles were produced from the aqueous silver nitrate and the fresh tea leaf extract and tested to PHP. Influence of different operating parameters such as applied heat flux to the evaporator section, filling ratio of working fluid, heat pipe inclination, nanoparticle concentration and response time on the thermal performance and efficiency of heat pipe was also experimentally studied. Results showed that using the nanoparticles leads to the reduction in temperature distribution and enhances the thermal performance of heat pipe. [24]

Heat transfer characteristics and flow analysis were investigated within straight circular pipe with twisted-tape insert. Numerical simulation was conducted for various Reynolds numbers along with different dimensions (1, 2, 2.5 and 3mm) of twisted-tape insert. Noticeable swirling flow inside the pipe was observed for twisted-tape insert as well as increment of pressure drop was also obtained. The enhancements achieved with the twisted-tape inserts was between 23% and 29% with higher enhancement achieved with the wider twisted-tape inserts. [25]

The performance parameters such as temperature difference between evaporator and condenser, thermal resistance and the overall heat transfer coefficient were evaluated on two turn closed loop PHP. The filling ratio is a critical parameter, which needs to be optimized to achieve maximum thermal performance and minimum thermal resistance for a given operating condition. A copper tube of 3 mm diameter and length of 1080 mm was used to construct the PHP. Varying heat load (10-100W) and fill ratio (20%-100% in steps of 20%) of working fluids was considered. The experimental results demonstrate the heat transfer characteristics, lower thermal

resistance and higher heat transfer coefficient of PHP were found to be better at a fill ratio of 60% for various heat input. The thermal resistance of closed loop pulsating heat pipe decreases with the increase of heat input. At the lower heat input (Q ≤ 30 W) the thermal resistance is decreased slowly and at higher heat input (Q ≤ 30 W) the difference is smaller. The thermal resistances have the results of Racetone < Rmethanol < Rethanol < Rwater [26].

Effect of fill ratios on CLPHP, working fluids and other experimental investigations were carried out to find the operating limit of heat pipe. Generally, a large FR (50% to 70%) is preferable for high heat fluxes and very long PHP channels. Above 70% FR, the PHP performance decreases for most conditions. At high FR, the bubbles tend to limit two phase fluid motion. Working fluids with high boiling point temperature and high latent heat require higher power loads for the phase change, which can be important when PHP is intended to dissipate high heat fluxes at high temperatures. A high $\frac{\partial P}{\partial T}|sat$ offers a greater driving force for fluid motion [27, 28, 29].

The operating frequency of the pulsating heat pipe will increase with the heating power. It occurs because of large driving force and the larger perturbation. The pulsating heat pipe should have one eigan frequency based on the temperature visualization. Although previous establishment was done by balancing forces such as driving force, inertial force and the frictional force. The result show that various structural parameter of pulsating heat pipe influences the eigan frequency differently. The frequency changes quickly for less turn number, mini capillary radius and higher filling ratios. The self-frequency of the driving forces can automatically reach the system eigan pulsating frequency. The system action frequency is got by the following equation. [30]

$$f = \frac{\omega}{2\pi} = \frac{1}{2\pi}\sqrt{(b^2 - a^2)} = \frac{1}{2\pi}\sqrt{\frac{nP_\circ}{L_e{}^2 N^2 \emptyset(1-\emptyset)\rho_l} - 256\left(\frac{\mu_l}{d^2 N \emptyset \rho_l}\right)^2} \qquad (4)$$

Although the fabrication process of pulsating heat pipes is comparatively easy but the operating limit, thermal performance and heat transfer process are very complex which is the actual motivation of present work.

CHAPTER 3: EXPERIMENTAL SETUP

An acceptable experimental setup is required for any experimental investigation. In this experiment, the setups were constructed separately so that the test could be run in the same conditions. Precise filling ratio of working fluid were maintained to observe the performance without any fault. Thermal resistance is the primary properties for this test. So, the experimental instruments were properly calibrated to minimize the error. Insulation was done in a suitable way to reduce heat loss. The brief discussion for the construction of the model is mentioned in this chapter.

3.1: Model setup

A capillary tube of copper was used for the construction. Three separate Closed Loop PHP were constructed for the experiment. First one is the plain capillary means no inserts inside the tube. Second one is constructed as similar dimensions as plain tube CLPHP but with a wire inserts. A long copper wire was placed inside the tube. Lastly the main focus of the study is a rosette like wire is inserted to CLPHP. Wire that inserted was a plain copper wire. A rosette shape insert is prepared by soldering the small diameter copper wire into the main copper wire at 90 degrees to each other after 16~18 mm distance. All the dimensions of the PHPs and insert structures are given in the table. CLPHP specifications for the current experiment are mentioned in the Table 3.1. In the 4th column the modified structure's specification has been shown. Due to the rosette shape insert in the CLPHP, the overall volume has reduced. Moreover, the length of the CLPHP is made close to the other CLPHPs.

3.1.1: CLPHP structure (Plain tube)

It's a basic structure of CLPHP of this experiment. A copper tube of 2.1mm diameter is used to construct the pipe. This diameter is valid for the PHP action because it satisfies the bond number from Eq. 2. There is no insert inside the pipe. U-shape bend is made with eight (8) turn number for this structure. Three sections were identified as evaporator, adiabatic and condenser region. The height of the evaporator is 50mm, adiabatic is about 100mm and the rest is condenser region mentioned in figure 3.1. Cross section of inner tube is showed in Fig. 3.3 (a). Total Nine (9) points were marked to setup. Three points in the evaporator, three in the adiabatic and rest are marked in the condenser. The k-type thermocouple is added in these nine points for

measuring the temperatures. All the connected points of thermocouple and CLPHPs were wrapped with heat tape for measuring the temperature without any other heat sources accidentally. The evaporator section is wrapped with heat tape to overcome possible short circuit. Nickel-Chromium wire is wrapped in the evaporator section for the heat source coil. Current will pass through the high resistive Nickel-Chromium wire for generating high heat. The adiabatic and evaporator sections are surrounded by the glass wool of 1 inch thickness for proper insulation of the setup. Then the setup is placed between wooden block and electrical connections were added. Full setup is placed in the wooded stand structure about 3 feet higher from the ground. A selector switch is connected with the 9 thermocouples for getting the temperature value for a specific point. A Variac is used to supply various voltage which is measured by the digital multimeter. Electric current is measured accurately by clamp on meter. Before conducting the experiment, the electrical safety has been checked carefully.

Table 3.1: Specification of three different types of CLPHP for this experiment

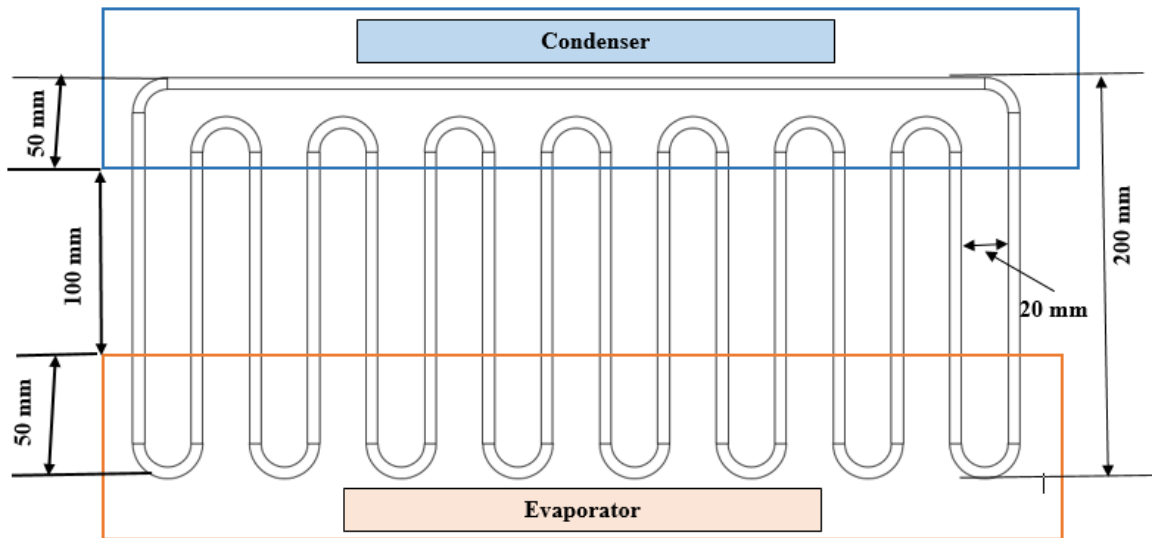| Contents	No wire inserts CLPHP (plain tube)	Wire inserted CLPHP	Rosette inserted CLPHP
Material	Copper	Copper	Copper
Length (mm)	3488	3490	3494
Diameter of the circular CLPHP (mm)	2.1	2.1	2.1
Insert wire diameter (mm)	N/A	0.7	0.7 (main wire)
Rosette wire (small) diameter (mm)	N/A	N/A	0.25 (fin wire)
Number of turns	8	8	8
Measured volume inside CLPHP (mL)	12.42	10.98	9.48

Figure 3.1: Schematic view of front cross-section with no wire insert (plain tube) CLPHP
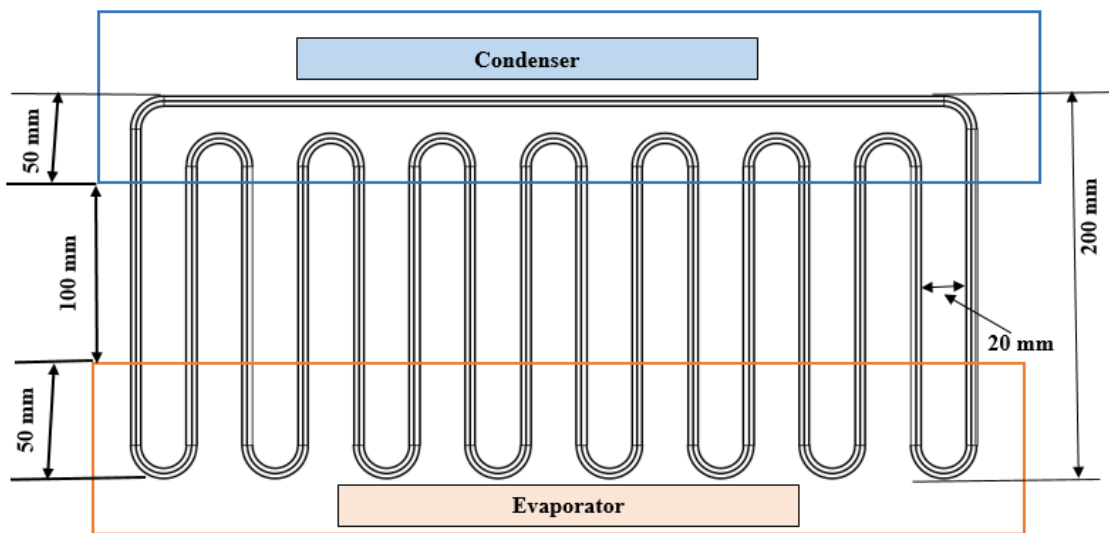

Figure 3.2: Schematic view of front cross-section with wire insert (WI) CLPHP

3.1.2: CLPHP structure (Wire insert)

In this case a straight copper wire of 0.7mm is inserted inside the copper tube of 2.1mm diameter. Total eight turns are made for the structure. The height of the evaporator section is about 50mm, adiabatic section is 100mm and rest of the height is for condenser section showed in Fig. 3.2. Inner tube cross-sectional sectional view is showed in Fig. 3.3 (b). Similar points are marked as plain tube CLPHPs and thermocouples are added to the respective points. The evaporator section is wrapped with heat tape to overcome possible short circuit. Nickel-Chromium wire is wrapped

in the evaporator section for the heat source coil. Current will pass through the high resistive Nickel-Chromium wire for generating high heat. The adiabatic and evaporator sections are surrounded by the glass wool of 1 inch thickness for proper insulation of the setup. Then the setup is placed between wooden block and electrical connections are added. Full setup is placed in the wooden stand structure about 3 feet higher from the ground.
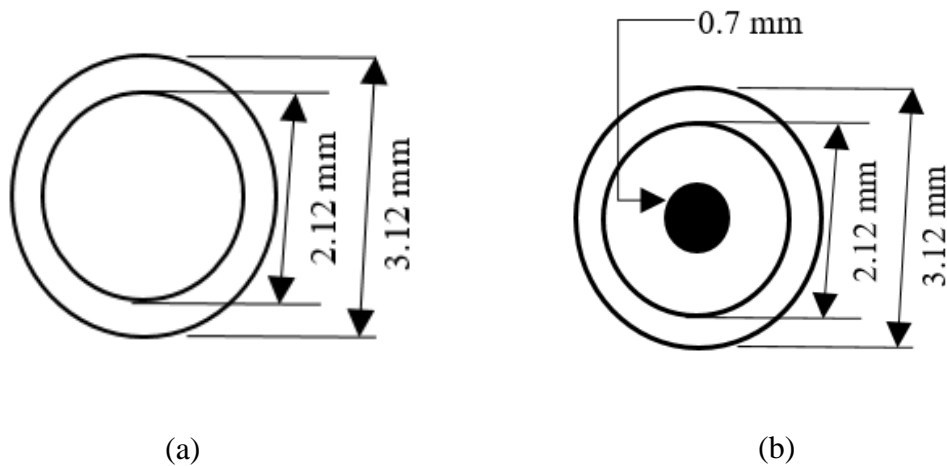

(a)   (b)

Figure 3.3: Inner tube cross-sectional view **(a)** With no wire insert (plain tube) CLPHP and **(b)** With wire insert (WI) CLPHP

3.1.3: Construction of rosette structure & CLPHP

The rosette shape insert is shown in Fig. 3.4 (a). A primary copper wire of diameter of 0.7mm has taken as main wire for rosette structure. After that, several copper wires with 0.25mm diameter, length of 10mm was soldered to the main wire. The distance between the soldered wires was about 10mm each. Then, the rosette was inserted to the copper tube with rotation. The cross-sectional of the rosette insert CLPHP is shown in Fig. 3.4 (b) and (c). The total length is equal to the length of Plain and wire inserts PHP. This rosette is inserted to the main copper tube of 2.1mm diameter. Similar shape and turn number were fabricated like the other setup showed in Fig 3.5. The remaining steps are as like other construction of plain tube CLPHPs.
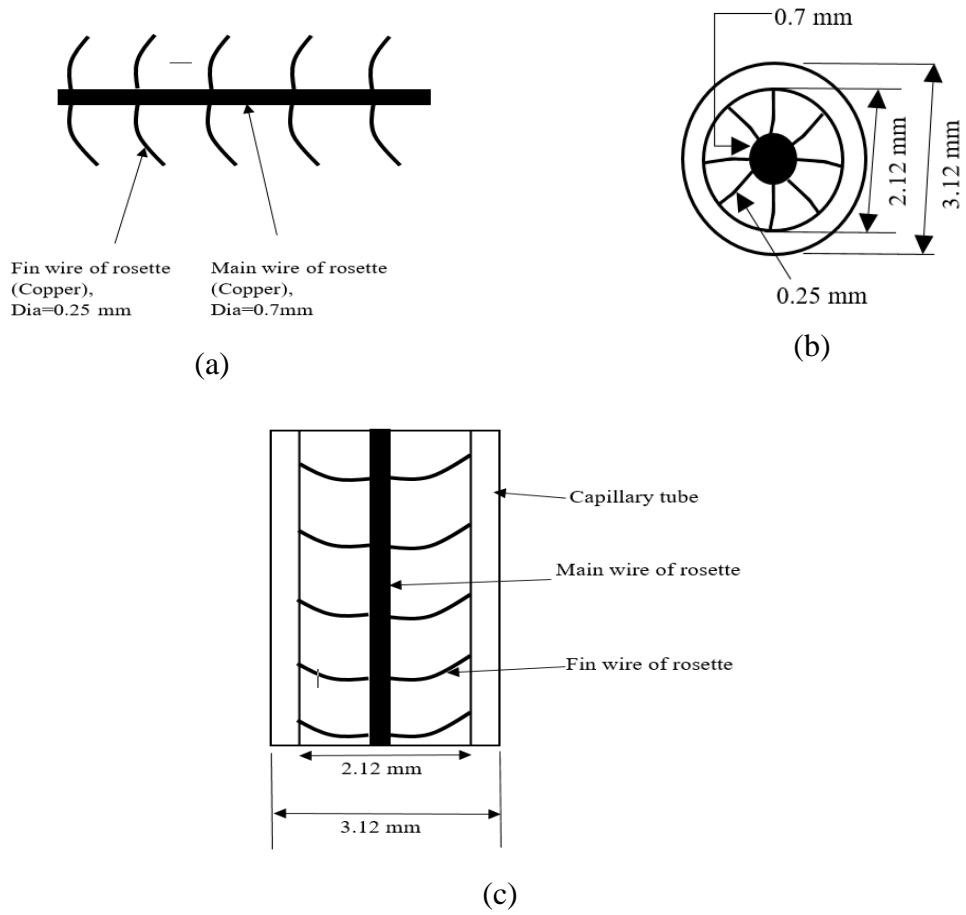
Figure 3.4: Schematic diagram of rosette insert **(a)** rosette construction geometry **(b)** Inner tube cross section **(c)** frontal section inner view of rosette insert
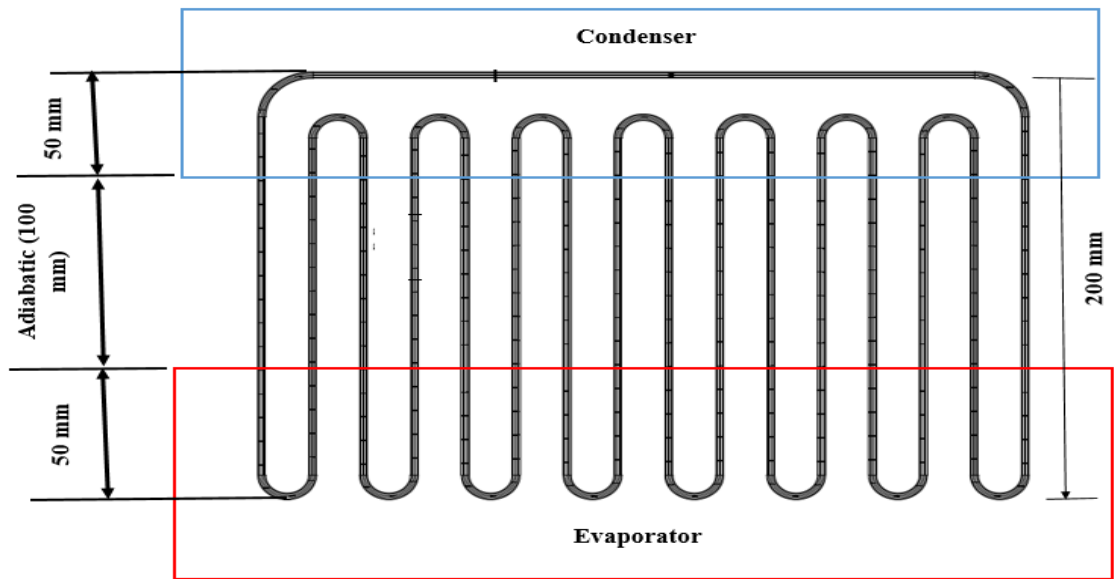

Figure 3.5: Schematic view of front cross-section with rosette insert (RI) CLPHP

3.2: Electrical Components

The main electrical components used in this experiment are as follows. Before measuring the values all the instruments are calibrated following standard rules.

3.2.1: Heating arrangement

AC supply is used in this experiment as the electric source. Then a variac is used to control the current and voltage for supplying electricity to the heater. A heater coil is fabricated by winding a nichrome wire on evaporator tube. A piece of nichrome wire of 0.25mm diameter wound at constant interval of 1.50 mm is used as heater, which is wrapped by insulating clothes to hinder the electricity from passing through the heating blocks.

Table 3.2: Specification of electric variac

Specifications		
Model No.	J8/T10091	
Input Voltage	~220 V	
Output Voltage	0-250 V	
Output Current	8A	
Frequency	50 Hz	**Figure 3.6:** Electric variac

3.2.2: Temperature measurements

K type nichrome wire is used to measure the temperature of various points of the CLPHPs. It is then connected to different marked points of selector switch. The reading of the temperature is recorded by the digital thermometer. The model and specifications are as below:

Table 3.3: Specification of digital thermometer

Specifications		
Manufacturer	HIOKI	
Model No.	3442	
Temperature range	~1300 ˚C	**Figure 3.7:** Digital Thermometer

3.2.3: Multimeter specification

Output voltage of electrical variac is measure by the digital multimeter of bellow specifications:

Table 3.4: Specification of digital multimeter

Specifications		
Manufacturer	INSTEK	
Model No.	GDM-356	**Figure 3.8:** Digital multimeter

3.2.4: Clamp on meter

The ampere of the electrical wire was measured by clamp on meter. For measuring the value the device first calibrated for accuracy. The wire just clamped with the meter and the data was shown in the display.

Table 3.5: Specification of clamp on meter

Specifications		
Manufacturer	HIOKI	
Model No.	3261	**Figure 3.9:** Clamp on meter

3.2.5: Selector Switch

A selector switch is used to get temperature value of thermocouple connected points on the CLPHPs. Total 12 points are available in the selector switch. Nine points are connected to the thermocouples.

3.3: Working Fluids

The working fluids used for this investigation are: acetone, ethanol, methanol and water. Effect on thermal performance of working fluid on different CLPHPs at different filling ratios. The properties of the liquids are as given bellow:

Table 3.6: Chemical properties of the working fluids

Property	Water	Ethanol	Methanol	Acetone
Boiling points (˚C)	100	78.3	64.7	56
Liquid density (kg/m^3)	997.1	785.5	786.3	784.6
Liquid Specific Heat (KJ/Kg ˚C)	4.183	2.513	2.535	2.34
Latent Heat (KJ/Kg)	2257	846	1101	518
dp/dT @80 ˚C	1946	4299	6395	6262
Dynamic Viscosity (pa-sec)×10^{-3}	0.8905	1.0820	0.5455	0.3166
Surface Tension (dynes/cm)	71.97	22.28	22.26	22.99
Thermal conductivity (W/m·K) –Liquid (at 20˚C)	0.598	0.179	0.202	0.161

3.4: Experimental Rig

Heating of the evaporator section of the PHP was done using a nichrome heater wire, wrapped outside the evaporator section. The evaporator section is made up of copper tubes. Copper is a good conductor of electricity and heat. When the current passes through heater for heating of evaporator section, there is a chance of short circuit of heater due to its direct contact with copper tubes. Therefore, heater was electrically insulated in order to avoid this problem. In order to minimize the heat loss from the evaporator section, the heating section was thermally insulated by wrapping glass-wool and finally, it was supported by wooden block. The input heating power to the evaporator was controlled using an AC variac for all the experiments. The current and voltage were monitored using a multimeter. The input voltage has been varied up to a maximum of 30 V in steps of 5 V. The schematic diagram of the test rig is showed in Fig 3.10.
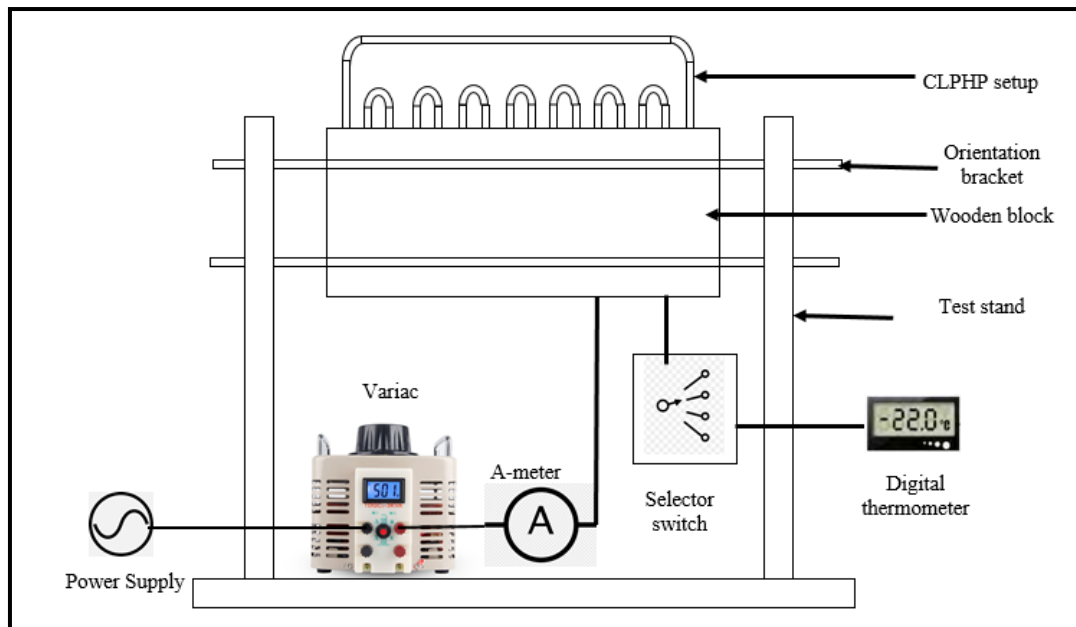
Figure 3.10: Schematic diagram of experimental setup of CLPHP

3.5: Experimental Process

I. Each of the CLPHPs were set between two wooden blocks. The evaporator and adiabatic region were insulated properly with glass wool to reduce heat loss. The test rig is shown in fig 3.10. It comprised a wooden stand, wooden block, variac, digital multimeter, digital thermometer, clamp on meter and selector switch.

II. Three CLPHPs were placed vertically in the wooden stand for the test. To perform the investigations, four working fluids were used: water, ethanol, methanol and acetone.

III. Before every test, the inside of the CLPHPs were cleaned, rinsed with distilled water and dried.

IV. For every single working fluid, total four filling ratios (20%, 40%, 60% and 80%) were used filled for each test to find the finest performance and the effect of fill ratio on CLPHPs.

V. In each of the tests, the electrical variac was used to maintain a constant output AC voltage and current. Digital multimeter and clamp on meter were used to register the output voltage and current readings. Total power input was computed from the recorded data. The applied heat was absorbed by the

evaporator liquids thus escalate the temperature and transferred towards condenser region. After a particular time, the temperature had maintained a steady-state condition.

VI.   The temperature of thermocouple points (showed in Fig. 3.14) is recorded by the digital thermometer at steady-state condition. A selector switch was utilized to show the temperature for each point.

VII. After completing one test, the above steps were followed for the other working fluids in three geometries CLPHP.

VIII. From the recorded data, thermal resistance is computed for respective conditions and analyzed thoroughly.

The lab experiment was conducted in Instrument and Measurement Lab, Department of Mechanical Engineering, BUET. Images from the lab are as following:
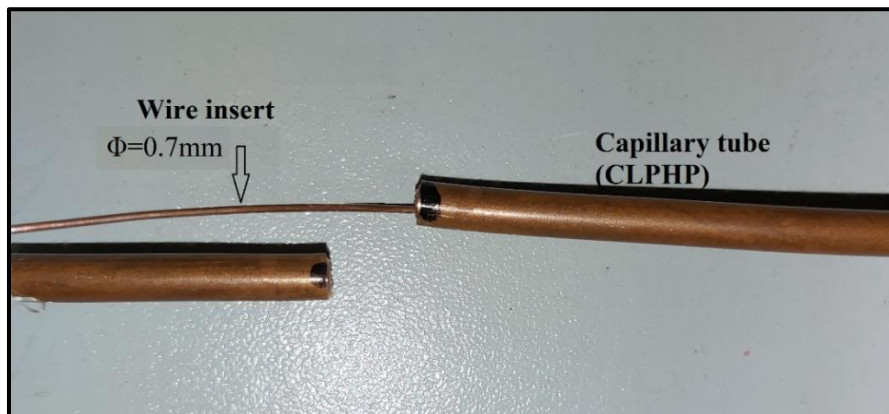
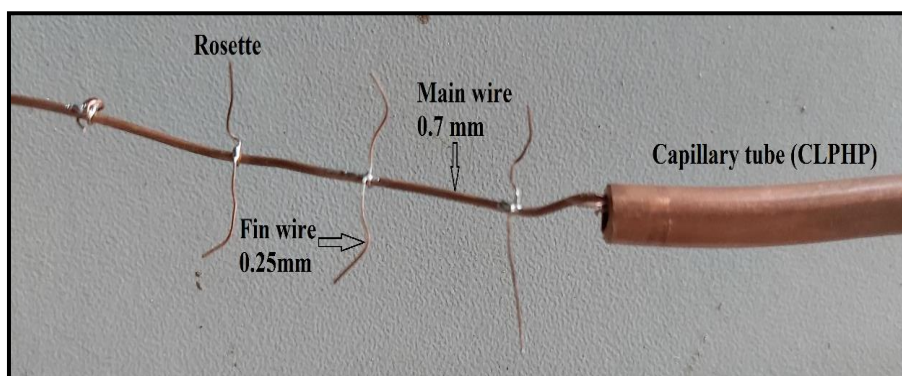**Figure 3.11:** Detail view of wire insert structure

Figure 3.12: Detail view of rosette structure

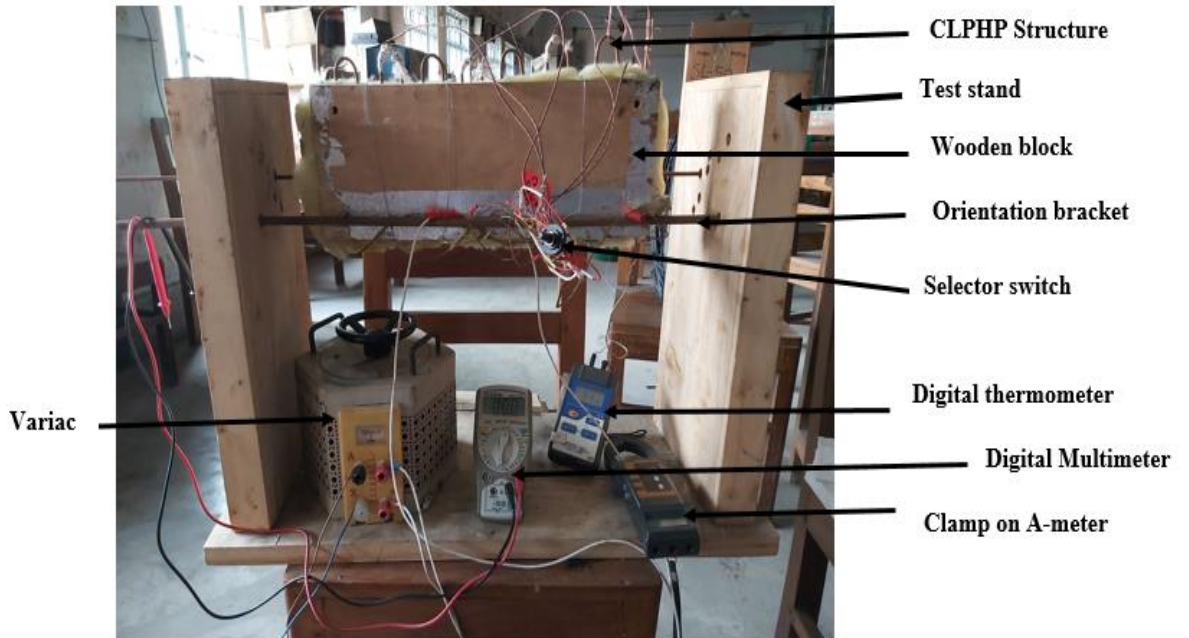**Figure 3.13:** Construction setup of CLPHP in lab.

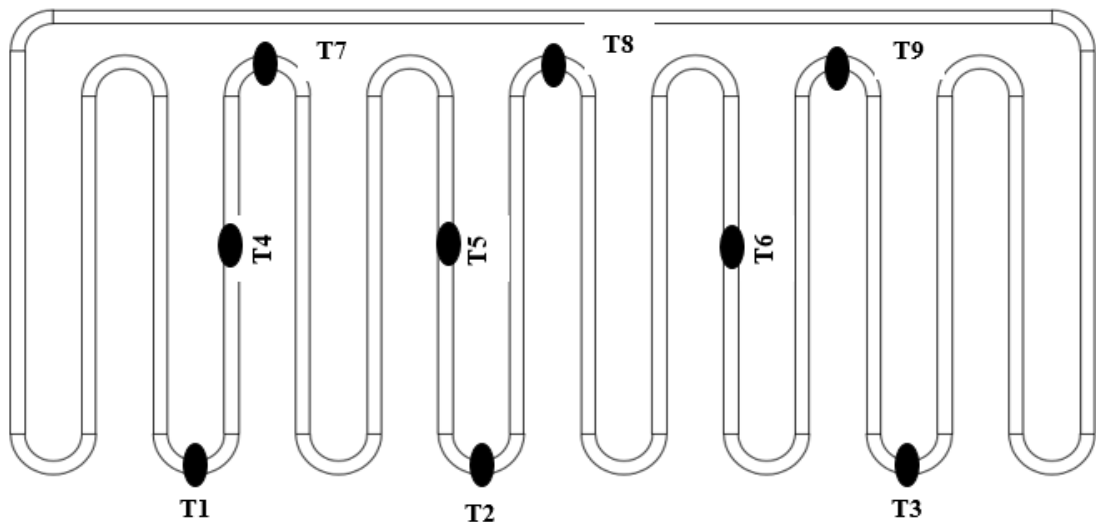**Figure 3.14:** Selected points on CLPHP for temperature measurements

3.6: Necessary Formula:

Heat   Input $Q=V*I*Cos\Theta$
(5)

Here, V=Output voltage of variac,

      I= Electrical Current,

CosΘ= Power factor=0.85,

Evaporator average temperature, $T_e = \dfrac{T1+T2+T3}{3}$ $\hspace{2cm}$ (6)

Adiabatic average temperature, $T_a = \dfrac{T4+T5+T6}{3}$ $\hspace{2cm}$ (7)

Condenser average temperature, $T_c = \dfrac{T7+T8+T9}{3}$ $\hspace{2cm}$ (8)

Thermal resistance, $R = \dfrac{T_e - T_c}{Q}$ $\hspace{2cm}$ (9)

Eq. 2 can be written as:

$$R = \frac{(T_e - T_c)}{Q_{input}}$$

$$or, R = \frac{(T_e - T_a)}{Q_{input}} + \frac{(T_a - T_c)}{Q_{input}}$$

$$or, R = R_a + R_c \hspace{2cm} (10)$$

Here,

T1, T2 and T3= Temperatures at evaporator region

T4, T5 and T6= Temperatures at adiabatic region

T6, T7 and T9= Temperatures at condenser region

T_e= Average temperature of the evaporator region

T_a= Average temperature of the adiabatic region

T_c= Average temperature of the condenser region

R_a= Thermal resistance of adiabatic region

R_c= Thermal resistance of condenser region

CHAPTER 4: RESULTS & DISCUSSIONS

One of the measured parameters is thermal resistance to determine thermal performance of Closed Loop Pulsating Heat Pipe (CLPHP). Temperature profiling could also be studied to realize the working conditions of CLPHP. In this experiment, the primary concern will be to learn the thermal performance with modified inserts (rosette) CLPHP. Thermal performance will be compared to the CLPHPs with no wire insert (plain tube-PT) and wire inserts (WI) will be analysed to get optimized conformation of CLPHP from this experiment. Total fifty-one experimental run have been undertaken with the three different conformations of CLPHP in this investigation. Temperature profiling, thermal resistance comparison will be analysed and discussed in this chapter.

4.1: Temperature Distributions

Heat was applied to the evaporator region with an increment of 5V each. Corresponding current was recorded and total power input was calculated. Total electrical resistance was maintained constant at evaporator region for the heating purpose. At first, each of the constructions were vacuumed by vacuum meter and prepared for the experiment. Test were performed in each of the CLPHPs with dry run condition (0% fill ratio) along with various fill ratios of different liquids (20%, 40%, 60% and 80%). Four types of working fluids were selected for this investigation: water, acetone, ethanol and methanol. All the data were recorded at steady state condition during the tests. Temperature profile were plotted against heat input with various fill ratios of different working fluids in three types CLPHPs: with no wire insert, wire insert and rosette insert. In this chapter, temperature of the evaporator, adiabatic and condenser region will be assigned as T_e, T_a and T_c respectively.

4.1.1: Distribution of Evaporator temperature (T_e), adiabatic temperature (T_a) and Condenser temperature (T_c)

In dry run condition in plain tube CLPHP, temperature of the three regions is plotted against heat input in Fig 4.1. It is observed that the temperature of each region (T_e, T_a and T_c) increases with heat inputs. During dry run condition, there was no fluids inside the tube, the temperature of evaporator, adiabatic and condenser region is increased due to heat conductivity of copper tube wall surface. Condenser is cooled

by free convection in atmospheric air. Although, it is desirable to maintain constant temperature due to constant isentropic system in the adiabatic region but construction of such a system is difficult to build.
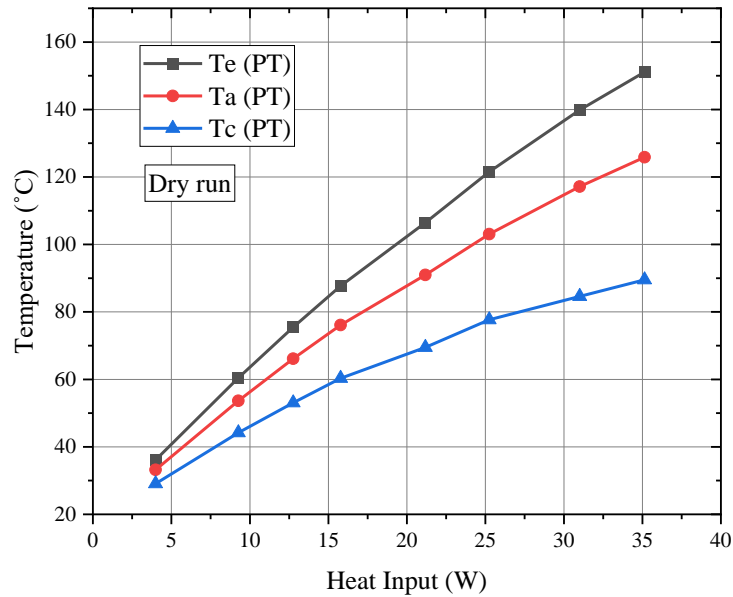

Figure 4.1: Temperature distribution of evaporator, adiabatic and condenser region of Plain tube CLPHP (Dry run)

In Fig. 4.2 for 20% water, it has been noticed that the temperature of the evaporator, adiabatic and condenser regions are increased with respect to heat input for plain tube CLPHP. The temperature of the three regions is increased at higher rate up to 25W and later the rate is slightly decreased. The condenser temperature also increases with respect to heat input but maintains lower temperature than evaporator due to heat dissipation in the atmosphere. The adiabatic temperature curve stays close to evaporator curve that means minimal loss in this region due to less heat transfer.

The amount of liquid phase in the CLPHP depends on the filling ratio (FR). A higher FR implies that there is more liquid phase than vapor phase. Tong [31] observed that vapor-liquid slug-train units are randomly distributed in the CLPHP after it is partially filled. When heat is applied to evaporator region, working fluid of wall adjacent layer heated by convective mode. Increase in heat input, the temperature of the working fluid rises and nucleate boiling starts at the wall surface. Further increase of heat input enhance the nucleation sites thus more bubbles will form that will provide high heat transfer from the evaporator surface. A pressure variation is experienced in between evaporator and condenser region thus provides pulsating motion of vapor-liquid slugs

48

towards the condenser region. When the temperature of the evaporator region rises to boiling point of the working fluids, rapid boiling decreases the presence of liquids with respect to vapor phase thus hinders heat transfer rate which is observed after 25W in Fig. 4.2.
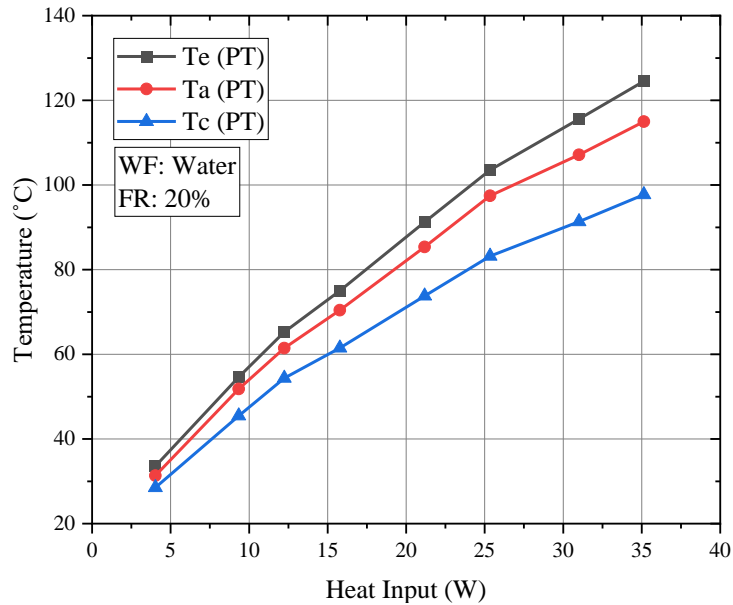

Figure 4.2: Thermal response of no wire insert (plain tube) CLPHP with water for 20% fill ratio.
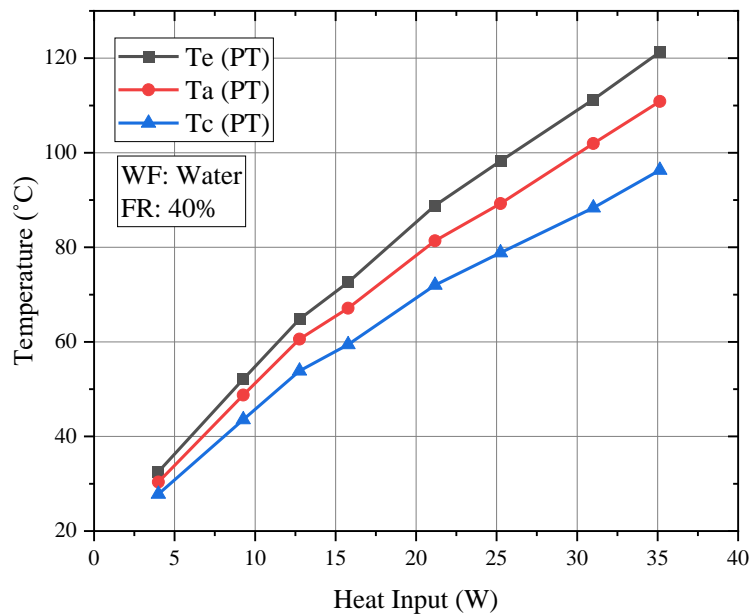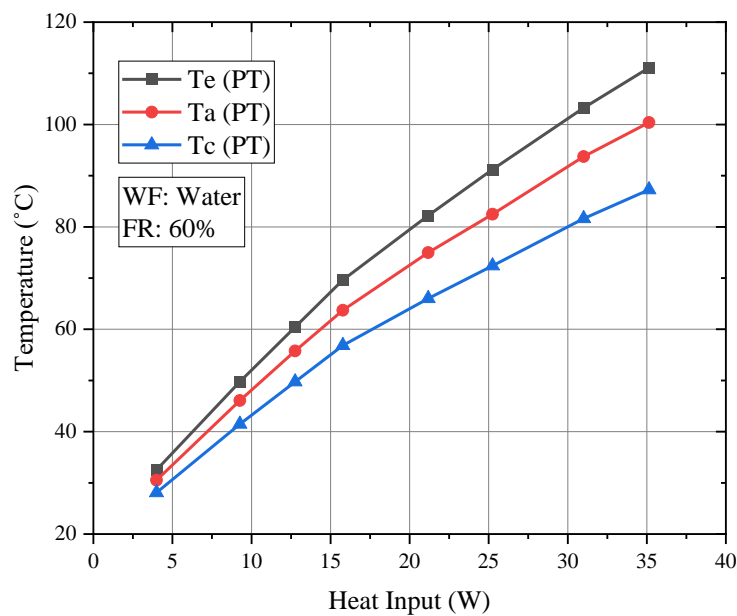

Figure 4.3: Thermal response of no wire insert (plain tube) CLPHP with water for 40% fill ratio.

Similar phenomena can be seen for 40% and 60% fill ratio of water in plain tube CLPHP. Fig 4.3 and Fig 4.4 depicts that the T_e, T_a and T_c are increases against heat input. The difference of T_e and T_c is increased with respect to heat input due to better condensation of working fluids illustrated in Fig 4.6. At higher heat input, the increase of nucleation boiling phenomena inside the CLPHP causes more bubble generation but after reaching boiling point of fluids, there is a change of trajectory in temperature curve is seen. It is happened because large size bubbles are formation at this stage restricts heat transfer. At this condition the loss in adiabatic region is greater than 20% FR.

Figure 4.4: Thermal response of no wire insert (plain tube) CLPHP with water for 60% fill ratio.
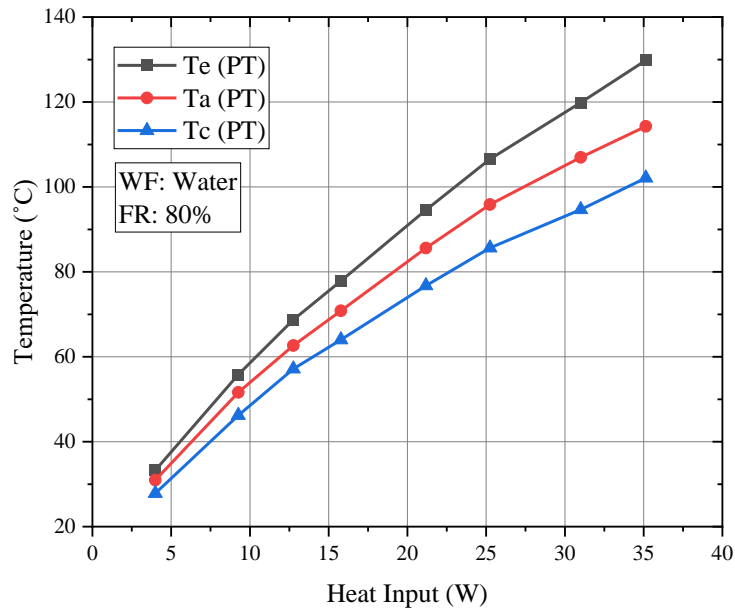
Figure 4.5: Thermal response of no wire insert (plain tube) CLPHP with water for 80% fill ratio.

At a higher FR: 80% of water in plain tube CLPHP, evaporator temperature is maintained greater temperature than the low FR. Fig 4.5 depicts that, higher FR means more presence of liquid phase that requires more heat to start nucleate boiling. As a result, the temperature of the evaporator showed higher temperature. Furthermore, the loss in the adiabatic region is also greater at this FR. Less pulsating action is happened due to less space available is also responsible for the adiabatic temperature. The is less space for vapor condensation which hampers the evaporation-condensation cycle thus shows higher condenser temperature than other FR. Similar scenario is observed for the other working fluids also.
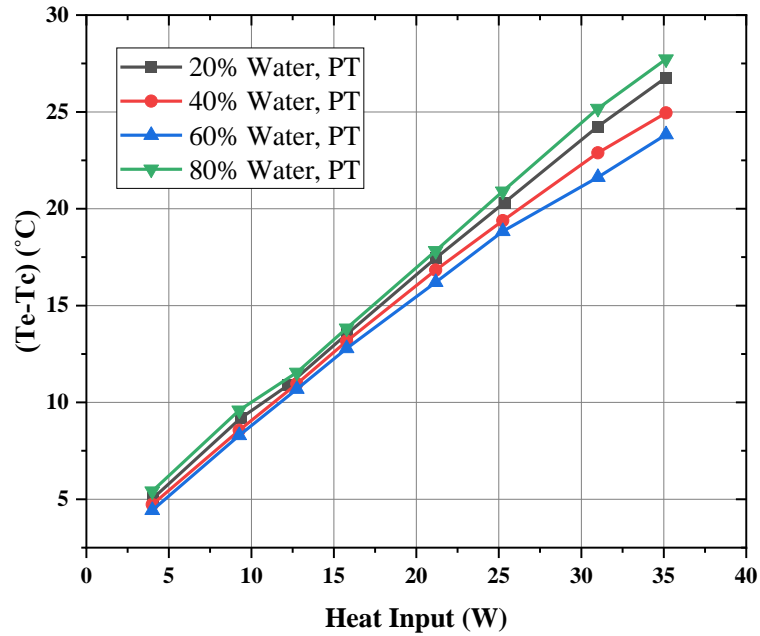
Figure 4.6: Te-Tc variation with various fill ratio with respect to Heat input

In Fig 4.6, the value of (Te-Tc) with respect to heat input are plotted with various fill ratio considering Fig. 4.2-4.5. It has been observed that the difference of temperature between the evaporator and condenser is increased with various fill ratio. For higher fill ratio of 80%, the value of (Te-Tc) is greater than other fill ratio which is because of less heat transfer between evaporator and condenser. Less available of space inside the CLPHP could not grow bubbles in adequate amount. For 20% fill ratio, presence of less mass in the CLPHP is not sufficient to provide better heat transfer. From this Fig 4.6, it is found that lowest temperature difference between evaporator and condenser region is obtained for 60% fill ratio that is optimum condition in this case.

4.2: Thermal Resistance of Various Working Conditions

From the temperature of evaporator and condenser region, thermal resistance can be calculated from Eq. 10. The calculated values of Ra, Rc and total resistance R is plotted against heat inputs in Fig 4.6 to Fig 4.9. Thermal resistance is the significant parameter to observe the thermal performance of any CLPHP. Heat transfer performance depends on the thermal resistance and lower thermal resistance is desirable for any CLPHP operation.

For dry run condition, Ra, Rc and R variation with respect to heat input are shown in Fig 4.6. Since there is no fluid present in the CLPHP for dry condition, Ra possess lower value than Rc. Temperature difference is less between evaporator and adiabatic

region than the adiabatic to condenser region. Heat is only transferred though the tube wall surface by conduction. Thermal resistance is almost same throughout the test.
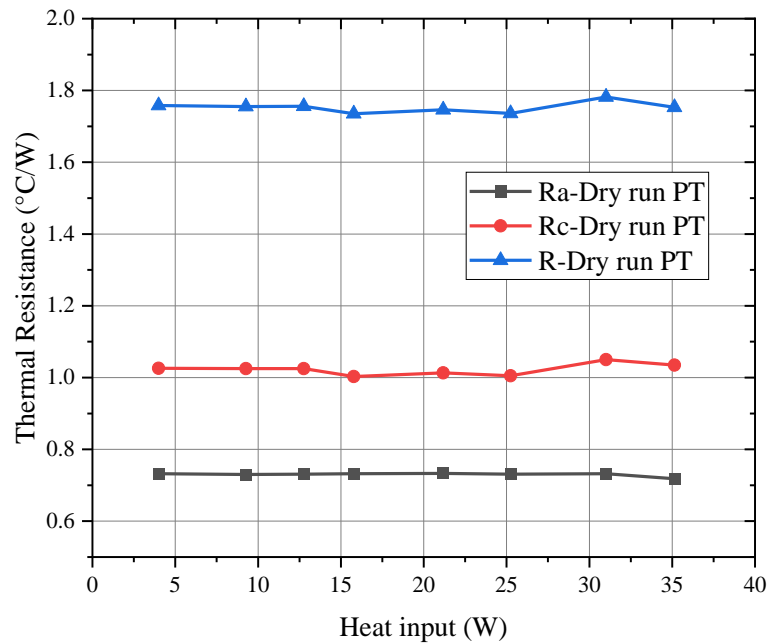

Figure 4.7: Variation of Ra, Rc and R of plain tube CLPHP (Dry run)

If working fluids are incorporated in the CLPHP, different observation is found. Considering Fig 4.7 to 4.9, it is noticed that Rc and Ra decreases against heat input gradually. Total thermal resistance R is the summation of Ra and Rc, is also decreased in value when heat input is increased. Rc is greater than Ra in almost all conditions which is obvious because condenser is responsible for the cooling which turns high temperature difference between adiabatic and condenser region. Total thermal resistance R drops quicker at lower heat input than higher heat. Initially the nucleate boiling rate in the CLPHP is high due to presence of adequate liquid in CLPHP which provides high pressure and density variance in the two regions. Pulsating action starts in the beginning of the experiments. Vapor-liquid slugs are able to move towards the condenser thus condensation is occurred. As heat input increases, surface temperature increment provides better condition for nucleation boiling but liquid content become lesser in quantity. As a result, the reduction rate of thermal resistance is slower.
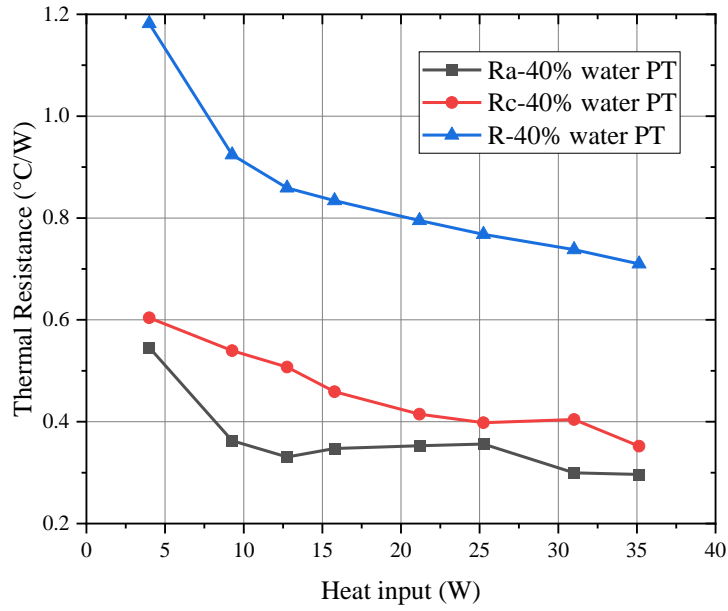
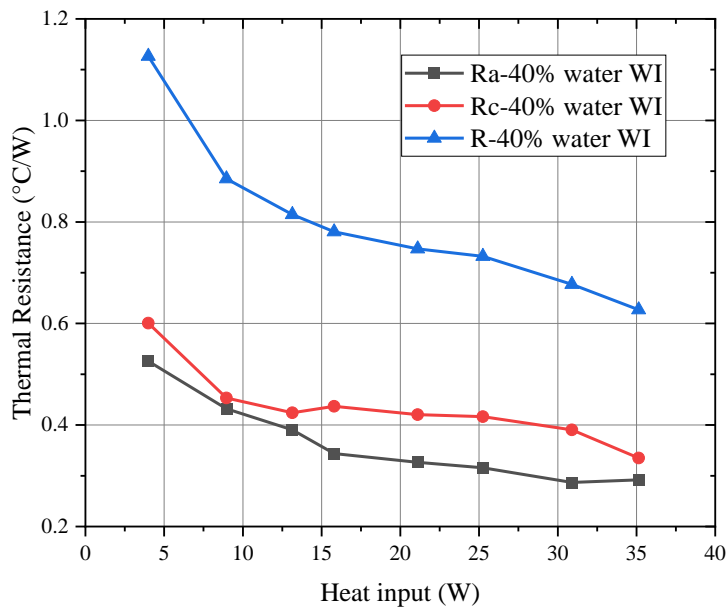**Figure 4.8:** Variation of Ra, Rc and R of plain tube CLPHP (WF: water, FR: 40%)

Figure 4.9: Variation of Ra, Rc and R of Wire insert CLPHP (WF: water, FR: 40%)
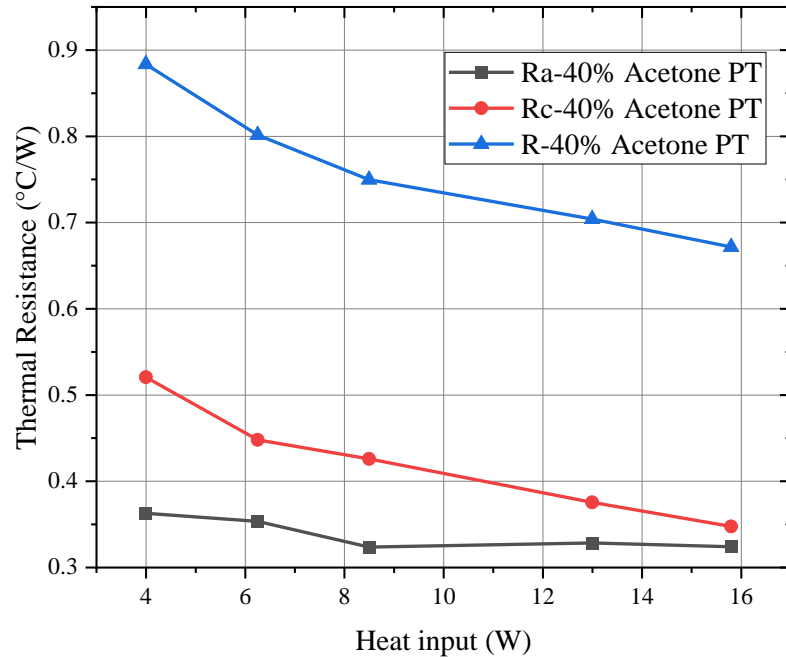
Figure 4.10: Variation of Ra, Rc and R of plain tube CLPHP (WF: acetone, FR: 40%)

In case of Rc, condensation is happened by collapse of bubble and by changing the phase from vapor to liquid. This is not happened in adiabatic region thus Rc showed larger value than Ra. Since adiabatic region situated close to evaporator and difference in temperature between these two regions remains low and steady.

Although heat loss in the adiabatic section is not desirable at all but fully adiabatic condition could not be obtained in actual. As a consequent, lower Ra is conserved between these two regions and gradually decreases at higher heat inputs shown for various fluids in figure 4.6-4.9. Similar trend can be obtained from other conditions and figures are given in the appendix III. As it is discussed that the thermal resistant R is inclusion of Ra and Rc so further study will be introduced on R only.

4.3: Effects of Fill Ratios on thermal performance

Study of thermal performance with varying fill ratios is oriented towards finding the optimal fill ratio for a PHP. Variation of temperature distribution curves and thermal resistance is necessary to understand the event. In this experiment, five fill ratios will be compared: 0% (dry run), 20%, 40%, 60% and 80%. Although, 0% fill ratio means there was no working fluid inside the tube, the other fill ratios were considered for the working fluids only. From the experimented data the following analysis has been illustrated with proper graphical representations.

4.3.1: Effects on Evaporator Temperature (T_e) for Various Fill Ratios

Fig. 4.10 to Fig. 4.12, illustrates the T_e distribution curve with respect to heat input of various fill ratios of different working fluids. Some representative graphs have been presented here. It is noticed from Fig. 4.10 that, T_e increases against heat input for various fill ratios of water in plain tube CLPHP because pressure in the evaporator will increase and boiling point will increase. FR 80%, possess high temperature against heat input. Since there is not enough space to intensify bubble growth due to nucleation boiling so, inadequate quantity of bubble will be formed. Besides, the more amount of liquid at 80% fill ratio requires greater amount of heat to start the pulsation. At 20% the T_e will locate under the 80% FR curve. The reason behind this occurrence is because the bubble growth rate is limited at low FR due to insufficient presence of liquid mass. Vapor-liquid presence is optimum for the 40% and 60% FR. Presence of liquid phase is adequate to continue proper nucleate boiling thus can maintain lower temperature in the evaporator throughout the tests. The differences in temperature of evaporator is visible after 10-15W heat inputs. Pulsating action may increase rapidly after that condition.
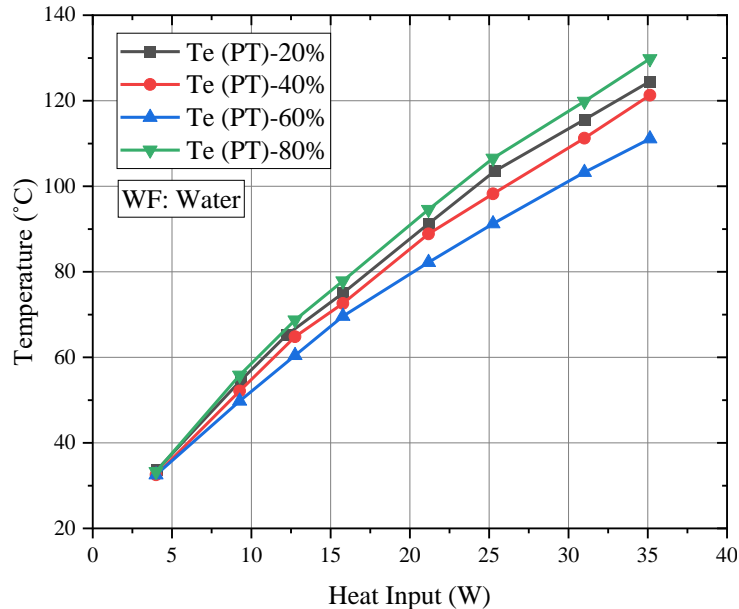

Figure 4.11: Variation in Te with water of different fill ratios on plain tube CLPHP
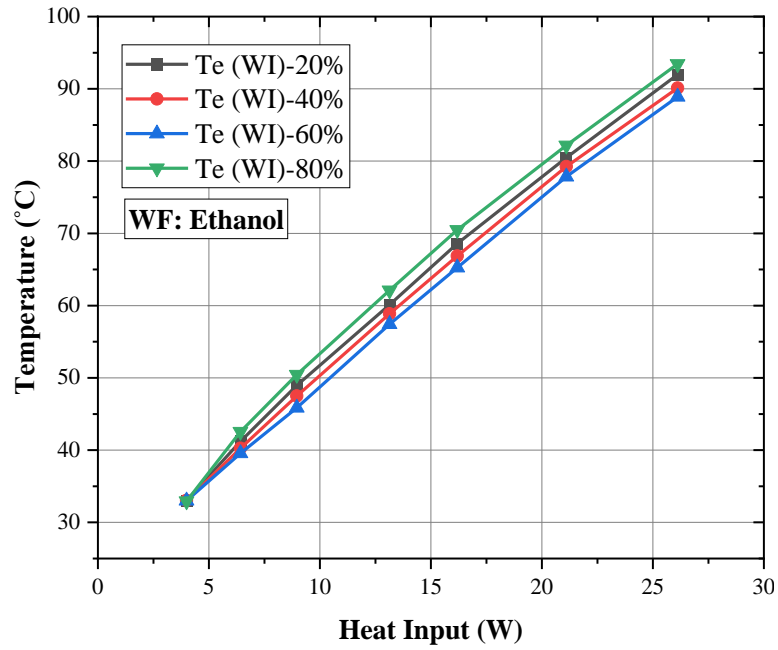
Figure 4.12: Variation in Te with ethanol of different fill ratios on wire insert CLPHP

The similar events are observed from the Fig. 4.11 and Fig. 4.12. In Fig. 4.11, ethanol is considered as working fluid for wire insert CLPHP. 60% FR shows minimal temperature of evaporator. The differences in temperature are visible after 10W. Pulsating movement is better for 60% FR and as a consequent, heat transfer is large.
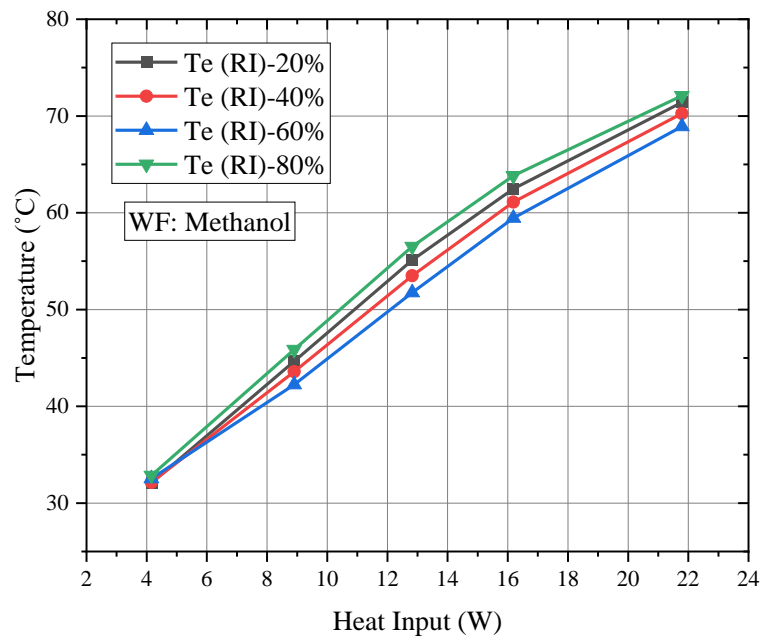

Figure 4.13: Variation in Te with methanol of different fill ratios on rosette insert CLPHP

Fig. 4.12 depicts the T_e distribution of methanol in rosette inserts. In this consideration, methanol shows increase in temperature steeper up to 16W for all FR and becomes flattens later. Since the boiling point of methanol is 64.7˚C, after reaching this temperature continuous bubble will form causes restriction in heat transfer. Similar trend can be obtained for other working fluids in different configuration are given in appendix C.

4.3.2: Effects of Filling Ratio on Thermal Resistance

Thermal resistance of Pulsating Heat Pipe is the key property for evaluation of thermal performance. Various fill ratios effect on thermal resistance are plotted against heat inputs. Thermal performance for working fluids operation is tested for 20% to 80% fill ratio increasing 20% steps. Detailed analysis study has been discussed for various conditions.

Fig 4.13 represents the thermal resistance of three CLPHPs for dry run conditions. Thermal resistance exhibits maximum value at this stage. There are no liquids (0% fill) inside the tubes, heat transfer took place only by conduction through the copper surface. However, when inserts are introduced, the thermal performance is increased slightly as inserts act like an additional conduction device.
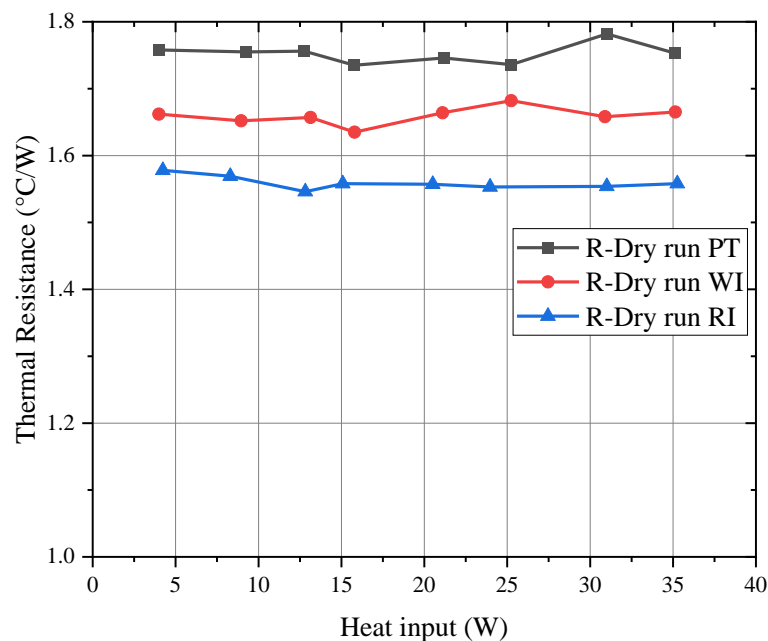

Figure 4.14: Variation of thermal resistance of dry run condition on different geometries of CLPHPs

Fig. 4.14 to 4.16 illustrates that thermal resistance for various fill ratio of ethanol. It is decreased when heat input increased. The decrement rate in CLPHP due to various fill ratio of working fluids, is expeditious up to 10W and becomes flatter at further heat input. This inspection is occurred due to lack of liquid mass presence at high heat input inside the CLPHP at high heat input.

Immediately after filling the CLPHP, the working fluid naturally distributes itself into various liquid vapor plug-bubble systems in a random fashion [31]. At low heat inputs, there are adequate amount of liquid presence in the tube thus initiates nucleation boiling at random nucleation sites in the evaporator sections. Variation of pressure and temperature between the condenser and evaporator region is generated and pumping actions of vapor-liquid plug become started. Further heat input provides sufficient temperature for the increment of nucleation sites thus bubble coalescence causes local void in the evaporator region [26]. This coalescence bubble will start to move towards the condenser region along with liquid slugs. Heat transfer occurred at higher rate at this time. Increase in nucleation sites agitates bubble growth in the evaporator region causes lack of liquid mass of working fluids. Latent heat transferring capacity reduces at high heat input and causes flatter curve of thermal resistance. The thermal resistance curves can be divided into two separate trend. From 4W to 10 W the value of thermal resistance drops quickly whereas it becomes flatter after 10W to rest. Since high heat input provides sufficient condition to increase the nucleation sites in the evaporator but low liquid inventory hinders in the bubble formation rate. As a result, less variation of thermal resistance is experienced. Similar explanation is valid for the plain tube and wire inserts CLPHPs also.

Although, thermal resistance decreases as heat input increases but different fill ratios of working fluids have showed different trend. For every PHP, an optimum working condition should be analyzed properly. It is observed from Fig 4.15 in plain tube CLPHP that higher fill ratio such as 80% ethanol retains higher value of thermal resistance compared to other. At high fill ratio, there is almost full area filled up with working fluids that causes minimum degree of freedom for vapor-liquid slug movement. Khandaker [29] also experienced such phenomenon. That means less degree of freedoms inside the CLPHP does not provide sufficient agitation to the bubble formations from the nucleation sites to a desired quantity. Inadequate bubbles could not perform better movement of the vapor-liquid slug thus higher thermal

resistance for this condition. Similar phenomena also explain the wire inserted CLPHP in Fig. 4.16
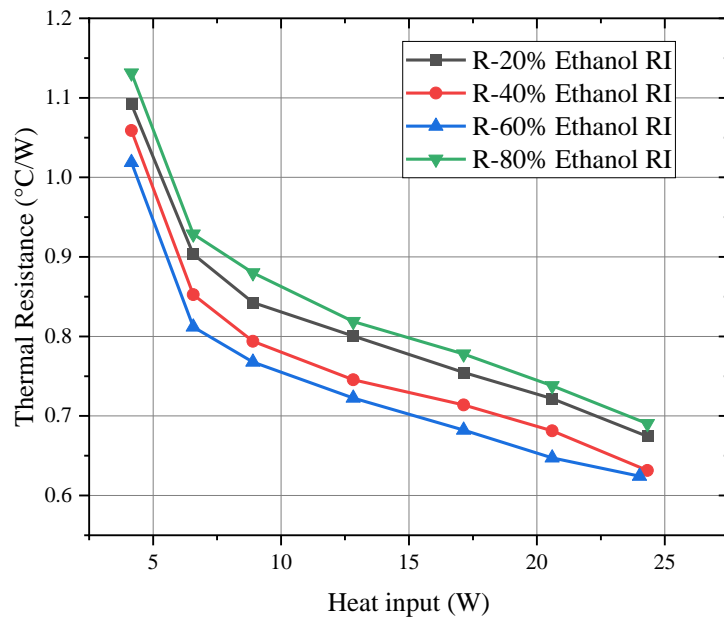

Figure 4.15: Variation of thermal resistance with various fill ratios of ethanol in rosette insert CLPHP.
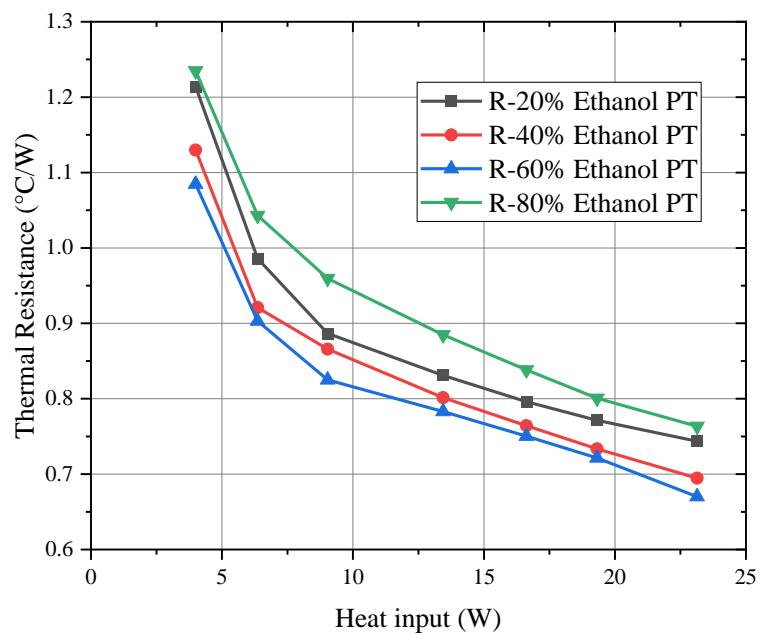

Figure 4.16: Variation of thermal resistance with ethanol of different fill ratio on plain tube CLPHP.

On the other hand, lower fill ratio such as 20%, the curve situated lower from the FR: 80% curve which is observed from the Fig 4.14. This fill ratio does not give the

lowest value of thermal resistance at all. Optimum working condition can be found for the 60% fill ratio where thermal resistance shows lowest thermal resistance. Besides, 40% fill ratio also performs better, close to 60% ratio. Yuwen [31] experienced that optimum fill ratio stays in between 40-70%. In this experiment 60% is obtained as optimum filling condition.

At very low fill ratio like 20%, there are little quantity of working fluid is present in the tube. Initially, the evaporator region provides sufficient heat to start nucleation boiling inside the CLPHP at low heat input. Thus, bubbles are formed rapidly at various nucleation sites inside surface which creates almost absence of liquid mass when the heat input is increased further. Due to low liquid mass in the tube, heat transfer occurred by the latent heat is not satisfactory at high heat input. Similar trend in thermal resistance is seen for 40% and 60% fill ratios. For 40% and 60% fill ratios, there are optimum amount of vapor liquid movement happened during operation which gives minimal value of resistance is obtained. In this case 60% fill ratio exhibits lowest value. The vapor-liquid slug presence condition provides sufficient liquid mass present inside the tube to continue the heat transfer loop properly.
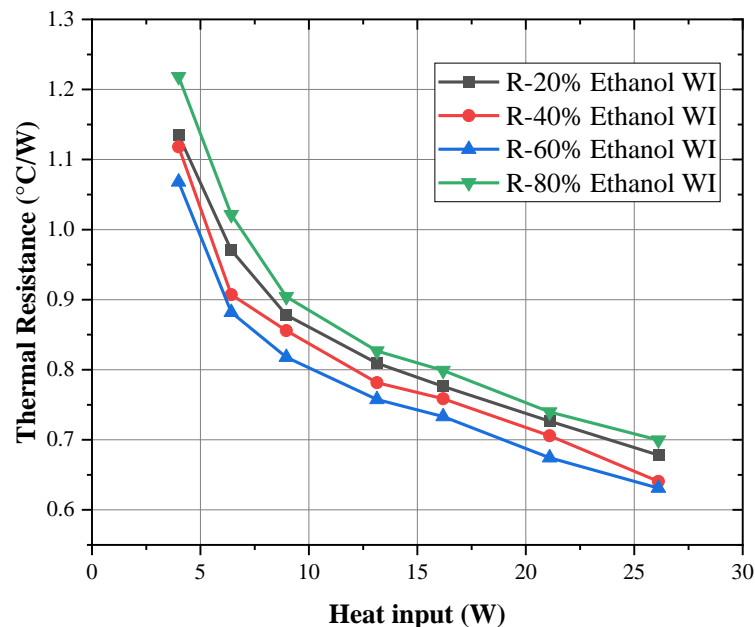

Figure 4.17: Variation of thermal resistance with ethanol of different fill ratio on wire insert CLPHP.

This phenomenon can be seen for the plain tube and wire inserts in Fig. 4.15 and Fig. 4.16. Zilong [14] experienced similar result in thermal resistance which brings our

61

characteristics result valid. Three different fluids (acetone, methanol and water) are also tested in three different conformations of CLPHPs and analogous curve patterns have been observed for various fill ratios of other fluids given in the appendix C.

4.4: Effect of Working Fluids on Thermal performance on CLPHPs

Various working fluids possess different properties which has a significant impact on PHP performance. In this section some representative conditions will be analyzed.

4.4.1: Effect of Working Fluids on Temperature distributions

From table 3.1, Acetone owns low specific heat (2.34 KJ/Kg ˚C) and latent heat (518 KJ/Kg) comparing to rest of fluids. Less heat is required for increasing the temperature of acetone liquids. Nucleation boiling will start earlier in acetone and exhibits lower evaporator temperature illustrated in Fig. 4.17. Although, Ethanol possesses lower latent heat (846 KJ/Kg) than methanol (1101 KJ/Kg) but ethanol exhibits higher evaporator temperature than methanol. It is because viscosity of methanol is lower than ethanol which increase the pulsating action than ethanol. On the other side, water having the highest latent heat (2257 KJ/Kg) and specific heat of (4.183 KJ/Kg ˚C) comparing the other fluids, it exhibits highest evaporator temperature. These properties having a great influence on the CLPHP performance significantly. So, the evaporator temperature is lower for methanol and acetone. Water possesses maximum latent heat and specific heat which delayed the nucleation boiling.
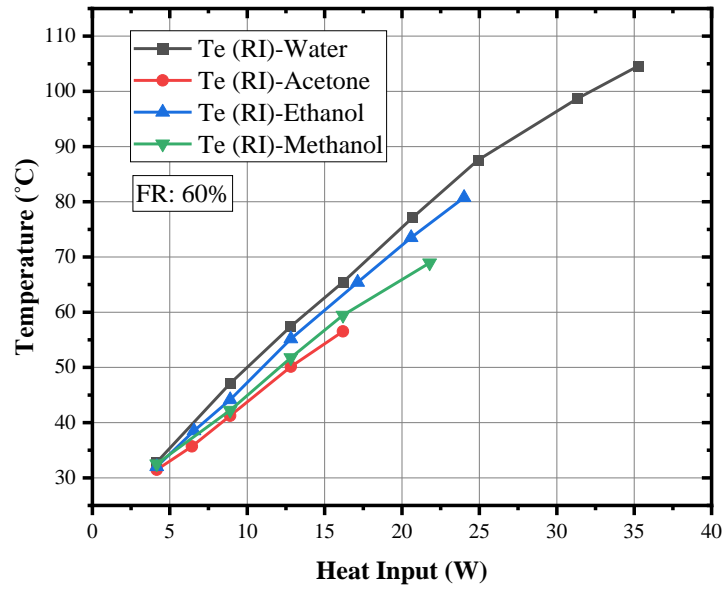
Figure 4.18: Variation of Evaporator temperature of different fluids on rosette insert CLPHP (FR: 60%)
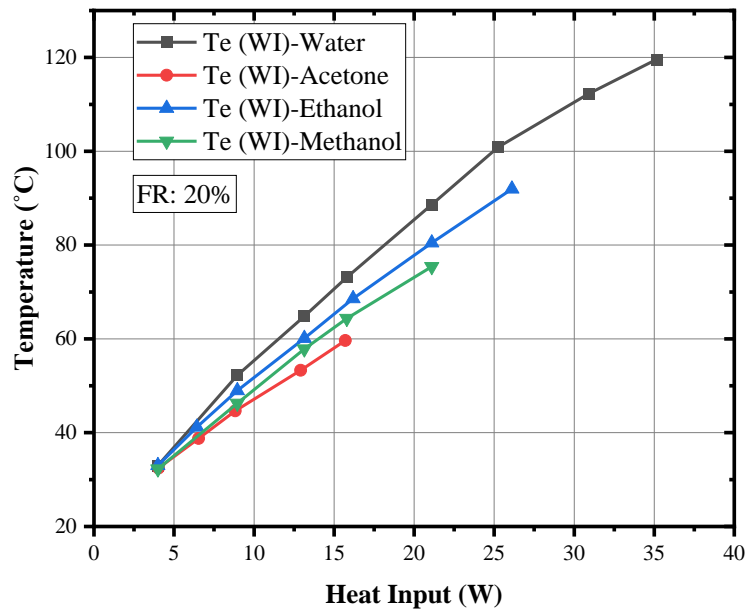

Figure 4.19: Variation of Evaporator temperature of different fluids on wire insert CLPHP (FR: 20%)

Fig. 4.18 presents the evaporator temperature of various liquids for wire inserts CLPHP of 20% FR. In this case, water shows higher temperature. High latent heat and specific heat delay in nucleation boiling. Ethanol shows slightly lower value than water due to Lower latent heat and specific heat than water. Methanol and acetone have an almost similar properties so it gives lowest temperature as much as possible. In case methanol ethanol, methanol exhibits lower temperature due to minimal

63

viscosity. Same analogous can be found for plain tube CLPHPs with 80% FR which is shown in Fig. 4.19.

4.4.2: Effect of Working Fluids on Thermal resistance

In this experiment, water, ethanol, methanol and acetone are considered for the tests. They possess variety of thermos-physical properties which can enhance thermal performance in a wide range. Fig. 4.20 represents the thermal resistance of rosette insert CLPHP with different working fluids against heat inputs at fixed fill ratio (20%). At 20% fill ratio the thermal resistance shows different curve trend. In rosette structure, the higher thermal resistance is found for water and lower value is achieved for acetone.

A relation can be established for thermal resistance as water>ethanol>methanol>acetone from the Fig. 4.20. Similar type of investigation is explained by Durga [27] that ratio of saturation pressure gradient to temperature, (dp/dT) and dynamic viscosity of working fluid define the pulsating nature of the working fluids.
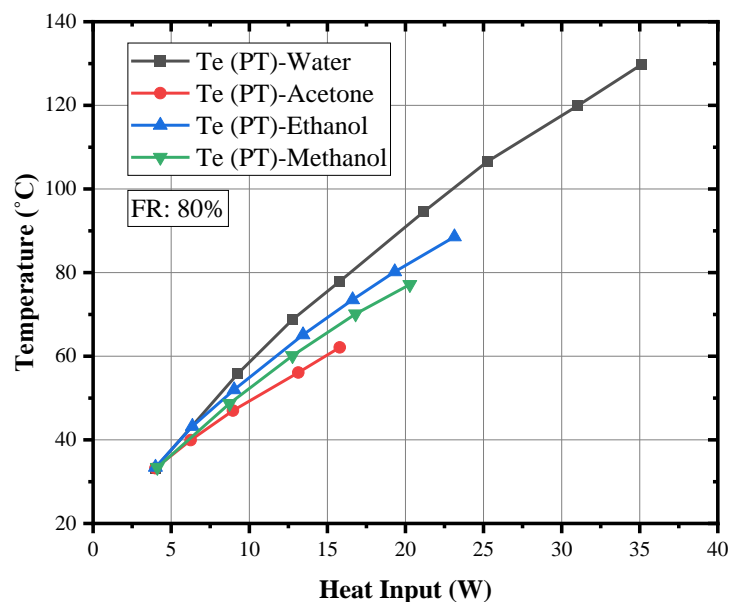

Figure 4.20: Variation of Evaporator temperature of different fluids on plain tube CLPHP (FR: 80%)
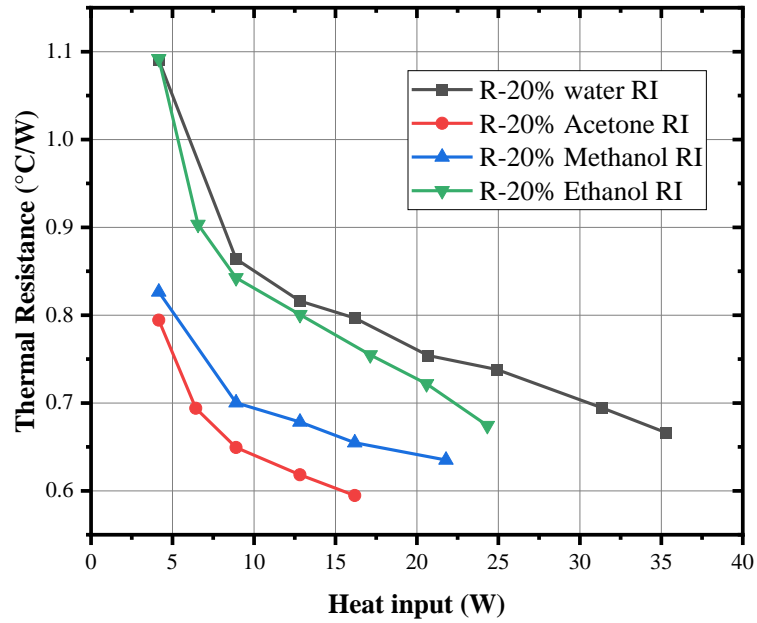
Figure 4.21: Thermal Resistance of various working fluids on rosette insert CLPHP (FR: 20%)

Shi [32] performed a test with acetone that helps to reduce thermal performance for higher (dp/dT) and low dynamic viscosity. Lower latent heat of liquids has an effect on CLPHP performance. Liquids having low latent heat requires less heating power to create nucleation sites for the bubble formations and early start-up of oscillating action.

Acetone having low latent heat, low dynamic viscosity and comparatively low saturation pressure gradient which makes the fluids to show better performance. Methanol and ethanol also perform preferable in this test. Ethanol owns a comparatively low latent heat than methanol, still methanol possesses low dynamic viscosity and pressure gradient contrast to ethanol. It means dynamic viscosity has an influence on thermal resistance. Water possesses higher latent heat and specific heat that require high heat to start working. As a consequent, it exhibits high thermal resistance. Similar results had been found by Babu and Reddy [33]. For the different filling ratio, similar event can be obtained represented in the Fig. 4.21 and Fig. 4.22.
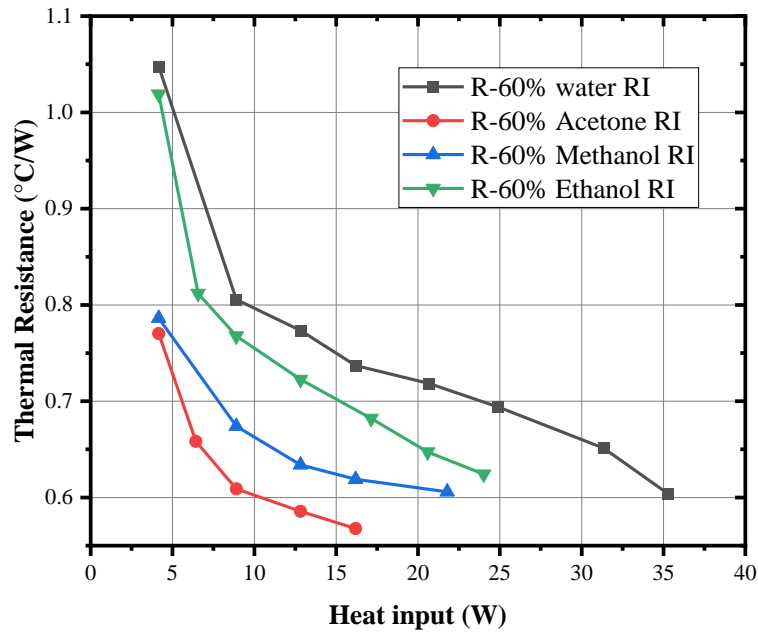
Figure 4.22: Thermal Resistance of various working fluids on rosette insert CLPHP
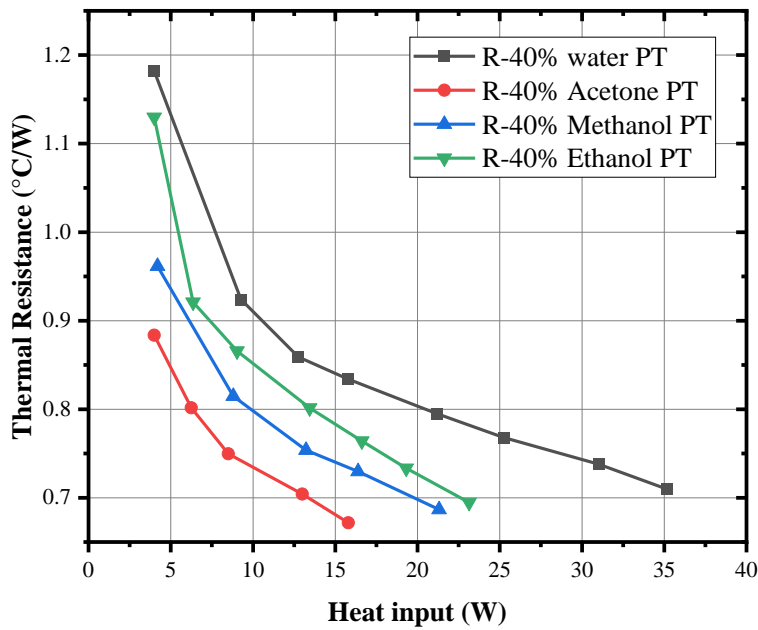(FR: 60%)

Figure 4.23: Thermal Resistance of various working fluids on plain tube CLPHP
(FR: 40%)

If plain tube and wire inserts CLPHPs are considered, almost equivalent curve representation can be observed for thermal resistance. Comparing these figures with rosette study, it can be concluded that modified inserts perform similar in these experiments. The curves pattern can be explained by the same analysis as discussed

above other configurations. Similar graphical depictions are given in the appendix C for various conditions.

4.5: Validation of thermal resistance

Experimented result of this test was compared with Rahman [11], B. Verma [34], H. Han [35,] KH Chien [36] who were conducted similar studies of plain tube and wire inserts investigations charged with water, ethanol and methanol. From Fig 4.23, it seems that the curves show similar trends. Rahman [11] experimented methanol and ethanol at 45˚ inclination of OLPHP with plain wire insert. Experimental value of this test shows better performance since design consideration is not identical for compared studies. So, experimental validity is situated within comparable limits.
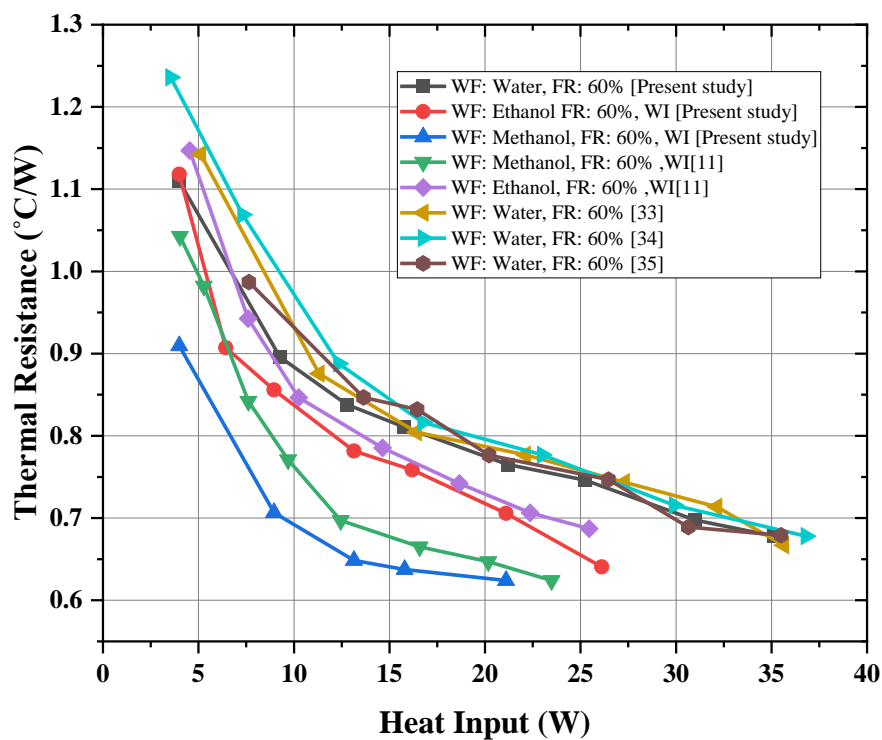
Figure 4.24: Validation of thermal resistance of present study with some previous studies

4.6: Comparative Study of Heat Transfer Phenomena of CLPHPs

In this investigation, a modified insert has been installed inside the CLPHP to study the thermal performance. The main idea of the modification of insert is to enhance the heat transfer performance of the CLPHP. However, a lot of experiment had been studied for plain tube and insert in CLPHPs. In this case, modified insert is designed as it could establish multimode of heat transfer within the PHP. Numerous nucleation

site can achieve to increase the bubble growth manner that could intensify the oscillating action of the PHP. It can be elucidated by following illustration.

4.6.1: Heat Flow Phenomena of Plain Tube and Wire Insert CLPHP

Fig 4.24 depicts a conventional CLPHP with no wire insert inside the capillary tube. When heat is applied to the CLPHP tube's outer wall, the temperature of the inner surface will increase also. Capillary tube is occupied by working fluids in random manner when it is charged partially. This heat will absorb by the working fluids from the inner surface of the evaporator and natural convection will occur at some extent (showed as green arrow). A few moments later, continuous convection heat transfer will rise the temperature of the fluids greater than saturated temperature and nucleate boiling will be started.
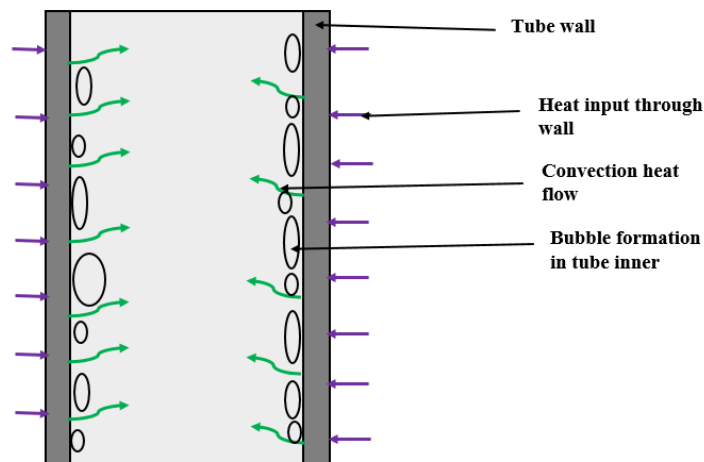

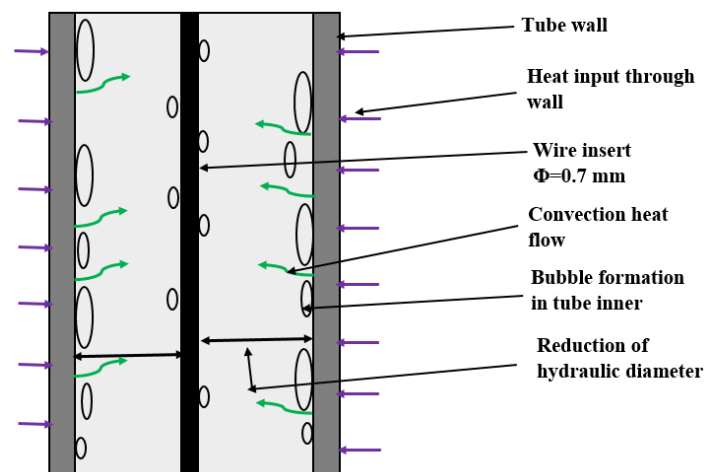**Figure 4.25:** Heat transfer phenomena in plain tube CLPHP

Figure 4.26: Heat transfer phenomena of wire insert CLPHP

Consequently, bubbles will be formed in the heat transfer surface and breaks away into small series of bubble then carried to the main stream of fluids. Certainly, large bubble will be formed when the bubble growth rate is high. The large bubble will create a pressure difference within evaporator and condenser region and movement of vapour-liquid slug will be started towards the condenser region. The similar heat transfer phenomena are experienced to the wire insert CLPHP shown in Fig. 4.25 In this case the net hydraulic diameter is reduced that causes the increase in surface tension of vapour-liquid slugs. As a result, overall oscillation will increase that improves the heat transfer rate in the CLPHP.

4.6.2: Heat Flow Phenomena of Rosette Insert CLPHP

In this experimental study, a modified insert geometry looks like a rosette is made with copper wire which is installed right in the centre of the CLPHP. The heat transfer concept is illustrated in Fig 4.26. When the heat is applied to the evaporator (showed as violet arrow) of CLPHP, heat will transfer to the inner surface of the tube by conduction. Working fluid present inside the capillary tube will absorbs heat from the inner surface.
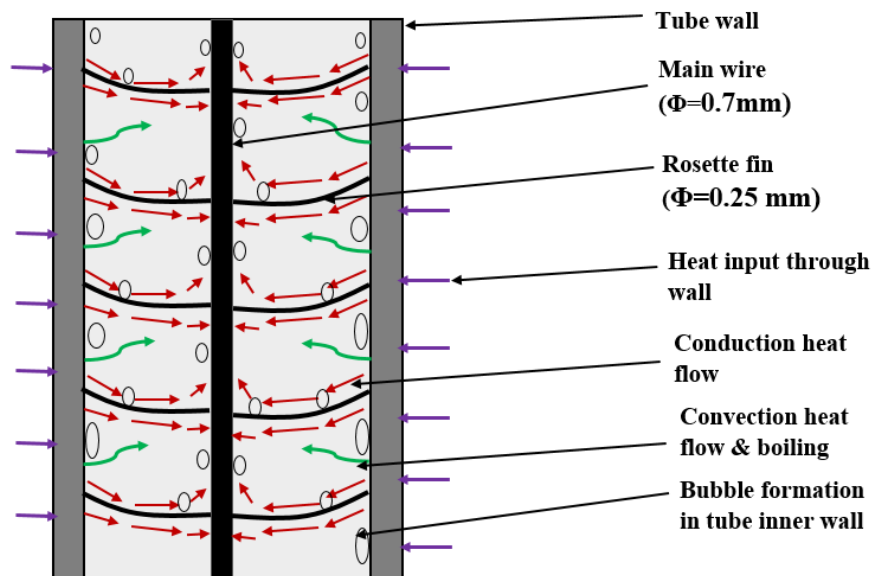

Figure 4.27: Heat transfer phenomena in evaporator of rosette insert CLPHP

In this case heat will be transferred by convective and boiling mode (showed as green arrow). After some extent, nucleate boiling will start in the CLPHP inner surface. Consequently, bubble will form at the heat transfer surface and then break away. This

small bubble will carry into the main stream of the working fluid to form a large bubble in the capillary tube. An addition of rosette inserts in the CLPHP, rosette will establish a conductive heat flow (shown as red arrow) in between the rosette fin wire and the inner surface of CLPHP. Conductive heat transfer will occur to the main wire of rosette structure through rosette fin. Average temperature will increase of the fluids adjacent to the main wire in the middle of the CLPHP. As a result, bubble growth rate will increase significantly.

The aforementioned discussions and graphical representations of the thermal resistance concise the research summery like that, the addition of conduction as well as convection heat transfer in the rosette structure could improve the thermal performance of the CLPHP significantly. The multimode heat transfer phenomenon is the prime cause for this improvement.

Fig. 4.27 illustrates the heat dissipation phenomenon from condenser region for the three CLPHPs. Since rosette will increase the nucleation sites in the evaporator than wire and plain configurations, so small sized bubble will be formed in the evaporator and could not coalescence large bubbles due to rosette. This large quantity bubble will move to the condenser where rosette will act as heat dissipating fin structure inside. It will dissipate large amount of heat from the large quantity bubbles and turns into liquid slugs in condenser. Here the small wires in the rosette will dissipates heat by conduction and convection (multimode) from maximum region of vapor-liquid slugs through condenser surface and condenses. When only wire is inserted the heat dissipation active points will lower than rosette and bubble size present in the condenser will be moderate due to less nucleation sites in the evaporator. Consequently, it will get more free space to coalescence comparatively big size bubble. Conventional plain will dissipate heat at minimum rate due to large sized bubble presence and less active heat dissipation area in condenser.
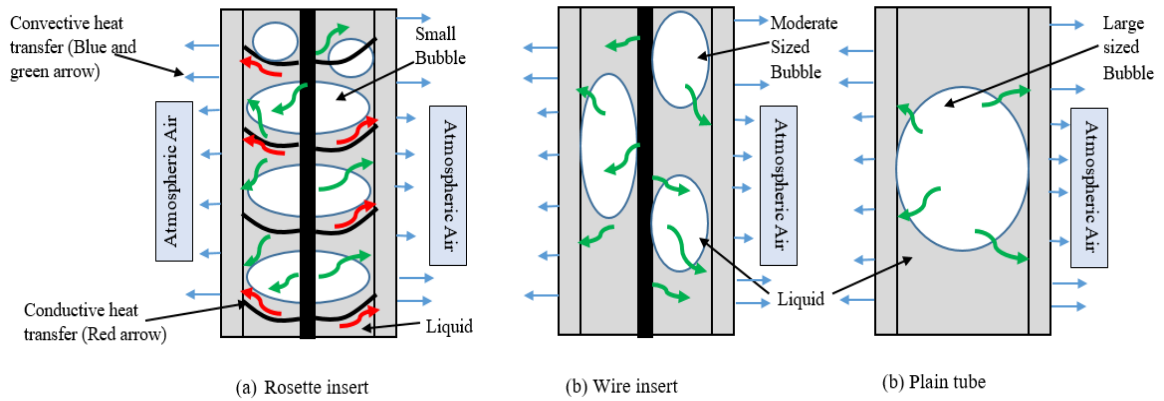
Figure 4.28: Heat dissipation phenomena in condenser (a) rosette insert (b) Wire insert (c) plain tube

4.7: Comparative Study for Rosette Insert CLPHP

It has been analyzed that modified insert like rosette could improve the thermal performance of the CLPHP. A comparative investigation has been made for the thermal performance of rosette insert CLPHP. The comparison is done with the no wire insert and wire insert CLPHP. Effects on the thermal performance and temperature distribution due to various CLPHP construction geometries with various working fluids have been discussed. Four different fluids (acetone, ethanol, methanol and water) are utilized for this test. These working fluids possess a variety of different properties itself. These fluids property have influences to the oscillating action in CLPHP.

4.7.1: Effects of various fluids on evaporator temperature

From Fig. 4.28, the variation of the evaporator temperature for three CLPHPs: plain tube (PT), wire insert (WI) and rosette insert (RI) has been shown when 40% of water is considered. At a lower heat input, the effect of fluids is not clear as differences in evaporator temperatures are marginal. But with the increase in heat input, the effect on evaporator temperature becomes visible. The maximum average temperature variation of evaporator is recorded as 110˚C (rosette insert), 115˚C (Wire insert) and 121˚C (plain tube) at 35W.

The presence of rosette fin in the rosette insert CLPHP maintains a lower temperature in the evaporator region with respect to heat input compared to other CLPHPs. The addition of rosette in the CLPHP provides a conductive mode of heat transfer from the

inner surface of the capillary tube, which increases the possibility of creating nucleation sites in the liquids at the centre of CLPHP. This heat is passed through the main wire of the rosette to the adiabatic and condenser region also adjacent fluids of the main wire take heat from it. Nucleation boiling is started earlier in the evaporator region than the wire inserts and plain tube CLPHPs. Consequently, more bubbles formation and growth in the rosette insert CLPHP will occur in the evaporator region, resulting in maintaining a lower temperature in the evaporator region.

If plain tube and wire insert CLPHPs are compared, wire insert shows lower temperature from the plain wire CLPHP. The hydrodynamic diameter of wire insert CLPHP is less compare to plain tube CLPHP. The reduction of hydrodynamic diameter causes high capillary pressure in the wire inserted CLPHPs. The fluid movement increases due to capillary pressure increases as compared to plain tube CLPHP. When the bubble gets collapsed at the condenser region, it returns to the evaporator through the inserted wire due to the wick action of wire.
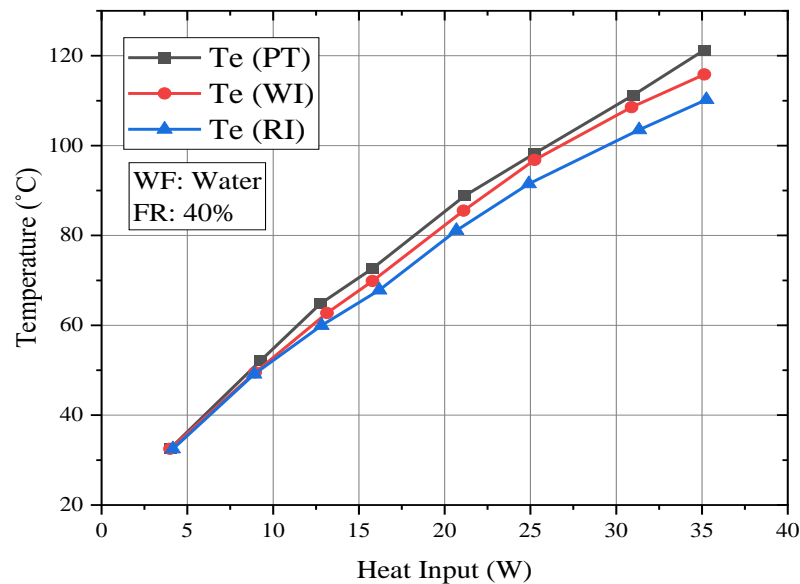
Figure 4.29: Effect of evaporator temperature in three different configuration of CLPHPs (WF: water, FR: 40%).
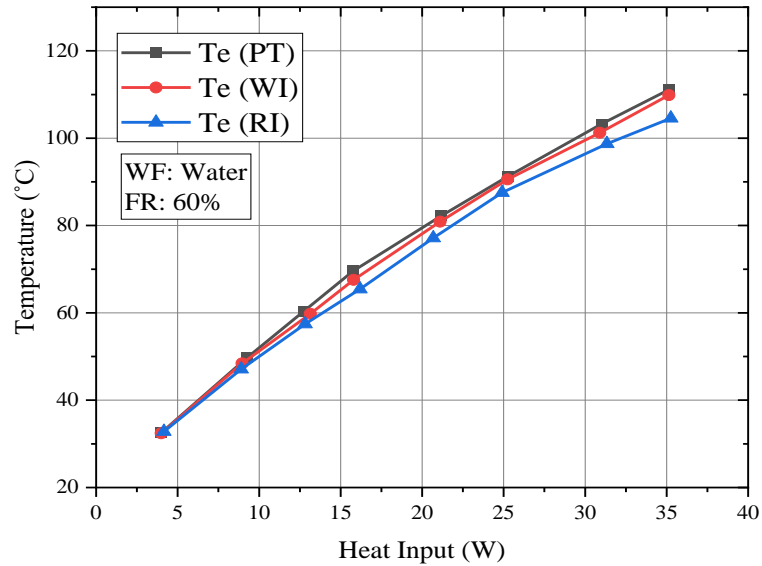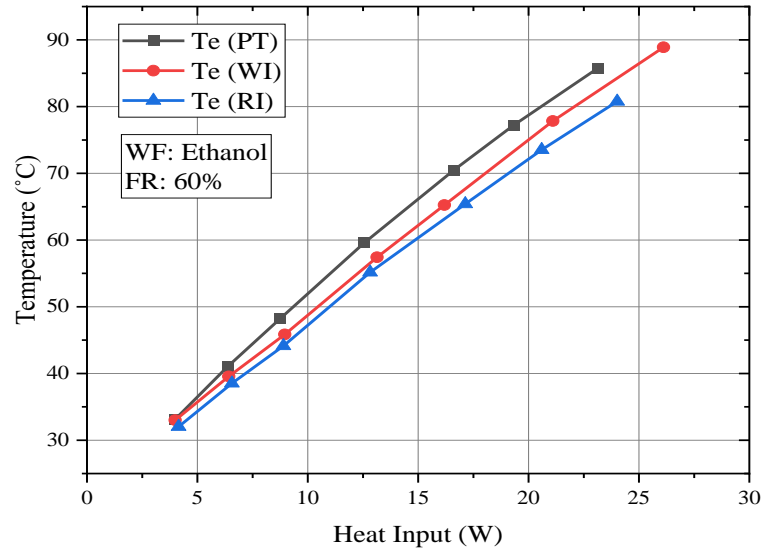
Figure 4.30: Effect of evaporator temperature in three different configuration of CLPHPs (WF: water, FR: 60%).

Similar observation has been found for the 60% fill ratio of water illustrated in Fig 4.29. Maximum evaporator temperatures during this experimental text of this condition are found as 111°C (for plain tube), 109°C (for wire insert) and 104°C (for rosette insert). In that case, liquid inventory inside the CLPHP becomes high which shows lower temperature than 40% fill ratio. After the filling of fluids, the liquids are orientated as vapour liquid slug in the capillary tube due to saturation temperature to pressure gradient of fluids. This optimum orientation for the boiling effect is observed for this fill ratio. After starting the heat input, the fluids change its orientation due to convective heat transfer from the tube inner wall. Further increase of heat in the evaporator creates nucleation sites for bubble growth which is found better for 60% fill ratios. More nucleation sites are formed at this condition thus large amount of heat transfers occur from the evaporator and dissipates in the condenser region as well. At 20% and 80% fill ratio, the similar trend in temperature curves is obtained showed in appendix C. For both case, rosette could maintain the low temperature from the other two CLPHP structures.

If different working fluid is considered for the same analysis on the three CLPHPs, the variation of evaporator temperature for ethanol, methanol and acetone are illustrated in Fig. 4.30 to Fig. 4.32. It is noticed that the temperature increases with respect to heat input as like water. The difference for different CLPHP structures is less at low heat input and becomes larger for further heat input. For acetone of 60%

fill ratio in Fig 4.30 depicts that the rosette insert CLPHP can maintain lower evaporator temperature from the plain tube and wire inserted CLPHPs. Since acetone possess low latent heat so, less amount of heat is required for evaporation. The similar phenomena as discussed before is responsible for this reason. Rosette insert CLPHP has reduced about 4% of overall temperature in the evaporator region than wire insert CLPHP. However, wire insert lowered 6% overall temperature from the plain tube CLPHP for acetone.
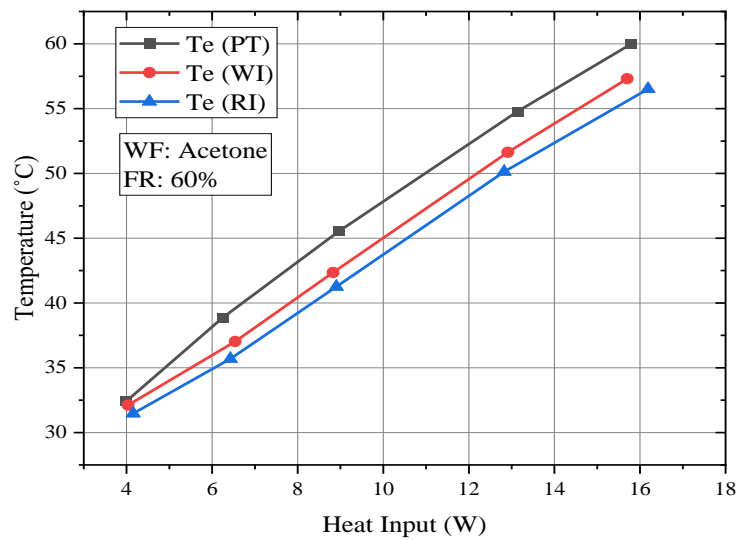
Figure 4.31: Effect of evaporator temperature in three different configuration of CLPHPs (WF: acetone, FR: 60%).

From Fig. 4.31, the variation of ethanol shows same trend in temperature curve while maximum variation is found at high heat input. In case of rosette insert CLPHP, high heat input increases the number of nucleation sites in the CLPHP and more isolated bubbles takes latent heat from the evaporator inner surface thus provides maximum temperature reduction. Wire insert could not perform like rosette. Here rosette fin provides a better heat transfer by conduction mode than wire and plain tube CLPHPs.

Figure 4.32: Effect of evaporator temperature in three different configuration of CLPHPs (WF: Ethanol, FR: 60%).
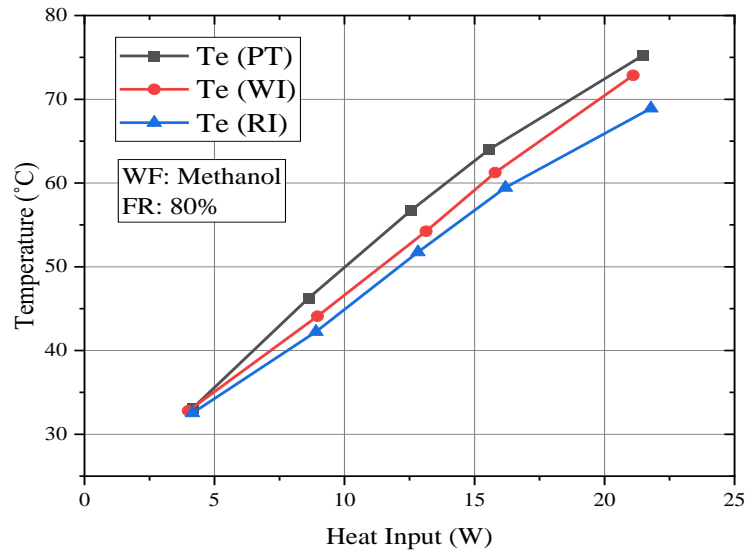

Figure 4.33: Effect of evaporator temperature in three different configuration of CLPHPs (WF: Methanol, FR: 80%).

Analogous performance and trend are obtained for methanol. Since acetone, ethanol and methanol possess low latent heat, specific heat as compare to water so, the temperature variation can be visible at low heat input. In Fig. 4.32, it is seen that the evaporator temperature curves of 80% methanol for different CLPHPs. Rest of the similar figures are given in appendix C.

4.7.2: Comparative Study of thermal resistance of rosette insert CLPHP

It has been elucidated that; the rosette can intensify the nucleation boiling effortlessly in CLPHP that provides more pulsating action. In Fig. 4.34 to Fig. 4.36, the comparison of thermal resistance curves of rosette insert CLPHP to the plain tube and wire inserts CLPHP is observed. Lutfur [11] experienced that, the thermos-physical properties of the working fluid coupled with the geometry of the device have profound implications on thermal performance of CLPHP. It is noticeable from the figures that, the thermal resistance is significantly lowered for the rosette insert CLPHP from plain tube and wire insert CLPHPs. Rosette fin in the CLPHP assists to transfer heat by conduction from the tube inner surface to the rosette primary wire along with convection heat transfer of tube wall and fluids.
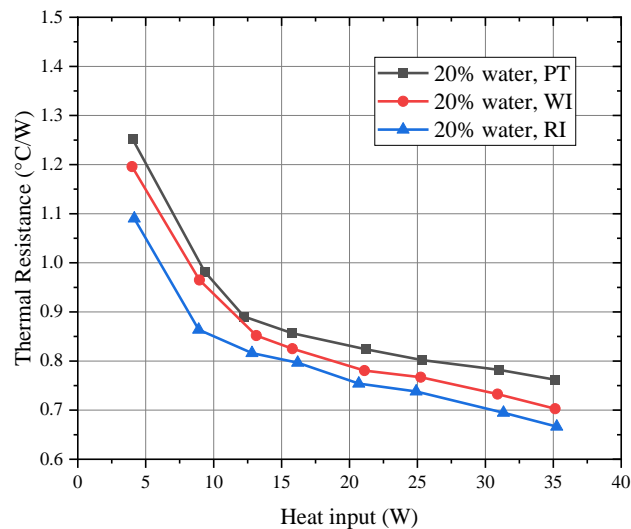
Figure 4.34: Variation of thermal resistance in plain tube, wire insert and rosette insert CLPHP (WF: Water, FR: 20%)

Although the thermal resistance is lower for rosette and wire insert CLPHP from the plain tube but the decrement rate is not uniform for various working fluids. Differences of properties for the working fluids are responsible for it. Additionally, CLPHP inserts will exhibit shear stress to the working fluids due to inserts. Since the flow is two-phase condition, the change in overall viscosity may affect in performance of inserts structure CLPHPs.
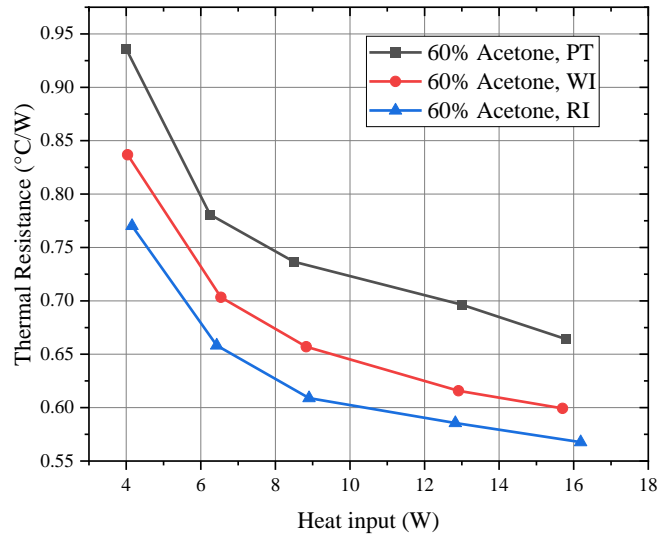
Figure 4.35: Variation of thermal resistance in different CLPHPs (WF: Acetone, FR: 60%)
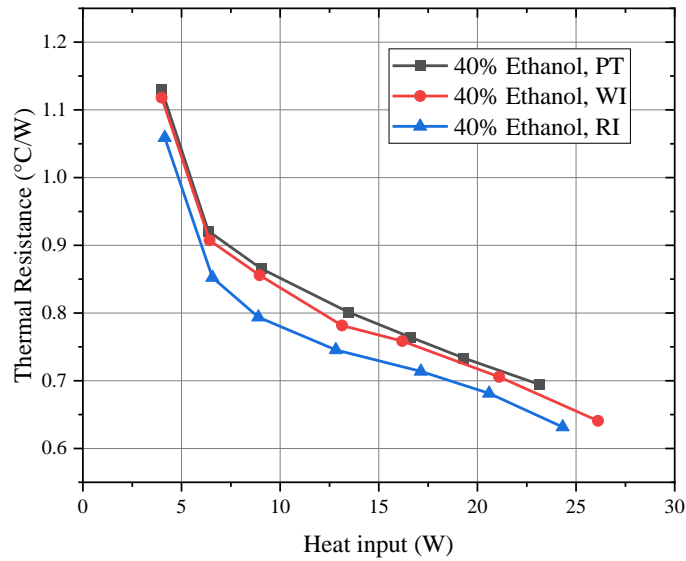

Figure 4.36: Variation of thermal resistance in different CLPHPs (WF: Ethanol, FR: 40%)

As a consequent, the nucleation boiling starts earlier than the plain and wire inserted CLPHPs. Formation of bubbles will be started earlier in rosette insert CLPHP resulting to maintain lower temperature in the evaporator region. Moreover, the condenser will dissipate heat from the working fluid at escalated rate which provides low temperature difference between evaporator and condenser region in rosette insert CLPHP. So, the thermal resistance becomes lower and shows high heat transfer.

Thermal resistance reduction rate is steeper at the beginning of the heat input and slower after some extent. Initially, the presence of liquid inventory in the CLPHP is

adequate quantity which starts nucleation boiling at the heat transfer surface of tube wall and large quantity of bubble will form from the liquid mass. As heat input increases further, the liquid mass becomes less quantity and lower abatement in thermal resistance is seen.

The reduction rate is not uniform for different working fluids. Table 4.1 is given for the reduction rate of the above figures.

Table 4.1: Reduction rate of thermal resistance for rosette insert CLPHP

Structure name	Comparable structure	Maximum decrement	Minimum decrement	Fill ratio
Rosette inserts	Plain tube	20% up to 12W	5% after 15W	FR:20%, WF: Water
	Wire inserts	15% up to 13W	7% after 15W	FR:20%, WF: Water
	Plain tube	16% after 10W	14% up to 8W	FR:60%, WF: Acetone
	Wire inserts	7% after 10W	5% up to 8W	FR:60%, WF: Acetone
	Plain tube	9% up to 15W	6% up to 5W	FR:40%, WF: Ethanol
	Wire inserts	8% up to 10W	2% up to 5W	FR:40%, WF: Ethanol

A conclusion can be drawn from the above table that an overall decrement of thermal resistance is approximately 10% for rosette with respect to plain tube and 7% decreases with respect to plain wire tube.

4.8: Performance Comparison of Thermal Resistance of Different Fluids

In Figs 4.36-4.38, the comparisons to find the optimum fill ratio and effective working fluids based on PHP performance. These comparisons could help to achieve the better geometry for the PHP operation along with the effective fill ratio and working fluid. In Fig 4.36, thermal resistance for the working fluids of 40% fill ratios is showed for all conditions. Fluids that possess high latent heat of evaporations, high

dynamic viscosity and high specific heat like water and ethanol showed high thermal performance. Comparatively lower latent heat, dynamic viscosity and specific heat working fluids such as methanol and acetone exhibits lower thermal resistance. Where insert of wire and rosette helps to improve the performance from plain tube. Comparing the rosette insert and wire insert with plain tube CLPHPs, rosette inserts showed lower thermal resistance due to multimode (Both convection and conduction) heat transfer. It is also noticeable that the thermal resistance decreases rapidly up to 10-12 W for acetone and methanol, 15W for water and ethanol. The decrement rate becomes slower for further heat input. For 40% fill ratio, the thermal resistance rating is found for low heat input as follows:

$(Water)_{PT}>(Water)_{WI}>(Ethanol)_{PT}>(Ethanol)_{WI}>(Water)_{RI}>(Methanol)_{PT}>(Ethanol)_{RI}>>(Methanol)_{WI}>(Acetone)_{PT}>>(Acetone)_{WI}>(Methanol)_{RI}(Acetone)_{RI}$

When heat input increases, the relation becomes:

$(Water)_{PT}>(Water)_{WI}>(Water)_{RI}>(Ethanol)_{PT}>(Ethanol)_{WI}(Methanol)_{PT}>(Ethanol)_{RI}>>(Acetone)_{PT}>(Methanol)_{WI}>(Methanol)_{RI}>(Acetone)_{WI}>(Acetone)_{RI}$
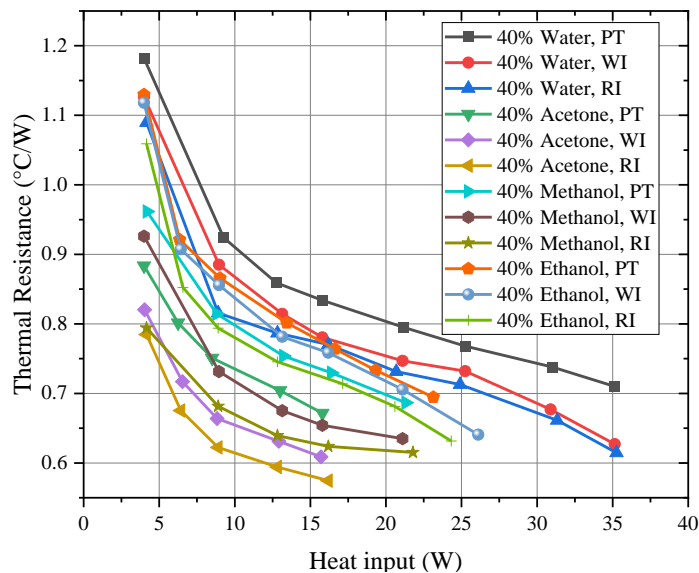

Figure 4.37: Thermal resistance of various working fluids (FR 40%) in different configuration of CLPHP
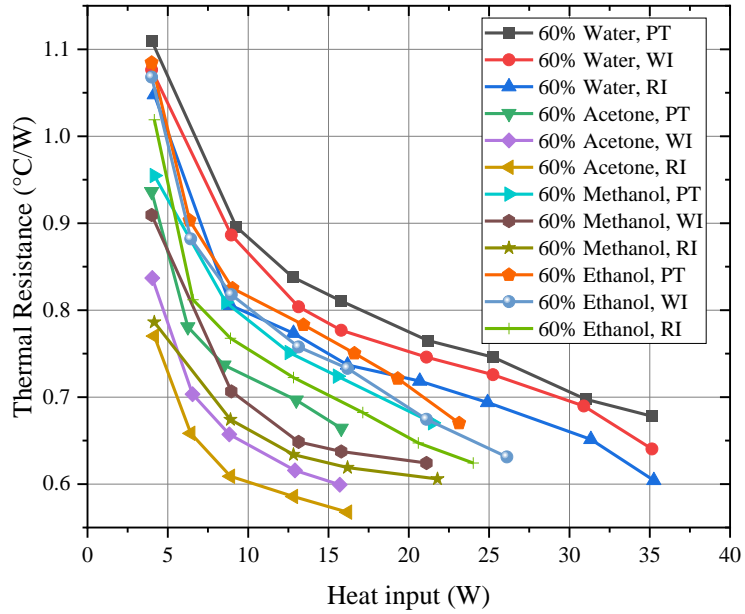
79

Figure 4.38: Thermal resistance of various working fluids (FR 60%) in different configuration of CLPHP

Similar phenomena can be observed for the various working fluids with 60% filling ratio in Fig. 4.37. Acetone in rosette insert CLPHP shows better thermal performance among all configurations. Acetone possess low latent heat of evaporation, low viscosity, specific heat that requires less heat to start the nucleate boiling which is the prime reason for showing low thermal resistance. Moreover, rosette agitates to start the nucleate boiling as well.

For 60% fill ratio, the thermal performance for various fluids can be related at low heat input as follows:

$(Water)_{PT} > (Water)_{WI} > (Ethanol)_{PT} > (Ethanol)_{WI} > (Water)_{RI} > (Methanol)_{PT} > (Ethanol)_{RI} >$ $> (Methanol)_{WI} > (Acetone)_{PT} > > (Methanol)_{RI} > (Acetone)_{WI} > (Acetone)_{RI}$

When heat input increases, the relation becomes like:

$(Water)_{PT} > (Water)_{WI} > (Water)_{RI} > (Ethanol)_{PT} > (Ethanol)_{WI} > (Methanol)_{PT} > (Ethanol)_{RI} >$ $> (Acetone)_{PT} > (Methanol)_{WI} > (Methanol)_{RI} > (Acetone)_{WI} > (Acetone)_{RI}$
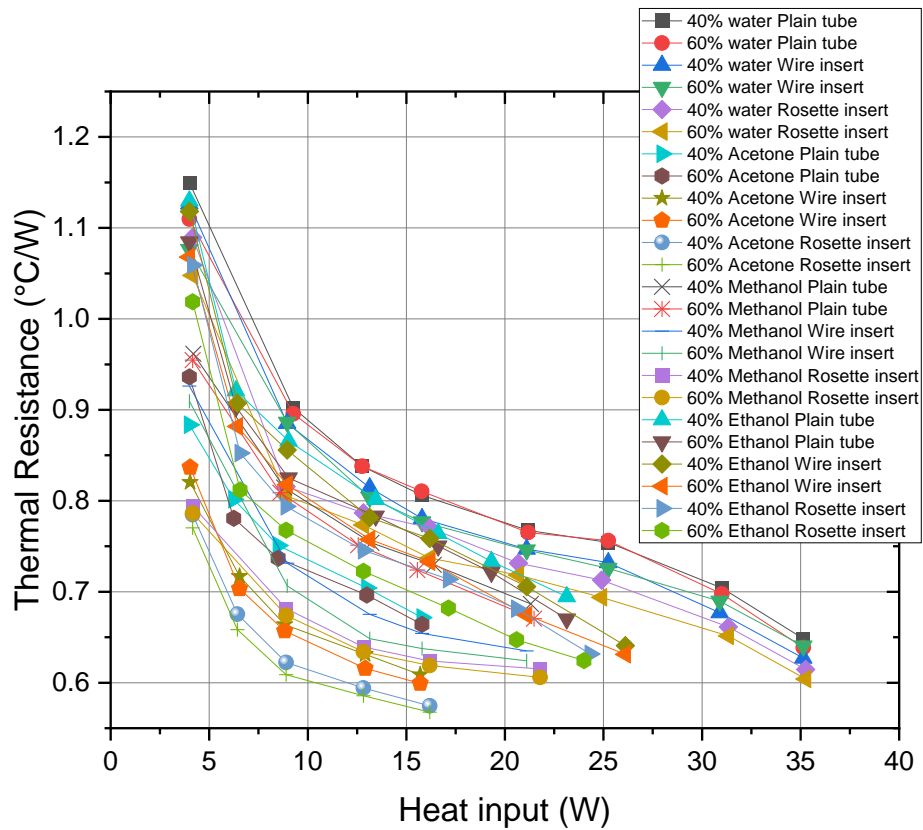
Figure 4.39: Thermal resistance of various working fluids (FR 40% & 60%) on no wire insert, wire insert and rosette insert CLPHP

Considering both fill ratio in Fig. 4.38, it is observed that acetone with 60% fill shows the lowest thermal resistance in a rosette configuration. Multimode heat transfer improves thermal performance. Although acetone with 40% fill also indicates better performance with rosette configuration. Low latent heat and low viscosity with low specific heat play a meaningful impact on the performance as well as multimode heat transfer due to rosette.

CHAPTER 5: DIMENSIONAL ANALYSIS

A dimensional analysis on thermal resistance is very complicated and difficult to perform. As variable increase the mathematical terms starts to be more complicated. In the previous chapter, it has been clearly shown and discussed that the thermal resistance of the CLPHP is significantly depends on the fluid properties such as latent heat of evaporation (h_{fg}), surface tension (σ), specific heat $(Cp_l,)$, viscosity (μ_l), conductivity (k_l) and finally vapor and liquid density(ρ_v, ρ_l) The temperature differences of the condenser and evaporator region is also has an effect on the thermal resistance. In addition, an insert inside the CLPHP showed significantly change of thermal resistance as well.

Now, an analysis can be carried out to find the dimensionless diameters that affects the thermal resistance of the CLPHP. In that case, the characteristics diameter for insert is considered as D_e which could be illustrates in the following Fig. 5.1.
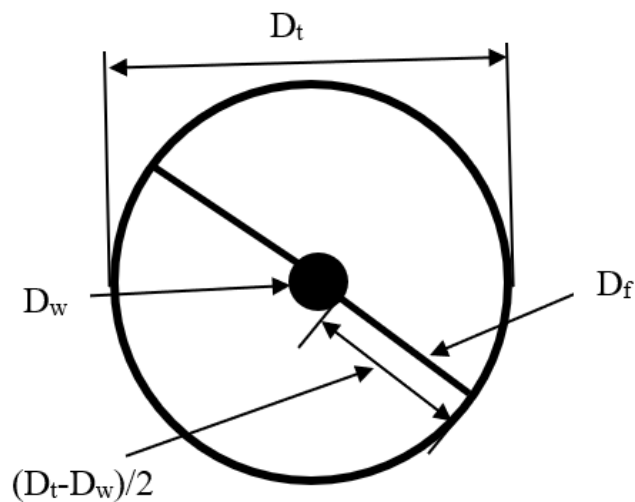
Figure 5.1: Cross-sectional view of rosette inserts in CLPHP

Assuming the tube inner diameter is D_t, main insert wire diameter, D_w, fin diameter is D_f and the characteristics diameter of the tube after rosette inserts D_e. The area of fin wire will be $\frac{D_t - D_w}{2}$ on each side of the main wire. Therefore, the effective diameter D_e can be obtained by the following equations:

$$\frac{\pi D_e{}^2}{4} = \frac{\pi D_t{}^2}{4} - \frac{\pi D_w{}^2}{4} - (D_f \times 2 \times \frac{D_t - D_w}{2})$$

$$\frac{\pi D_e{}^2}{4} = \frac{\pi D_t{}^2}{4} - \frac{\pi D_w{}^2}{4} - \frac{4\pi \ (D_f \times (D_t - D_w))}{4\pi}$$

$$D_e{}^2 = D_t{}^2 - D_w{}^2 - \frac{4}{\pi}\overline{D}$$

Let assume, $\overline{D} = D_f \times (D_t - D_w)$;

$$D_e{}^2 = D_t{}^2 - D_w{}^2 - \frac{4}{\pi}\overline{D}$$

$$D_e = \sqrt{D_t{}^2 - D_w{}^2 - \frac{4}{\pi}\overline{D}} \tag{11}$$

So, D_e will be considered as a characteristic parameter for the analysis.

However, from the studies from the previous chapter, thermal resistance

$$R = f\left(\sigma, \mu_l, k_l, \rho_l, \rho_v, cp_l, h_{fg}, \Delta T, D_e\right) \tag{12}$$

$$f\left(R, \sigma, \mu_l, k_l, \rho_l, \rho_v, cp_l, h_{fg}, \Delta T, D_e\right) = constant \tag{13}$$

Here, the number of variable terms is 10 and the fundamental dimensions are 4. Hence, there are total 6 π-terms when Buckingham-π theorem is applied.

$$f(\pi_1, \pi_2, \pi_3, \pi_4, \pi_5, \pi_6) = constant \tag{14}$$

Simplifying and applying Buckingham-π theorem, the π-terms expression will as be following:

$$\pi_1 = \rho_l{}^{a1}\Delta T^{b1}D_e{}^{c1}\sigma^{d1}R$$

$$\pi_2 = \rho_l{}^{a2}\Delta T^{b2}D_e{}^{c2}\sigma^{d2}\mu_l$$

$$\pi_3 = \rho_l{}^{a3}\Delta T^{b3}D_e{}^{c3}\sigma^{d3}k_l$$

$$\pi_4 = \rho_l{}^{a4}\Delta T^{b4}D_e{}^{c4}\sigma^{d4}\rho_v$$

$$\pi_5 = \rho_l{}^{a5}\Delta T^{b5}D_e{}^{c5}\sigma^{d5}Cp_l$$

$$\pi_6 = \rho_l{}^{a6}\Delta T^{b6}D_e{}^{c6}\sigma^{d6}h_{fg}$$

Equating the exponents of fundamental dimensions, the above π-terms can be achieved. Detail steps are shown in Appendix E. Then, substituting the π-terms in Eq. 14

$$\frac{R}{\Delta T}\sqrt{\frac{\sigma^3 D_e}{\rho_l}} = f\left(\frac{\rho_v}{\rho_l}, \frac{\Delta T \rho_l C p_l D_e}{\sigma}, \frac{h_{fg}}{\sigma D_e^{2}}, \mu_l\sqrt{\frac{D_e^{5}}{\sigma \rho_l}}, \Delta T k_l \sqrt{\frac{\rho_l D_e}{\sigma^3}}\right) \tag{15}$$

The brief of the following graphical analysis could reveal the dominating dimensionless parameter for the thermal resistance. All the required data have been taken from book [38] and table 3.6. Since, the experiment was conducted by measuring the tube surface temperature, it is not possible to get the actual temperature of the liquid inside the tube. For this reason, all the properties of the liquids have been taken for saturated condition. As in the earlier chapters the detail analysis of CLPHP geometry structures have been shown already, this time the main focus will be only to effect of π-terms on the thermal resistance. So, the filling ratio is considered as 60% and representative data is drawn for only 16W for the four liquids.
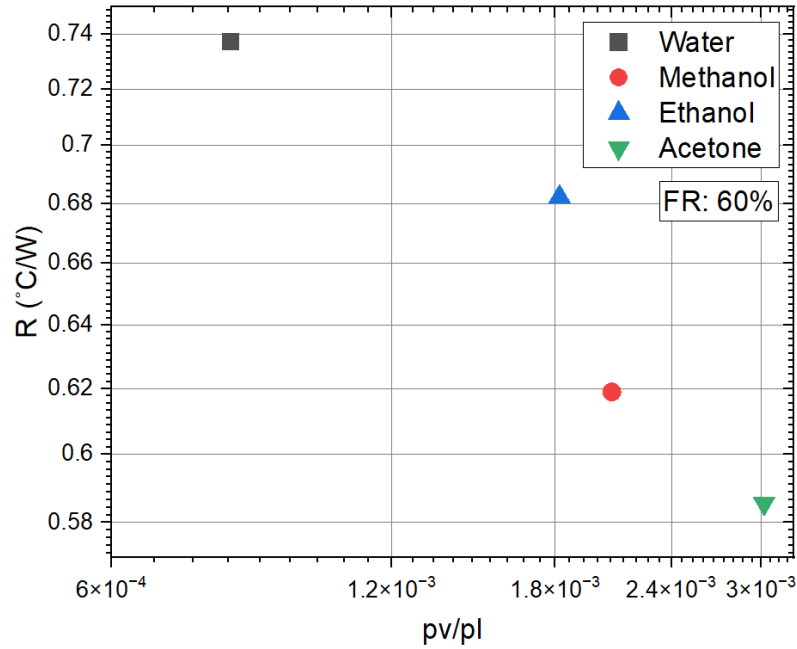
Figure 5.2: Effect of $\frac{\rho_v}{\rho_l}$ on the thermal resistance (Rosette inserts and FR: 60%)

From Fig. 5.2, it is clear that for the increase in ratio of $\frac{\rho_v}{\rho_l}$ exhibits the declining of thermal resistance for different liquids. Moreover, it is clearly noticed that the acetone depicts low thermal resistance at high ratio whereas water with lower ratio showed low thermal resistance. Considering, the term $\frac{\Delta T \rho_l C p_l D_e}{\sigma}$ in Fig. 5.3, the thermal resistance is also varied for different working fluids.
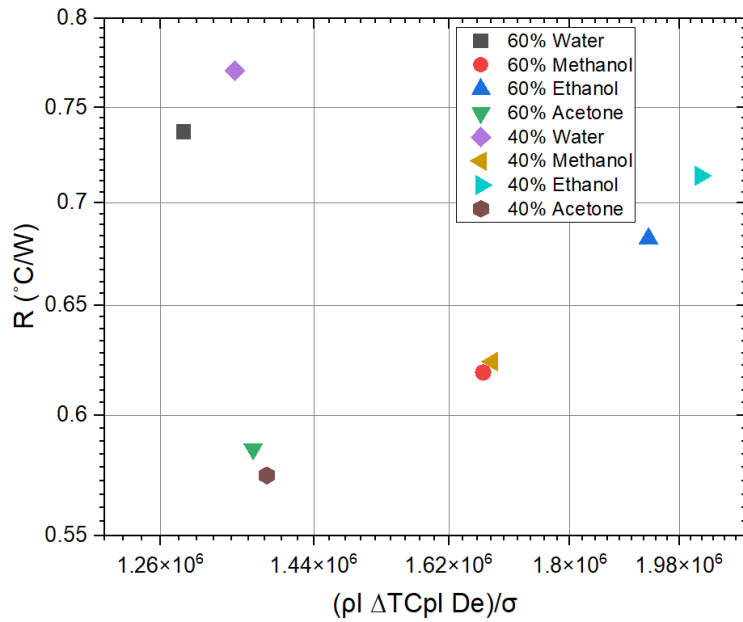
Figure 5.3: Effect of $\frac{\Delta T \rho_l Cp_l D_e}{\sigma}$ on thermal resistance (Rosette inserts and FR: 40% & 60%)
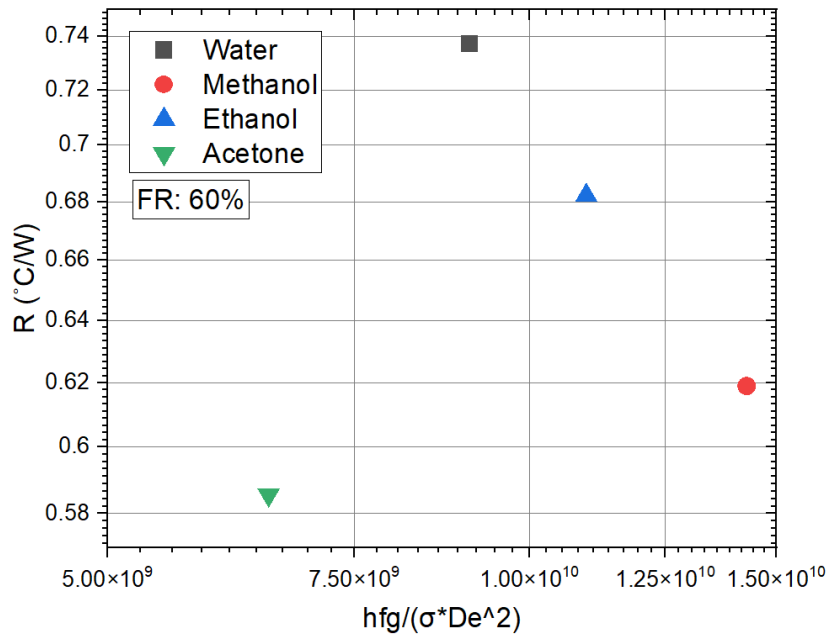

Figure 5.4: Effect of $\frac{h_{fg}}{\sigma D_e^2}$ on thermal resistance (Rosette inserts and FR: 60%)

From Fig. 5.4 to 5.6, similar variations are seen including some exceptions. The trend line analysis is not the main target of this dimensional study but, it can be said that the dimensional terms have an effect on the thermal resistance.
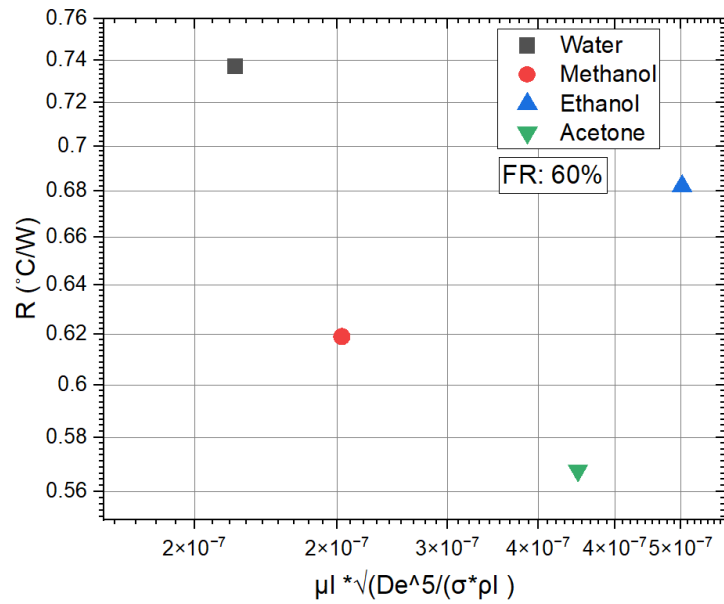
Figure 5.5: Effect of $\mu_l\sqrt{\dfrac{D_e{}^5}{\sigma\rho_l}}$ on thermal resistance (Rosette inserts and FR: 60%)
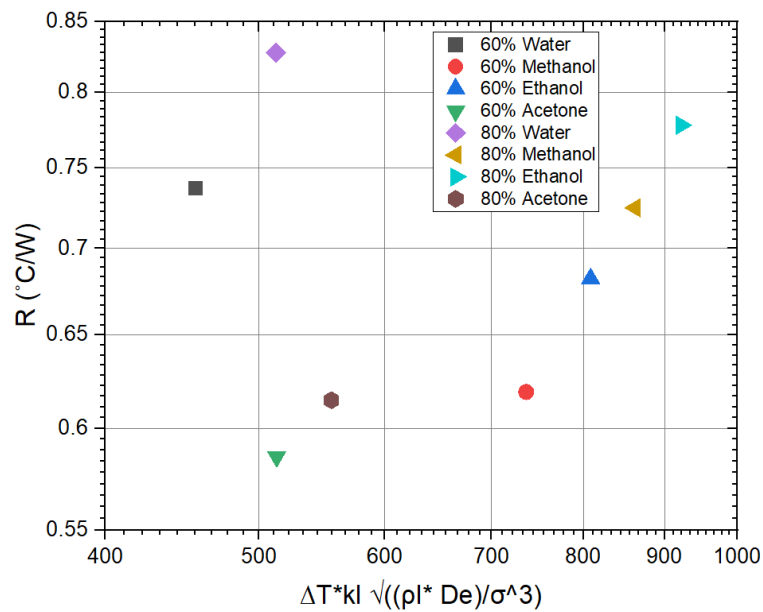
Figure 5.6: Effect of $\Delta Tk_l\sqrt{\dfrac{\rho_l D_e}{\sigma^3}}$ on thermal resistance (Rosette inserts and FR: 60% & 80%)

The above graphical representations are drawn to show the effect of the π-terms over the thermal resistance. The main focus of these depictions is to define a clear idea that thermal resistance is actually depends on these dimensionless π-terms.

Now, the comparison effect of the dimensionless parameter on three different geometries of CLPHPs are illustrated in the Fig. 5.7 and Fig. 5.8. Here, two

parameters are considered $\Delta T k_l \sqrt{\frac{\rho_l D_e}{\sigma^3}}$ and $\frac{\Delta T \rho_l C p_l D_e}{\sigma}$. From the Fig. 5.7, It can be seen

that the thermal resistance is decreasing for all CLPHPs with respect to $\Delta T k_l \sqrt{\frac{\rho_l D_e}{\sigma^3}}$.
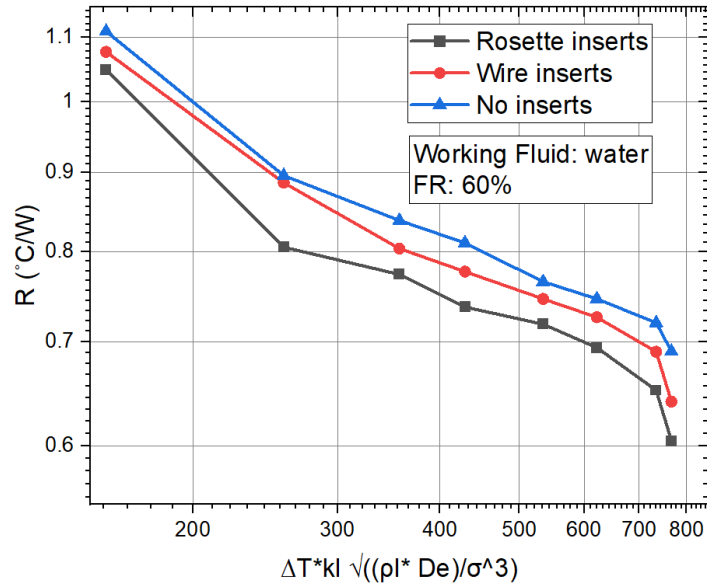
Figure 5.7: Effect of $\Delta T k_l \sqrt{\frac{\rho_l D_e}{\sigma^3}}$ on thermal resistance for three different CLPHPs
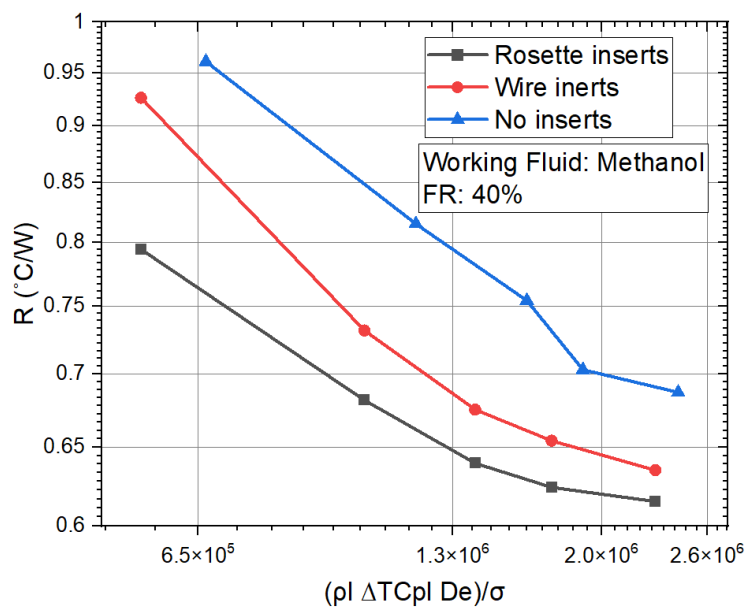(WF: Water and FR: 60%)

Figure 5.8: Effect of $\frac{\Delta T \rho_l C p_l D_e}{\sigma}$ on thermal resistance for three different CLPHPs

(WF: Methanol and FR: 40%)

The surface tension (σ), the characteristics diameter (D_e) and ΔT are the main parameters in this case due to different inserts inside CLPHPs. Rosette inserts CLPHP showed lower thermal resistance because of the lower value of D_e and σ which was already discussed from the experimental analysis in the previous chapter. If the effect on thermal resistance due to $\frac{\Delta T \rho_l C p_l D_e}{\sigma}$ is plotted similar trend can be achieved which is depicted in Fig. 5.8.

From the above discussions, it can be concluded that the dimensionless parameters have an effect on the thermal resistance not only for the various working fluids but also for the inserts of CLPHPs. The main goal of this study is also aligned with this analysis.

CHAPTER 6: CONCLUSIONS AND RECOMMENDATIONS

Experimental study has been carried out in the Closed-loop pulsating heat pipe (CLPHP) with different working fluids at varying filling ratios. The thermal performance parameter depends on the properties of working fluids, filling ratios and geometries. A modified insert which is rosette like insert improves the overall thermal performance than the traditional wire inserts and plain tube CLPHPs. The following major conclusions can be drawn from the present study:

1. CLPHP fill ratio affects its performance significantly. Very low fill ratio causes minimal liquid inventory at higher heat input and very high fill can prevent proper bubble generation due to less space available inside CLPHP. 60% is the optimum fill ratio based on the experimental data.

2. For acetone and methanol rapid decrement of thermal resistance is obtained up to 10-12W of heat supply. On the other hand, this phenomenon is observed up to 15W for water and ethanol due to high specific heat and boiling point of liquids. Further heat supply yields slow change of thermal resistance because of less presence of liquid mass with compared vapour. After reaching the boiling points, rapid boiling also lowers the presence of liquid mass quickly resulting low heat transfer.

3. Among the acetone, ethanol, methanol and water, acetone showed the lowest thermal resistance due to low latent heat and specific heat but offers low working range due to its lower boiling point.

4. Thermal resistance in rosette insert exhibits the lowest value with respect to plain tube and plain wire insert CLPHP at all experimental conditions. Insertion of rosette introduces an additional conduction heat transfer phenomena to the CLPHP along with convection and boiling to the CLPHP. Consequently, the early nucleate boiling is started and exhibits lower thermal resistance from the plain tube and plain wire insert CLPHP. Best performance was achieved in case of rosette insert due to very high fin conduction effect, wall heat removal and availability of more possible nucleation zones. An overall decrement of thermal resistance is approximately 10% for rosette with compare to plain tube and it is

observed approximately 7% decrement with respect to plain wire insert CLPHP.

5. Acetone with 60% fill ratio exhibits the lowest thermal resistance of 0.568 ˚C/W in the rosette insert CLPHP. Usual convection and boiling along with conduction heat transfer in the rosette insert plays a vital role to reduce the thermal resistance significantly from plain tube and plain wire insert CLPHP.

Usual modes of heat transfer are convection and boiling in heat pipe. In the present study, a special type of insert (rosette like structure) is used which introduces conduction mode of heat transfer (along with convection and boiling) in heat pipe for the first time. Significant improvement of thermal performance has been observed by using this rosette insert.

Recommendations

The present experimental study concludes that the rosette insert can improve the thermal performance significantly compared to plain tube and plain wire insert CLPHP but a certain number of recommendations also require for further attention. The future study should be based on following recommendations:

- Working fluid flow behaviour of the rosette insert CLPHP could be considered for further study.

- Experimental investigation can be performed by using nano fluid and mixer of two different fluids.

- Experiment can be conducted by changing parameters of the rosette like size, shape, wire diameter and so on for optimizing the performance of heat pipe.

- The overall experimental work can be simulated numerically by a comprehensive mathematical modelling with suitable numerical model scheme so that the effect of bubble dynamics can be visualized.

- An empirical co-relation could be made by various graphical analysis of the dimensionless parameters.

REFERENCES

[1] R.S. Gaugler, "*Heat transfer device*", US Patent 2350348 (1944)

[2] P.D. Dunn, D.A. Reay, *The heat pipe, Physics in Technology* 35 (1973) 172-201

[3] G. F. Smyrnov and G. A. Savchenkov, (USSR Patent 504065), 1971

[4] H. Akachi, "*Structure of a heat pipe*", U.S. Patent Number 4921041, 1990

[5] Groll, M., and Khandekar, S., "*Pulsating Heat Pipes: Progress and Prospects*", Proc. International Conference on Energy and the Environment, Shanghai, China, 2003, vol. 1, pp. 723–730

[6] Srikrishna Parthasarathi, Siddharth Nagarajan, Shambhavi Desai, S. Umamaheswara Reddy, G. S. V. L. Narasimham . "*Effect of bend radius and insulation on adiabatic section on the performance of a single closed loop pulsating heat pipe: experimental study and heat transfer correlation*" Heat and Mass Transfer (2021)

[7] Yuwen Zhang, Amir Faghri. "*Advances and Unsolved Issues in Pulsating Heat Pipes*" Heat Transfer Engineering, issue 1, Vol. 29, pp. 20–44. (2008)

[8] S. Khandekar, Manfred Groll, P. Charoensawan. "*Closed and open loop pulsating Heat pipes*".13th international Heat pipe conference, Shanghai, China, September 21-25. (2004)

[9] A. Hasanpour, M. Farhadi, K. Sedighi. "*A review study on twisted tape inserts on turbulent flow heat exchangers: The overall enhancement ratio criteria*" International Communications in Heat and Mass Transfer. (2014)

[10] Ahmed Ramadhan Al-Obaidi, Issa Chaer. "*Study of the flow characteristics, pressure drop and augmentation of heat performance in a horizontal pipe with and without twisted tape inserts*" International Communications in Heat and Mass Transfer. (2021)

[11] M Lutfor Rahmana , Fariha Mira, Sumaiya Nawrina, R A Sultana, and Mohammad Alib "*Effect of fin and insert on the performance characteristics of Open Loop Pulsating Heat Pipe (OLPHP)*" 6th BSME International Conference on Thermal Engineering (ICTE 2014), Vol. 105, pp. 105-112. (2015)

[12] Grover, G M., "*Evaporation-condensation heat transfer device*", US Patent application, 2 December 1963, Published US Patent No. 3229759. (1966)

[13] B. Zohuri, "*Heat Pipe Design and Technology*". Chapter 1: Basic Principles of Heat Pipes and History

[14] Zilong Deng, Yi Zheng, Xiangdong Liu, Bingpeng Zhu, Yongping Chen. "*Experimental study on thermal performance of an anti-gravity pulsating heat pipe and its application on heat recovery utilization*" Applied Thermal Engineering, Vol 125, pp. 1368-1378

[15] M. Arab, M. Soltanieh, M.B. Shafii "*Experimental investigation of extra-long pulsating heat pipe application in solar water heaters.*" Experimental Thermal and Fluid Science, Vol 42, pp. 6-15

[16] Yuwen Zhang a, A. Faghri, M.B. Shafii, "*Analysis of liquid–vapor pulsating flow in a U-shaped miniature tube.*" International Journal of Heat and Mass Transfer, Vol 45, pp. 2501–2508. (2002)

[17] Marco Marengo, Vadim S. Nikolayev. "*Pulsating heat pipes: Experimental analysis, design and application*", International Journal of Heat and Mass Transfer. (2005)

[18] A. Hasanpour, M. Farhadi, K. Sedighi, "*A review study on twisted tape inserts on turbulent flow heat exchangers: The overall enhancement ratio criteria*", International Communications in Heat and Mass Transfer 55 (2014) 53–62

[19] M. Zufar, P. Gunnasegaran, H.M. Kumar, K.C. Ng. "*Numerical and experimental investigations of hybrid nanofluids on pulsating heat pipe performance*" International Journal of Heat and Mass Transfer, Vol. 146, pp. 118887. (2020)

[20] Piyanun Charoensawan, Sameer Khandekar, Manfred Groll, Pradit Terdtoon, "*Closed loop pulsating heat pipes Part A: parametric experimental investigations.*" Applied Thermal Engineering, Vol. 23, pp. 2009-2020. (2003)

[21] Durga Bastakoti, Hongna Zhang, Da Li, Weihua Cai, Fengchen Li. "*An overview on the developing trend of pulsating heat pipe and its performance.*" Applied Thermal Engineering, Vol. 141, pp. 305-332. (2018)

[22] Jason Clement, Xia Wang, "*Experimental investigation of pulsating heat pipe performance with regard to fuel cell cooling application*", Applied Thermal Engineering 50 (2013) 268-274

[23] D. Mangini, M. Mameli, D. Fioriti, S. Filippeschi, L. Araneo, M. Marengod. "*Hybrid Pulsating Heat Pipe for space applications with non-uniform heating patterns: Ground and micro-gravity experiments.*" Applied Thermal Engineering, Vol 126, pp. 1029-43

[24] M.M. Sarafraz, F. Hormozi, S.M. Peyghambarzadeh. "*Thermal performance and efficiency of a thermosyphon heat pipe working with a biologically ecofriendly nanofluid.*" International Communications in Heat and Mass Transfer, Vol. 57, pp. 297-303. (2014)

[25] Ahmed Ramadhan Al-Obaidi, Issa Chaer. "*Study of the flow characteristics, pressure drop and augmentation of heat performance in a horizontal pipe with and without twisted tape inserts*" Case Studies in Thermal Engineering, Vol. 25, pp. 10964. (2021)

[26] Dharmapal A Baitule, Pramod R Pachghare, "*Experimental analysis of closed loop Pulsating heat pipe with variable filling Ratio*" International Journal of Mechanical Engineering and Robotic Research, ISSN 2278 – 0149, Vol. 2, No. 3, July 2013

[27] Brian Holley, Amir Faghri. "*Analysis of pulsating heat pipe with capillary wick and varying channel diameter*" International Journal of Heat and Mass Transfer, Vol. 48, pp. 2635–2651. (2005)

[28] Himel Barua, Mohammad Ali, Md. Nuruzzaman, M. Quamrul Islam, Chowdhury M. Feroz. "*Effect of filling ratio on heat transfer characteristics and performance of a closed loop pulsating heat pipe*". 5th BSME International Conference on Thermal Engineering, Procedia Engineering. (2013)

[29] Honghai Yang, S. Khandekar and M. Groll. "*Operational limit of closed loop pulsating heat pipes*". Applied Thermal Engineering, Vol: 28, pp. 49-59. (2008)

[30] Wei Qu, Yuhua Li, Tongze Ma. "Frequency analysis on pulsating Heat Pipe". Proceedings of IPACK2007, ASME InterPACK'07.

[31] B.Y Tong, T.N. Wong, K.T. Ooi. "*Closed-loop Pulsating Heat Pipe.*" Applied Thermal Engineering, Vol. 21, pp. 1845-18. (2001)

[32] S. Shi, X. Cui, H. Han, J. Weng, Z. Li, "*A study of the heat transfer performance of a pulsating heat pipe with ethanol-based mixtures*", Appl. Therm. Eng. V.102, pp. 1219-1227. (2016)

[33] E.R. Babu, G.V. Gnanendra Reddy, "*Effect of working fluids on thermal performance of closed loop pulsating heat pipe*", J. Eng. Sci. Technol. V.11, pp. 872–880. (2016)

[34] Bhawna Verma*, Vijay Lakshmi Yadav, Kaushal Kumar Srivastava. "*Experimental Studies on Thermal Performance of a Pulsating Heat Pipe with Methanol/DI Water*". Journal of Electronics Cooling and Thermal Control, Vol. 3, pp. 27-34. (2013)

[35] Hua Han, Xiaoyu Cui*, Yue Zhu, Shende Sun. "*A comparative study of the behavior of working fluids and their properties on the performance of pulsating heat pipes (PHP)*", International Journal of Thermal Sciences V.82, pp. 138-147. (2014)

[36] Chih-Yung Tseng a, Kai-Shing Yang a, Kuo-Hsiang Chien a, Ming-Shan Jeng a, Chi-Chuan Wang. "*Investigation of the performance of pulsating heat pipe subject to uniform/alternating tube diameters*", Experimental Thermal and Fluid Science V.54, pp. 85–92. (2014)

[37] Khandekar, S*., "Closed Loop Pulsating Heat Pipes - Part B: Visualization and Semi-Empirical Modeling",* Appl. Therm. Eng., 23 (2003), 16, pp. 2021–2033

[38] Yunus A. Çengel, Afshin J. Ghajar, "*Heat and Mass Transfer- Fundamentals and Applications*", Fifth edition-2015, McGraw-Hill Education.

Heat input/power =Q

Average evaporator temperature: Te

Average adiabatic temperature= Ta

Average condenser temperature=Tc

Thermal resistance (evaporator and adiabatic) =Ra

Thermal resistance (evaporator and adiabatic) =Rc

Total thermal resistance = R

DR PT: Dry run-on Plain tube CLPHP

Table APP. 1: Data table for dry run-on plain tube CLPHP

Sl No.	Q (W)	Te (˚C)	Ta (˚C)	Tc (˚C)	Ra (˚C/W)	Rc (˚C/W)	R (˚C/W)	Identification
1	4.00	36.12	33.20	29.10	0.732	1.026	1.758	DR PT
2	9.27	60.44	53.68	44.18	0.730	1.025	1.755	DR PT
3	12.76	75.48	66.16	53.08	0.731	1.025	1.756	DR PT
4	15.78	87.68	76.13	60.30	0.732	1.003	1.735	DR PT
5	21.17	106.47	90.95	69.50	0.733	1.013	1.746	DR PT
6	25.24	121.52	103.07	77.70	0.731	1.005	1.736	DR PT
7	31.01	139.85	117.15	84.59	0.732	1.050	1.782	DR PT
8	35.14	151.11	125.88	89.51	0.718	1.035	1.753	DR PT

Table APP. 2: Data table for dry run-on wire insert CLPHP

Sl No.	Q (W)	Te (˚C)	Ta (˚C)	Tc (˚C)	Ra (˚C/W)	Rc (˚C/W)	R (˚C/W)	Identification
1	4.00	35.88	33.01	29.24	0.718	0.944	1.662	DR WI
2	8.96	58.48	52.03	43.68	0.720	0.932	1.652	DR WI
3	13.14	74.14	64.67	52.37	0.721	0.936	1.657	DR WI
4	15.80	85.11	73.75	59.28	0.719	0.916	1.635	DR WI
5	21.10	103.21	88.12	68.10	0.715	0.949	1.664	DR WI
6	25.24	119.98	101.91	77.52	0.716	0.966	1.682	DR WI
6	30.90	137.69	115.63	86.46	0.714	0.944	1.658	DR WI
6	35.14	149.71	124.62	91.20	0.714	0.951	1.665	DR WI

Table APP. 3: Data table for dry run-on rosette CLPHP

Sl No.	Q (W)	Te (°C)	Ta (°C)	Tc (°C)	Ra (°C/W)	Rc (°C/W)	R (°C/W)	Identification
1	4.23	35.12	32.12	28.44	0.708	0.870	1.578	DR RI
2	8.30	54.08	48.23	41.06	0.705	0.864	1.569	DR RI
3	12.82	70.22	61.14	50.39	0.708	0.838	1.546	DR RI
4	15.09	79.14	68.44	55.64	0.709	0.849	1.558	DR RI
5	20.51	98.11	83.63	66.18	0.706	0.851	1.557	DR RI
6	23.96	111.51	94.71	74.29	0.701	0.852	1.553	DR RI
7	31.01	135.21	113.60	87.02	0.697	0.857	1.554	DR RI
8	35.26	147.33	123.43	92.40	0.678	0.880	1.558	DR RI

Table APP. 4: Data table for (WF: Water, FR: 20%) on plain tube CLPHP

Sl No.	Q (W)	Te (°C)	Ta (°C)	Tc (°C)	Ra (°C/W)	Rc (°C/W)	R (°C/W)	Identification
1	4.03	33.57	31.34	28.52	0.554	0.698	1.252	20% water
2	9.34	54.63	51.82	45.46	0.301	0.681	0.982	20% water
3	12.24	65.25	61.46	54.35	0.310	0.581	0.891	20% water
4	15.78	75.02	70.44	61.50	0.290	0.567	0.857	20% water
5	21.17	91.23	85.37	73.78	0.277	0.547	0.824	20% water
6	25.34	103.52	97.45	83.20	0.240	0.562	0.802	20% water
7	31.01	115.58	107.13	91.33	0.273	0.509	0.782	20% water
8	35.14	124.52	114.99	97.74	0.271	0.491	0.762	20% water

Table APP. 5: Data table for (WF: Water, FR: 40%) on plain tube CLPHP

Sl No.	Q (W)	Te (°C)	Ta (°C)	Tc (°C)	Ra (°C/W)	Rc (°C/W)	R (°C/W)	Identification
1	4.00	32.53	30.35	27.81	0.546	0.636	1.182	40% water
2	9.27	52.12	48.76	43.56	0.363	0.561	0.924	40% water
3	12.76	64.82	60.60	53.86	0.331	0.528	0.859	40% water
4	15.78	72.61	67.13	59.45	0.347	0.487	0.834	40% water
5	21.17	88.86	81.39	72.03	0.353	0.442	0.795	40% water
6	25.24	98.25	89.26	78.86	0.356	0.412	0.768	40% water
7	31.01	111.25	101.96	88.37	0.300	0.438	0.738	40% water
8	35.14	121.28	110.86	96.33	0.297	0.413	0.710	40% water

Table APP. 6: Data table for (WF: Water, FR: 60%) on plain tube CLPHP

Sl No.	Q (W)	Te (°C)	Ta (°C)	Tc (°C)	Ra (°C/W)	Rc (°C/W)	R (°C/W)	Identification
1	4.00	32.53	30.51	28.10	0.506	0.604	1.110	60% water
2	9.27	49.77	46.10	41.47	0.396	0.500	0.896	60% water
3	12.76	60.43	55.76	49.74	0.366	0.472	0.838	60% water
4	15.78	69.62	63.71	56.83	0.375	0.436	0.811	60% water
5	21.17	82.21	74.99	66.01	0.341	0.424	0.765	60% water
6	25.24	91.23	82.49	72.40	0.346	0.400	0.746	60% water
7	31.01	103.25	93.74	81.62	0.307	0.391	0.698	60% water
8	35.14	111.10	100.39	87.27	0.305	0.373	0.678	60% water

Table APP. 7: Data table for (WF: Water, FR: 80%) on plain tube CLPHP

Sl No.	Q (W)	Te (°C)	Ta (°C)	Tc (°C)	Ra (°C/W)	Rc (°C/W)	R (°C/W)	Identification
1	4.00	33.27	30.96	27.85	0.578	0.779	1.357	80% water
2	9.27	55.82	51.61	46.22	0.454	0.582	1.036	80% water
3	12.76	68.71	62.66	57.16	0.474	0.431	0.906	80% water
4	15.78	77.85	70.82	64.02	0.446	0.431	0.876	80% water
5	21.17	94.58	85.60	76.75	0.424	0.418	0.842	80% water
6	25.24	106.54	95.86	85.64	0.423	0.405	0.828	80% water
7	31.01	119.85	106.96	94.67	0.416	0.396	0.812	80% water
8	35.14	129.82	114.27	102.09	0.443	0.346	0.789	80% water

Table APP. 8: Data table for (WF: Acetone, FR: 20%) on plain tube CLPHP

Sl No.	Q (W)	Te (°C)	Ta (°C)	Tc (°C)	Ra (°C/W)	Rc (°C/W)	R (°C/W)	Identification
1	4.00	33.34	31.69	29.13	0.412	0.641	1.053	20% Acetone
2	6.25	39.51	37.05	33.96	0.394	0.494	0.888	20% Acetone
3	8.50	45.15	42.28	38.65	0.338	0.427	0.765	20% Acetone
4	12.99	55.32	51.11	45.91	0.324	0.400	0.724	20% Acetone
5	15.80	61.40	57.05	50.56	0.275	0.411	0.686	20% Acetone

Table APP. 9: Data table for (WF: Acetone, FR: 40%) on plain tube CLPHP

Sl No.	Q (W)	Te (°C)	Ta (°C)	Tc (°C)	Ra (°C/W)	Rc (°C/W)	R (°C/W)	Identification
1	4.00	32.76	31.31	29.23	0.363	0.521	0.884	40% Acetone
2	6.25	39.24	37.03	34.23	0.354	0.448	0.802	40% Acetone
3	8.50	44.75	42.00	38.38	0.324	0.426	0.750	40% Acetone
4	12.99	55.00	50.73	45.85	0.329	0.376	0.704	40% Acetone
5	15.80	60.64	55.52	50.03	0.324	0.348	0.672	40% Acetone

Table APP. 10: Data table for (WF: Acetone, FR: 60%) on plain tube CLPHP

Sl No.	Q (W)	Te (˚C)	Ta (˚C)	Tc (˚C)	Ra (˚C/W)	Rc (˚C/W)	R (˚C/W)	Identification
1	4.00	32.42	30.71	28.68	0.428	0.508	0.936	60% Acetone
2	6.25	38.87	36.72	33.99	0.344	0.437	0.781	60% Acetone
3	8.96	45.52	42.49	38.92	0.338	0.398	0.737	60% Acetone
4	13.14	54.78	50.25	45.63	0.345	0.352	0.696	60% Acetone
5	15.80	60.00	54.92	49.51	0.322	0.342	0.664	60% Acetone

Table APP. 11: Data table for (WF: Acetone, FR: 80%) on plain tube CLPHP

Sl No.	Q (W)	Te (˚C)	Ta (˚C)	Tc (˚C)	Ra (˚C/W)	Rc (˚C/W)	R (˚C/W)	Identification
1	4.00	33.20	30.92	28.77	0.572	0.538	1.110	80% Acetone
2	6.25	39.93	37.09	34.30	0.454	0.446	0.901	80% Acetone
3	8.96	47.00	43.10	39.62	0.435	0.388	0.824	80% Acetone
4	13.14	56.10	50.48	46.01	0.428	0.340	0.768	80% Acetone
5	15.80	62.11	55.60	50.28	0.412	0.337	0.749	80% Acetone

Table APP. 12: Data table for (WF: Ethanol, FR: 20%) on plain tube CLPHP

Sl No.	Q (W)	Te (˚C)	Ta (˚C)	Tc (˚C)	Ra (˚C/W)	Rc (˚C/W)	R (˚C/W)	Identification
1	4.28	33.62	31.46	28.42	0.504	0.710	1.214	20% Ethanol
2	6.36	42.15	39.24	35.88	0.458	0.528	0.986	20% Ethanol
3	8.98	50.49	46.91	42.52	0.398	0.489	0.887	20% Ethanol
4	12.71	62.28	57.87	51.72	0.347	0.484	0.831	20% Ethanol
5	16.62	72.52	67.18	59.29	0.321	0.475	0.796	20% Ethanol
6	19.32	79.60	73.46	64.70	0.318	0.454	0.771	20% Ethanol
7	23.13	88.00	81.16	70.80	0.296	0.448	0.744	20% Ethanol

Table APP. 13: Data table for (WF: Ethanol, FR: 40%) on plain tube CLPHP

Sl No.	Q (W)	Te (˚C)	Ta (˚C)	Tc (˚C)	Ra (˚C/W)	Rc (˚C/W)	R (˚C/W)	Identification
1	4.28	33.42	31.37	28.58	0.479	0.651	1.130	40% Ethanol
2	6.36	41.89	39.18	36.03	0.426	0.495	0.921	40% Ethanol
3	9.03	50.00	46.25	42.18	0.415	0.451	0.866	40% Ethanol
4	12.48	60.50	55.85	50.50	0.373	0.429	0.802	40% Ethanol
5	16.62	71.60	65.80	58.90	0.349	0.415	0.764	40% Ethanol
6	19.32	78.50	71.46	64.33	0.365	0.369	0.733	40% Ethanol
7	23.13	86.58	79.11	70.51	0.323	0.372	0.695	40% Ethanol

Table APP. 14: Data table for (WF: Ethanol, FR: 60%) on plain tube CLPHP

Sl No.	Q (W)	Te (°C)	Ta (°C)	Tc (°C)	Ra (°C/W)	Rc (°C/W)	R (°C/W)	Identification
1	4.00	33.13	31.06	28.80	0.518	0.567	1.085	60% Ethanol
2	6.36	41.00	38.05	35.26	0.464	0.439	0.903	60% Ethanol
3	8.74	48.20	44.90	40.99	0.378	0.447	0.825	60% Ethanol
4	12.56	59.58	55.04	49.75	0.362	0.422	0.783	60% Ethanol
5	16.62	70.49	65.01	58.02	0.330	0.421	0.750	60% Ethanol
6	19.32	77.19	70.60	63.26	0.341	0.380	0.721	60% Ethanol
7	23.13	85.74	78.53	70.24	0.312	0.358	0.670	60% Ethanol

Table APP. 15: Data table for (WF: Ethanol, FR: 80%) on plain tube CLPHP

Sl No.	Q (W)	Te (°C)	Ta (°C)	Tc (°C)	Ra (°C/W)	Rc (°C/W)	R (°C/W)	Identification
1	4.00	33.43	31.24	28.50	0.548	0.687	1.235	80% Ethanol
2	6.36	43.22	40.10	36.59	0.491	0.552	1.043	80% Ethanol
3	9.03	51.98	47.87	43.31	0.455	0.504	0.960	80% Ethanol
4	13.44	65.14	59.64	53.25	0.409	0.475	0.885	80% Ethanol
5	16.62	73.52	67.09	59.59	0.387	0.451	0.838	80% Ethanol
6	19.32	80.20	72.74	64.73	0.386	0.415	0.801	80% Ethanol
7	23.13	88.55	78.89	70.89	0.418	0.346	0.763	80% Ethanol

Table APP. 16: Data table for (WF: Methanol, FR: 20%) on plain tube CLPHP

Sl No.	Q (W)	Te (°C)	Ta (°C)	Tc (°C)	Ra (°C/W)	Rc (°C/W)	R (°C/W)	Identification
1	4.15	33.42	31.52	29.24	0.457	0.550	1.007	20% Methanol
2	8.61	47.63	44.08	40.50	0.412	0.416	0.828	20% Methanol
3	12.56	58.25	53.55	48.55	0.374	0.398	0.772	20% Methanol
4	15.56	66.00	60.55	54.24	0.350	0.405	0.756	20% Methanol
5	21.48	78.25	71.53	62.85	0.313	0.404	0.717	20% Methanol

Table APP. 17: Data table for (WF: Methanol, FR: 40%) on plain tube CLPHP

Sl No.	Q (W)	Te (°C)	Ta (°C)	Tc (°C)	Ra (°C/W)	Rc (°C/W)	R (°C/W)	Identification
1	4.19	33.42	31.26	29.39	0.515	0.446	0.961	40% Methanol
2	8.80	47.14	43.61	39.97	0.401	0.414	0.815	40% Methanol
3	13.22	57.42	52.63	47.45	0.363	0.391	0.754	40% Methanol
4	16.39	65.26	59.25	53.74	0.367	0.336	0.703	40% Methanol
5	21.31	77.00	69.98	62.36	0.329	0.358	0.687	40% Methanol

Table APP. 18: Data table for (WF: Methanol, FR: 60%) on plain tube CLPHP

Sl No.	Q (W)	Te (°C)	Ta (°C)	Tc (°C)	Ra (°C/W)	Rc (°C/W)	R (°C/W)	Identification
1	4.15	33.10	31.08	29.13	0.485	0.469	0.955	60% Methanol
2	8.61	46.25	42.78	39.28	0.403	0.406	0.809	60% Methanol
3	12.56	56.74	51.91	47.31	0.384	0.367	0.751	60% Methanol
4	15.56	64.00	58.39	52.73	0.361	0.363	0.724	60% Methanol
5	21.48	75.25	67.86	60.86	0.344	0.326	0.670	60% Methanol

Table APP. 19: Data table for (WF: Methanol, FR: 80%) on plain tube CLPHP

Sl No.	Q (W)	Te (°C)	Ta (°C)	Tc (°C)	Ra (°C/W)	Rc (°C/W)	R (°C/W)	Identification
1	4.11	33.42	31.52	29.15	0.462	0.576	1.038	80% Methanol
2	8.74	48.69	44.74	40.76	0.452	0.456	0.908	80% Methanol
3	12.77	60.12	54.44	49.52	0.445	0.386	0.830	80% Methanol
4	16.81	70.12	62.80	56.69	0.435	0.363	0.799	80% Methanol
5	20.28	77.15	68.20	61.51	0.441	0.330	0.771	80% Methanol

Table APP. 20: Data table for (WF: Water, FR: 20%) on wire insert CLPHP

Sl No.	Q (W)	Te (°C)	Ta (°C)	Tc (°C)	Ra (°C/W)	Rc (°C/W)	R (°C/W)	Identification
1	4.00	33.01	30.72	28.23	0.573	0.623	1.196	20% Water
2	8.96	52.26	49.66	43.61	0.290	0.675	0.965	20% Water
3	13.14	64.82	60.19	53.63	0.352	0.499	0.852	20% Water
4	15.80	73.12	67.49	60.09	0.356	0.469	0.825	20% Water
5	21.10	88.64	81.86	72.17	0.321	0.459	0.781	20% Water
6	25.24	100.87	93.79	81.51	0.280	0.487	0.767	20% Water
7	30.90	112.25	104.07	89.61	0.265	0.468	0.733	20% Water
8	35.14	119.58	110.34	94.87	0.263	0.440	0.703	20% Water

Table APP. 21: Data table for (WF: Water, FR: 40%) on wire insert CLPHP

Sl No.	Q (W)	Te (°C)	Ta (°C)	Tc (°C)	Ra (°C/W)	Rc (°C/W)	R (°C/W)	Identification
1	4.00	32.50	30.40	28.00	0.526	0.601	1.126	40% Water
2	8.96	49.52	45.65	41.59	0.432	0.453	0.885	40% Water
3	13.14	62.75	57.62	52.05	0.390	0.424	0.814	40% Water
4	15.80	69.85	64.42	57.52	0.344	0.437	0.781	40% Water
5	21.10	85.52	78.63	69.76	0.327	0.420	0.747	40% Water
6	25.24	96.81	88.84	78.33	0.316	0.416	0.732	40% Water
7	30.90	108.54	99.68	87.62	0.287	0.390	0.677	40% Water
8	35.14	115.85	105.59	93.82	0.292	0.335	0.627	40% Water

Table APP. 22: Data table for (WF: Water, FR: 60%) on wire insert CLPHP

Sl No.	Q (W)	Te (˚C)	Ta (˚C)	Tc (˚C)	Ra (˚C/W)	Rc (˚C/W)	R (˚C/W)	Identification
1	4.00	32.42	30.34	28.12	0.521	0.556	1.076	60% Water
2	8.96	48.43	44.40	40.49	0.450	0.436	0.886	60% Water
3	13.14	59.78	55.00	49.22	0.364	0.440	0.804	60% Water
4	15.80	67.55	62.23	55.28	0.337	0.440	0.777	60% Water
5	21.10	80.89	74.04	65.15	0.325	0.421	0.746	60% Water
6	25.24	90.55	82.88	72.23	0.304	0.422	0.726	60% Water
7	30.90	101.25	92.60	79.94	0.280	0.410	0.690	60% Water
8	35.14	109.87	99.73	87.37	0.289	0.352	0.640	60% Water

Table APP. 23: Data table for (WF: Acetone, FR: 80%) on wire insert CLPHP

Sl No.	Q (W)	Te (˚C)	Ta (˚C)	Tc (˚C)	Ra (˚C/W)	Rc (˚C/W)	R (˚C/W)	Identification
1	4.00	33.00	30.99	28.11	0.503	0.721	1.224	80% Water
2	8.96	54.52	50.24	45.99	0.478	0.474	0.952	80% Water
3	13.14	67.85	62.24	56.16	0.427	0.463	0.890	80% Water
4	15.80	76.25	70.01	62.55	0.395	0.472	0.867	80% Water
5	21.10	92.52	84.05	74.97	0.401	0.430	0.832	80% Water
6	25.24	104.52	94.14	84.40	0.411	0.386	0.797	80% Water
7	30.90	117.52	105.23	94.11	0.398	0.360	0.758	80% Water
8	35.14	126.52	112.76	101.40	0.392	0.323	0.715	80% Water

Table APP. 24: Data table for (WF: Acetone, FR: 20%) on wire insert CLPHP

Sl No.	Q (W)	Te (˚C)	Ta (˚C)	Tc (˚C)	Ra (˚C/W)	Rc (˚C/W)	R (˚C/W)	Identification
1	4.03	32.46	30.90	28.79	0.387	0.523	0.910	20% Acetone
2	6.54	38.77	36.53	33.88	0.342	0.405	0.748	20% Acetone
3	8.83	44.64	42.08	38.52	0.290	0.403	0.693	20% Acetone
4	12.91	53.32	49.62	44.84	0.287	0.370	0.657	20% Acetone
5	15.70	59.67	55.81	49.88	0.246	0.378	0.624	20% Acetone

Table APP. 25: Data table for (WF: Acetone, FR: 40%) on wire insert CLPHP

Sl No.	Q (W)	Te (˚C)	Ta (˚C)	Tc (˚C)	Ra (˚C/W)	Rc (˚C/W)	R (˚C/W)	Identification
1	4.03	32.51	31.11	29.20	0.346	0.474	0.820	40% Acetone
2	6.54	38.11	36.01	33.42	0.321	0.396	0.717	40% Acetone
3	8.83	43.65	40.90	37.79	0.312	0.352	0.664	40% Acetone
4	12.91	52.41	48.52	44.26	0.301	0.330	0.631	40% Acetone
5	15.70	58.40	53.84	48.84	0.290	0.318	0.609	40% Acetone

Table APP. 26: Data table for (WF: Acetone, FR: 60%) on wire insert CLPHP

Sl No.	Q (W)	Te (°C)	Ta (°C)	Tc (°C)	Ra (°C/W)	Rc (°C/W)	R (°C/W)	Identification
1	4.03	32.12	30.64	28.74	0.366	0.471	0.837	60% Acetone
2	6.54	37.03	34.91	32.43	0.324	0.379	0.703	60% Acetone
3	8.83	42.36	39.74	36.56	0.297	0.360	0.657	60% Acetone
4	12.91	51.64	48.10	43.69	0.274	0.342	0.616	60% Acetone
5	15.70	57.31	52.87	47.90	0.283	0.317	0.599	60% Acetone

Table APP. 27: Data table for (WF: Acetone, FR: 80%) on wire insert CLPHP

Sl No.	Q (W)	Te (°C)	Ta (°C)	Tc (°C)	Ra (°C/W)	Rc (°C/W)	R (°C/W)	Identification
1	4.03	32.75	30.79	28.72	0.486	0.514	1.000	80% Acetone
2	6.54	39.64	37.06	34.32	0.394	0.419	0.813	80% Acetone
3	8.83	45.65	42.44	39.06	0.364	0.383	0.747	80% Acetone
4	12.91	54.24	49.89	45.37	0.337	0.350	0.687	80% Acetone
5	15.70	60.21	55.22	50.00	0.318	0.332	0.650	80% Acetone

Table APP. 28: Data table for (WF: Ethanol, FR: 20%) on wire insert CLPHP

Sl No.	Q (W)	Te (°C)	Ta (°C)	Tc (°C)	Ra (°C/W)	Rc (°C/W)	R (°C/W)	Identification
1	4.00	33.02	30.97	28.49	0.513	0.622	1.135	20% Ethanol
2	6.43	41.21	38.22	34.97	0.465	0.505	0.971	20% Ethanol
3	8.96	48.97	45.05	41.10	0.437	0.441	0.878	20% Ethanol
4	13.14	60.12	55.09	49.49	0.383	0.427	0.809	20% Ethanol
5	16.19	68.59	63.05	56.02	0.342	0.434	0.776	20% Ethanol
6	21.10	80.47	73.84	65.14	0.314	0.412	0.727	20% Ethanol
7	26.11	91.97	84.39	74.26	0.290	0.388	0.678	20% Ethanol

Table APP. 29: Data table for (WF: Ethanol, FR: 40%) on wire insert CLPHP

Sl No.	Q (W)	Te (°C)	Ta (°C)	Tc (°C)	Ra (°C/W)	Rc (°C/W)	R (°C/W)	Identification
1	4.00	33.03	30.89	28.57	0.537	0.582	1.118	40% Ethanol
2	6.43	40.25	37.30	34.42	0.459	0.448	0.907	40% Ethanol
3	8.96	47.50	43.85	39.83	0.407	0.449	0.856	40% Ethanol
4	13.14	58.88	54.16	48.61	0.360	0.422	0.781	40% Ethanol
5	16.19	66.87	61.35	54.59	0.341	0.418	0.759	40% Ethanol
6	21.10	79.24	72.59	64.35	0.315	0.391	0.706	40% Ethanol
7	26.11	90.11	82.13	73.38	0.306	0.335	0.641	40% Ethanol

Table APP. 30: Data table for (WF: Ethanol, FR: 60%) on wire insert CLPHP

Sl No.	Q (W)	Te (°C)	Ta (°C)	Tc (°C)	Ra (°C/W)	Rc (°C/W)	R (°C/W)	Identification
1	4.00	33.00	31.01	28.73	0.497	0.571	1.068	60% Ethanol
2	6.43	39.55	36.92	33.88	0.409	0.473	0.882	60% Ethanol
3	8.96	45.87	42.62	38.54	0.363	0.455	0.818	60% Ethanol
4	13.14	57.42	53.13	47.47	0.327	0.431	0.758	60% Ethanol
5	16.19	65.25	60.27	53.38	0.307	0.426	0.733	60% Ethanol
6	21.10	77.85	71.05	63.62	0.322	0.352	0.674	60% Ethanol
7	26.11	88.90	80.88	72.42	0.307	0.324	0.631	60% Ethanol

Table APP. 31: Data table for (WF: Ethanol, FR: 80%) on wire insert CLPHP

Sl No.	Q (W)	Te (°C)	Ta (°C)	Tc (°C)	Ra (°C/W)	Rc (°C/W)	R (°C/W)	Identification
1	4.00	32.93	30.61	28.07	0.582	0.637	1.218	80% Ethanol
2	6.43	42.56	39.41	36.00	0.490	0.531	1.021	80% Ethanol
3	8.96	50.44	46.51	42.34	0.439	0.465	0.904	80% Ethanol
4	13.14	62.11	57.28	51.25	0.368	0.459	0.827	80% Ethanol
5	16.19	70.49	63.37	57.56	0.440	0.359	0.799	80% Ethanol
6	21.10	82.17	74.19	66.56	0.378	0.362	0.740	80% Ethanol
7	26.11	93.45	83.22	75.18	0.392	0.308	0.700	80% Ethanol

Table APP. 32: Data table for (WF: Methanol, FR: 20%) on wire insert CLPHP

Sl No.	Q (W)	Te (°C)	Ta (°C)	Tc (°C)	Ra (°C/W)	Rc (°C/W)	R (°C/W)	Identification
1	4.00	32.27	30.74	28.47	0.383	0.567	0.950	20% Methanol
2	8.96	46.28	43.53	39.55	0.307	0.445	0.752	20% Methanol
3	13.14	57.84	54.19	48.64	0.278	0.422	0.700	20% Methanol
4	15.80	64.36	59.96	53.73	0.279	0.395	0.673	20% Methanol
5	21.10	75.41	70.15	61.61	0.249	0.405	0.654	20% Methanol

Table APP. 33: Data table for (WF: Methanol, FR: 40%) on wire insert CLPHP

Sl No.	Q (W)	Te (°C)	Ta (°C)	Tc (°C)	Ra (°C/W)	Rc (°C/W)	R (°C/W)	Identification
1	4.00	32.74	30.95	29.04	0.448	0.478	0.926	40% Methanol
2	8.96	45.15	42.17	38.60	0.333	0.399	0.731	40% Methanol
3	13.14	56.15	52.36	47.28	0.288	0.387	0.675	40% Methanol
4	15.80	62.87	57.85	52.54	0.318	0.336	0.654	40% Methanol
5	21.10	74.52	68.03	61.12	0.308	0.327	0.635	40% Methanol

Table APP. 34: Data table for (WF: Methanol, FR: 60%) on wire insert CLPHP

Sl No.	Q (W)	Te (°C)	Ta (°C)	Tc (°C)	Ra (°C/W)	Rc (°C/W)	R (°C/W)	Identification
1	4.00	32.79	31.07	29.16	0.431	0.479	0.909	60% Methanol
2	8.96	44.10	40.97	37.77	0.349	0.357	0.707	60% Methanol
3	13.14	54.25	50.21	45.73	0.308	0.341	0.649	60% Methanol
4	15.80	61.25	56.35	51.18	0.310	0.327	0.637	60% Methanol
5	21.10	72.85	66.27	59.68	0.312	0.312	0.624	60% Methanol

Table APP. 35: Data table for (WF: Methanol, FR: 80%) on wire insert CLPHP

Sl No.	Q (W)	Te (°C)	Ta (°C)	Tc (°C)	Ra (°C/W)	Rc (°C/W)	R (°C/W)	Identification
1	4.00	33.03	31.38	29.13	0.413	0.563	0.976	80% Methanol
2	8.96	47.51	43.93	39.98	0.400	0.441	0.841	80% Methanol
3	13.14	59.10	53.96	48.93	0.391	0.382	0.774	80% Methanol
4	15.80	65.62	59.94	53.99	0.360	0.377	0.736	80% Methanol
5	19.89	74.10	66.10	59.57	0.402	0.328	0.731	80% Methanol

Table APP. 36: Data table for (WF: Water, FR: 20%) on rosette insert CLPHP

Sl No.	Q (W)	Te (°C)	Ta (°C)	Tc (°C)	Ra (°C/W)	Rc (°C/W)	R (°C/W)	Identification
1	4.15	32.25	30.66	27.72	0.383	0.708	1.090	20% Water
2	8.90	51.58	48.85	43.89	0.307	0.557	0.864	20% Water
3	12.82	62.39	58.55	51.92	0.299	0.517	0.816	20% Water
4	16.19	71.22	66.15	58.32	0.313	0.484	0.797	20% Water
5	20.69	84.55	78.67	68.95	0.284	0.470	0.754	20% Water
6	24.90	95.31	87.53	76.93	0.312	0.426	0.738	20% Water
7	31.33	107.64	98.48	85.87	0.292	0.402	0.695	20% Water
8	35.26	114.58	105.43	91.08	0.260	0.407	0.667	20% Water

Table APP. 37: Data table for (WF: Water, FR: 40%) on rosette insert CLPHP

Sl No.	Q (W)	Te (°C)	Ta (°C)	Tc (°C)	Ra (°C/W)	Rc (°C/W)	R (°C/W)	Identification
1	4.15	32.47	30.56	27.94	0.460	0.630	1.090	40% Water
2	8.90	49.14	45.53	41.88	0.406	0.410	0.816	40% Water
3	12.82	59.98	54.77	49.89	0.406	0.381	0.787	40% Water
4	16.19	67.85	61.31	55.38	0.404	0.366	0.770	40% Water
5	20.69	81.11	72.74	65.98	0.405	0.327	0.731	40% Water
6	24.90	91.49	81.92	73.74	0.384	0.328	0.713	40% Water
7	31.33	103.52	93.08	82.80	0.333	0.328	0.661	40% Water
8	35.26	110.25	99.68	88.58	0.300	0.315	0.615	40% Water

Table APP. 38: Data table for (WF: Water, FR: 60%) on rosette insert CLPHP

Sl No.	Q (W)	Te (°C)	Ta (°C)	Tc (°C)	Ra (°C/W)	Rc (°C/W)	R (°C/W)	Identification
1	4.15	32.83	31.09	28.48	0.419	0.629	1.048	60% Water
2	8.90	47.11	43.79	39.94	0.373	0.433	0.806	60% Water
3	12.82	57.44	52.96	47.52	0.349	0.424	0.774	60% Water
4	16.19	65.45	60.37	53.52	0.314	0.423	0.737	60% Water
5	20.69	77.14	71.02	62.28	0.296	0.423	0.718	60% Water
6	24.90	87.54	80.63	70.26	0.277	0.416	0.694	60% Water
7	31.33	98.71	89.88	78.30	0.282	0.370	0.651	60% Water
8	35.26	104.58	94.36	83.28	0.290	0.314	0.604	60% Water

Table APP. 39: Data table for (WF: Water, FR: 80%) on rosette insert CLPHP

Sl No.	Q (W)	Te (°C)	Ta (°C)	Tc (°C)	Ra (°C/W)	Rc (°C/W)	R (°C/W)	Identification
1	4.15	32.43	30.54	27.65	0.455	0.696	1.151	80% Water
2	8.90	53.25	49.67	45.09	0.402	0.515	0.917	80% Water
3	12.82	65.21	60.31	54.14	0.382	0.481	0.863	80% Water
4	16.19	74.54	68.46	61.14	0.376	0.452	0.828	80% Water
5	20.69	87.63	80.49	71.28	0.345	0.445	0.790	80% Water
6	24.90	98.69	89.50	79.55	0.369	0.400	0.769	80% Water
7	31.33	111.26	99.87	88.87	0.363	0.351	0.715	80% Water
8	35.26	118.25	104.08	93.81	0.402	0.291	0.693	80% Water

Table APP. 40: Data table for (WF: Acetone, FR: 20%) on rosette insert CLPHP

Sl No.	Q (W)	Te (°C)	Ta (°C)	Tc (°C)	Ra (°C/W)	Rc (°C/W)	R (°C/W)	Identification
1	4.15	32.33	30.99	29.03	0.323	0.472	0.794	20% Acetone
2	6.43	37.25	35.37	32.79	0.293	0.401	0.694	20% Acetone
3	8.90	43.44	40.93	37.66	0.282	0.367	0.649	20% Acetone
4	12.82	52.44	49.38	44.51	0.239	0.380	0.618	20% Acetone
5	16.19	58.75	55.22	49.12	0.218	0.377	0.595	20% Acetone

Table APP. 41: Data table for (WF: Acetone, FR: 40%) on rosette insert CLPHP

Sl No.	Q (W)	Te (°C)	Ta (°C)	Tc (°C)	Ra (°C/W)	Rc (°C/W)	R (°C/W)	Identification
1	4.15	32.12	30.67	28.86	0.349	0.436	0.785	40% Acetone
2	6.43	36.42	34.41	32.08	0.313	0.363	0.675	40% Acetone
3	8.90	42.45	39.82	36.91	0.295	0.327	0.622	40% Acetone
4	12.82	51.33	47.58	43.71	0.292	0.302	0.594	40% Acetone
5	16.19	57.55	52.84	48.25	0.291	0.284	0.575	40% Acetone

Table APP. 42: Data table for (WF: Acetone, FR: 60%) on rosette insert CLPHP

Sl No.	Q (W)	Te (°C)	Ta (°C)	Tc (°C)	Ra (°C/W)	Rc (°C/W)	R (°C/W)	Identification
1	4.15	31.47	29.86	28.27	0.388	0.383	0.770	60% Acetone
2	6.43	35.69	33.65	31.46	0.317	0.341	0.658	60% Acetone
3	8.90	41.26	38.69	35.84	0.289	0.320	0.609	60% Acetone
4	12.82	50.13	46.61	42.62	0.274	0.311	0.586	60% Acetone
5	16.19	56.52	51.94	47.33	0.283	0.285	0.568	60% Acetone

Table APP. 43: Data table for (WF: Acetone, FR: 80%) on rosette insert CLPHP

Sl No.	Q (W)	Te (°C)	Ta (°C)	Tc (°C)	Ra (°C/W)	Rc (°C/W)	R (°C/W)	Identification
1	4.15	32.36	30.38	28.62	0.477	0.424	0.900	80% Acetone
2	6.43	38.64	36.03	33.65	0.406	0.370	0.777	80% Acetone
3	8.90	44.64	41.04	38.37	0.404	0.300	0.704	80% Acetone
4	12.82	53.36	48.98	44.89	0.342	0.319	0.660	80% Acetone
5	16.19	59.47	53.99	49.52	0.339	0.276	0.615	80% Acetone

Table APP. 44: Data table for (WF: Ethanol, FR: 20%) on rosette insert CLPHP

Sl No.	Q (W)	Te (°C)	Ta (°C)	Tc (°C)	Ra (°C/W)	Rc (°C/W)	R (°C/W)	Identification
1	4.15	32.87	30.84	28.33	0.489	0.603	1.092	20% Ethanol
2	6.57	40.00	37.36	34.07	0.402	0.501	0.903	20% Ethanol
3	8.90	47.25	44.06	39.75	0.358	0.485	0.843	20% Ethanol
4	12.82	58.78	54.65	48.51	0.322	0.479	0.801	20% Ethanol
5	17.14	68.88	63.64	55.95	0.306	0.449	0.755	20% Ethanol
6	20.60	76.58	70.56	61.71	0.292	0.430	0.722	20% Ethanol
7	24.32	83.46	76.56	67.06	0.284	0.391	0.674	20% Ethanol

Table APP. 45: Data table for (WF: Ethanol, FR: 40%) on rosette insert CLPHP

Sl No.	Q (W)	Te (°C)	Ta (°C)	Tc (°C)	Ra (°C/W)	Rc (°C/W)	R (°C/W)	Identification
1	4.15	32.27	30.13	27.87	0.513	0.546	1.059	40% Ethanol
2	6.57	39.22	36.88	33.62	0.357	0.496	0.853	40% Ethanol
3	8.90	45.85	42.56	38.78	0.369	0.425	0.794	40% Ethanol
4	12.82	56.54	52.18	46.98	0.340	0.405	0.745	40% Ethanol
5	17.14	66.84	60.58	54.61	0.365	0.349	0.714	40% Ethanol
6	20.60	75.07	68.12	61.03	0.337	0.344	0.681	40% Ethanol
7	24.32	82.25	74.65	66.89	0.312	0.319	0.632	40% Ethanol

Table APP. 46: Data table for (WF: Ethanol, FR: 60%) on rosette insert CLPHP

Sl No.	Q (W)	Te (°C)	Ta (°C)	Tc (°C)	Ra (°C/W)	Rc (°C/W)	R (°C/W)	Identification
1	4.15	32.03	30.05	27.80	0.477	0.542	1.019	60% Ethanol
2	6.57	38.52	36.06	33.19	0.374	0.438	0.812	60% Ethanol
3	8.90	44.14	41.25	37.31	0.325	0.443	0.768	60% Ethanol
4	12.82	55.17	51.38	45.90	0.296	0.427	0.723	60% Ethanol
5	17.14	65.41	59.75	53.72	0.330	0.352	0.682	60% Ethanol
6	20.60	73.52	67.30	60.19	0.302	0.346	0.647	60% Ethanol
7	24.01	80.78	73.94	65.79	0.285	0.339	0.624	60% Ethanol

Table APP. 47: Data table for (WF: Ethanol, FR: 80%) on rosette insert CLPHP

Sl No.	Q (W)	Te (°C)	Ta (°C)	Tc (°C)	Ra (°C/W)	Rc (°C/W)	R (°C/W)	Identification
1	4.15	32.85	30.69	28.15	0.521	0.611	1.131	80% Ethanol
2	6.57	41.22	38.26	35.12	0.451	0.478	0.929	80% Ethanol
3	8.90	49.52	45.77	41.69	0.421	0.459	0.880	80% Ethanol
4	12.82	60.52	55.23	50.02	0.412	0.407	0.819	80% Ethanol
5	17.14	70.41	63.02	57.08	0.431	0.347	0.778	80% Ethanol
6	20.60	77.50	69.83	62.30	0.372	0.366	0.738	80% Ethanol
7	24.32	84.29	73.92	67.50	0.426	0.264	0.690	80% Ethanol

Table APP. 48: Data table for (WF: Methanol, FR: 20%) on rosette insert CLPHP

Sl No.	Q (W)	Te (°C)	Ta (°C)	Tc (°C)	Ra (°C/W)	Rc (°C/W)	R (°C/W)	Identification
1	4.15	32.08	30.74	28.65	0.323	0.504	0.826	20% Methanol
2	8.90	44.65	42.50	38.42	0.242	0.458	0.700	20% Methanol
3	12.82	55.12	51.76	46.42	0.262	0.416	0.678	20% Methanol
4	16.19	62.48	58.19	51.88	0.265	0.390	0.655	20% Methanol
5	21.79	71.41	65.59	57.58	0.267	0.368	0.635	20% Methanol

Table APP. 49: Data table for (WF: Methanol, FR: 40%) on rosette insert CLPHP

Sl No.	Q (W)	Te (°C)	Ta (°C)	Tc (°C)	Ra (°C/W)	Rc (°C/W)	R (°C/W)	Identification
1	4.15	32.15	30.75	28.85	0.337	0.457	0.794	40% Methanol
2	8.90	43.59	40.72	37.52	0.322	0.360	0.682	40% Methanol
3	12.82	53.49	49.79	45.29	0.289	0.351	0.639	40% Methanol
4	16.19	61.10	56.33	51.00	0.295	0.329	0.624	40% Methanol
5	21.79	70.25	63.84	56.85	0.294	0.321	0.615	40% Methanol

Table APP. 50: Data table for (WF: Methanol, FR: 60%) on rosette insert CLPHP

Sl No.	Q (W)	Te (°C)	Ta (°C)	Tc (°C)	Ra (°C/W)	Rc (°C/W)	R (°C/W)	Identification
1	4.15	32.54	30.90	29.27	0.396	0.391	0.786	60% Methanol
2	8.90	42.25	39.37	36.25	0.324	0.351	0.674	60% Methanol
3	12.82	51.76	47.63	43.63	0.322	0.312	0.634	60% Methanol
4	16.19	59.46	54.45	49.44	0.309	0.310	0.619	60% Methanol
5	21.79	68.92	61.98	55.72	0.319	0.287	0.606	60% Methanol

Table APP. 51: Data table for (WF: Methanol, FR: 80%) on rosette insert CLPHP

Sl No.	Q (W)	Te (°C)	Ta (°C)	Tc (°C)	Ra (°C/W)	Rc (°C/W)	R (°C/W)	Identification
1	4.15	32.87	31.18	28.93	0.406	0.541	0.947	80% Methanol
2	8.90	45.87	42.25	38.70	0.407	0.398	0.805	80% Methanol
3	12.82	56.52	51.69	46.75	0.377	0.385	0.762	80% Methanol
4	16.19	63.83	58.04	52.10	0.358	0.367	0.725	80% Methanol
5	21.79	72.10	63.55	56.50	0.393	0.323	0.716	80% Methanol

SAMPLE CALCULATION

Sample Calculation: 01

Plain tube CLPHP: 60% water

From table: 6

Observation no: 7

Heat input, Q= 31.008 Watt

Average Evaporator temperature: T_e=108.47 ˚C

Average adiabatic temperature: T_a=96.35 ˚C

Average Condenser temperature: T_c=86.84 ˚C

From equation no: 8 from chapter 3,

$$Ra = \frac{T_e - T_a}{Q_{input}} = \frac{108.47 - 96.35}{31.008} = .39087 \approx 0.39 \text{ ˚C/W}$$

$$Rc = \frac{(T_a - T_c)}{Q_{input}} = \frac{96.35 - 86.84}{31.008} = 0.30669 \approx 0.31 \text{ ˚C/W}$$

Net thermal resistance, $R = \frac{(T_e - T_c)}{Q_{input}} = \frac{108.47 - 86.84}{31.008} = 0.6974 \approx 0.697$ ˚C/W

Sample Calculation: 02

Wire insert CLPHP: 20% Ethanol

From table: 32

Observation no: 6

Heat input, Q= 21.1004 Watt

Average Evaporator temperature: T_e=79.59 ˚C

Average adiabatic temperature: T_a=70.89 ˚C

Average Condenser temperature: T_c=64.26 ˚C

From equation no: 9 in chapter 3,

$$Ra = \frac{T_e - T_a}{Qinput} = \frac{79.59 - 70.89}{21.1004} = 0.4123 \approx 0.41 \text{ °C/W}$$

$$Rc = \frac{(T_a - T_c)}{Q_{input}} = \frac{70.89 - 64.26}{21.1004} = 0.3142 \approx 0.31 \text{°C/W}$$

Net thermal resistance, $R = \frac{(T_e - T_c)}{Q_{input}} = \frac{79.59 - 64.26}{21.1004} = 0.7265 \approx 0.727 \text{ °C/W}$

Sample Calculation: 03

Rosette insert CLPHP: 60% Methanol

From table: 50

Observation no: 3

Heat input, Q= 12.8284 Watt

Average Evaporator temperature: T_e=49.89 °C

Average adiabatic temperature: T_a=45.89 °C

Average Condenser temperature: T_c=41.76 °C

From equation no: 9 in chapter 3,

$$Ra = \frac{T_e - T_a}{Qinput} = \frac{49.89 - 45.89}{12.8284} = 0.3118 \approx 0.31 \text{ °C/W}$$

$$Rc = \frac{(T_a - T_c)}{Q_{input}} = \frac{45.89 - 41.76}{12.8284} = 0.3219 \approx 0.32 \text{°C/W}$$

Net thermal resistance, $R = \frac{(T_e - T_c)}{Q_{input}} = \frac{49.89 - 41.76}{12.8284} = 0.6337 \approx 0.634 \text{ °C/W}$

EXPERIMENTAL GRAPHS

WF: Ethanol
FR: 80%

WF: Methanol
FR: 20%

WF: Methanol
FR: 40%
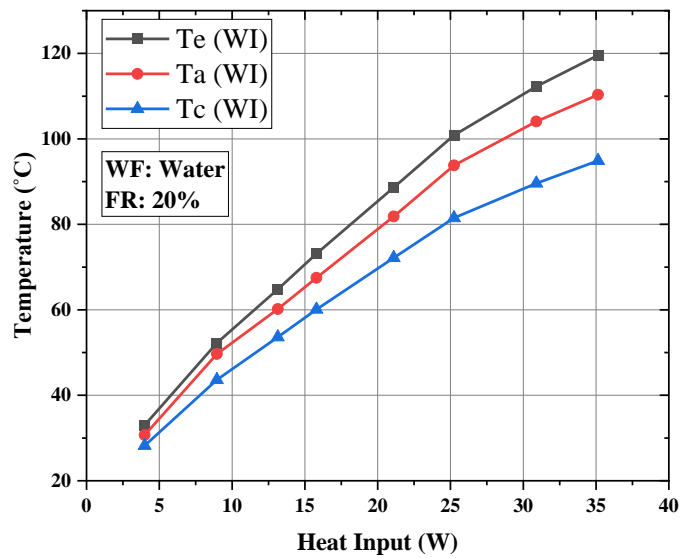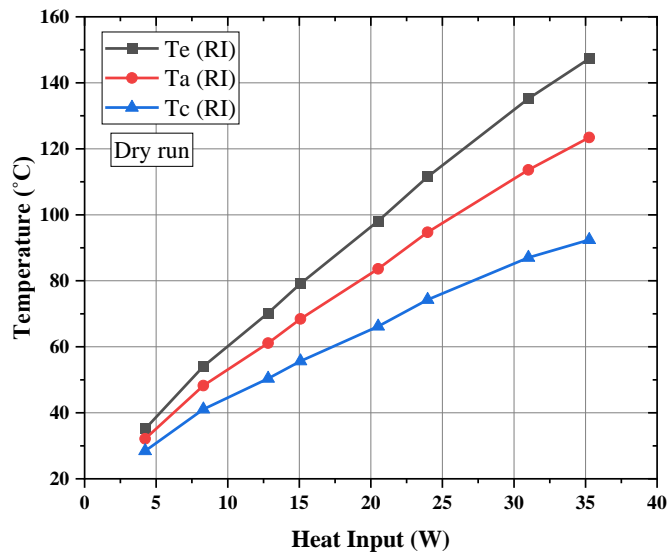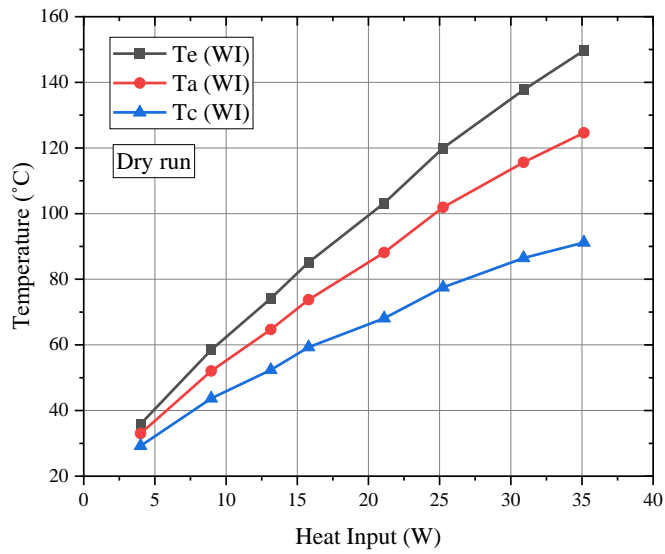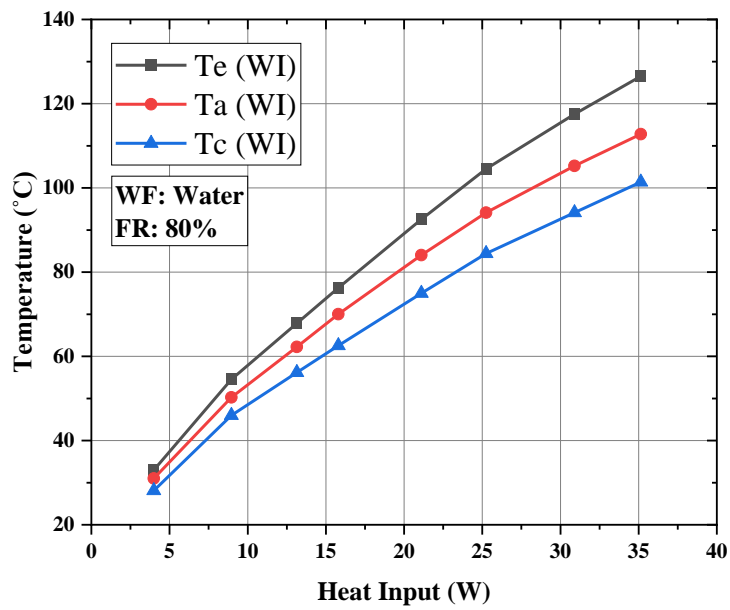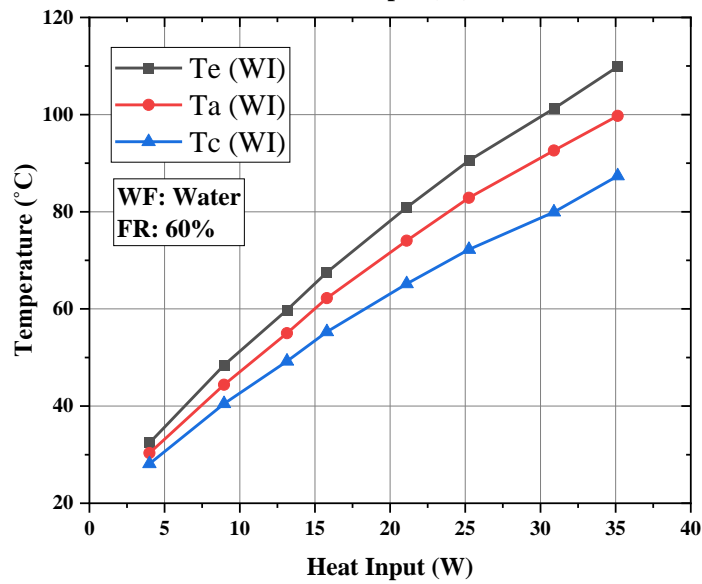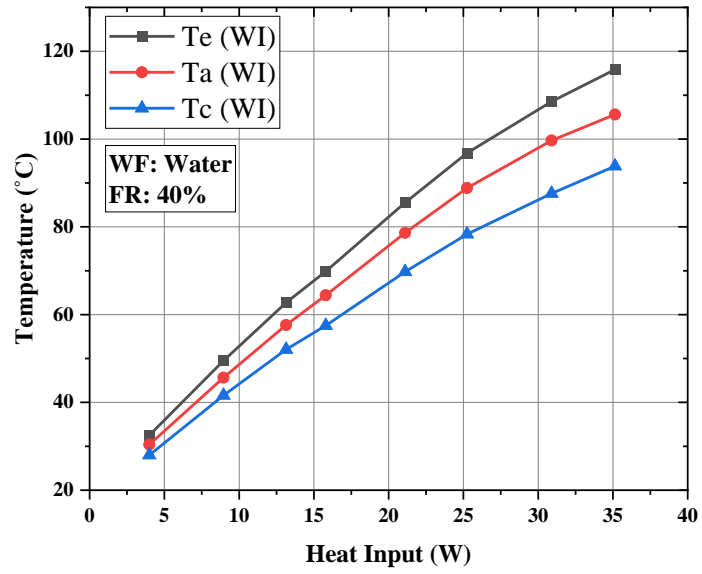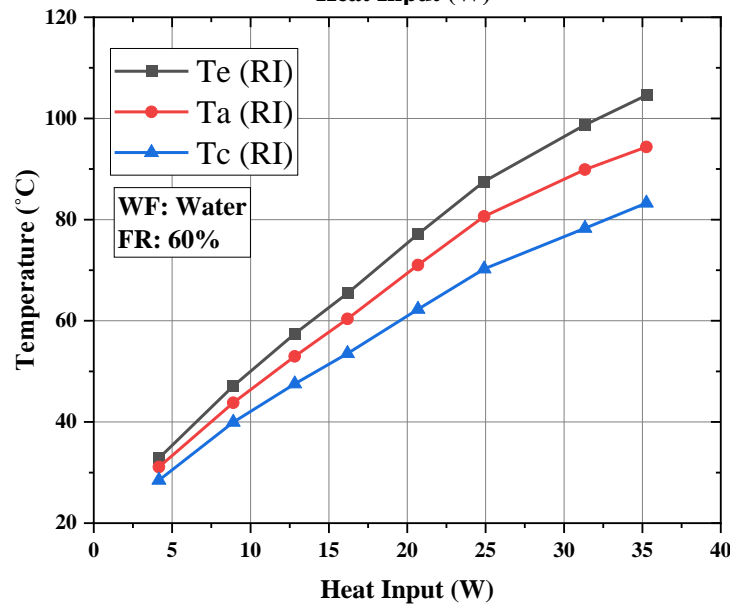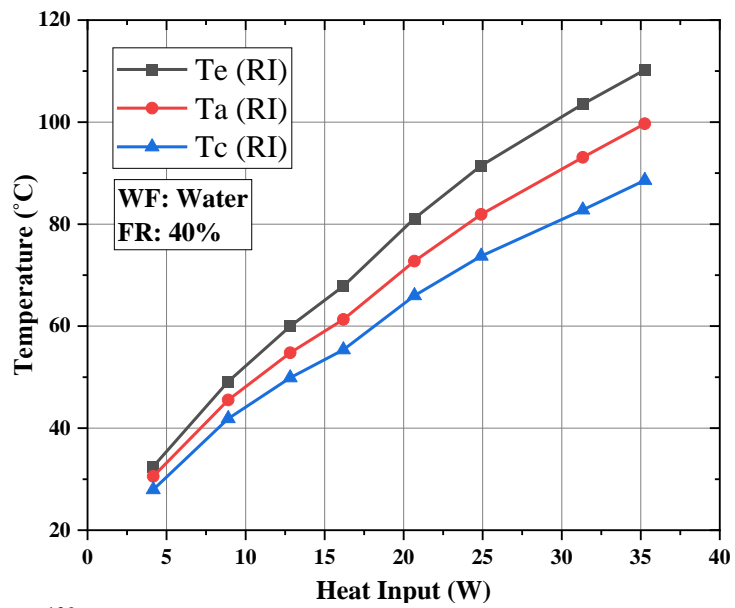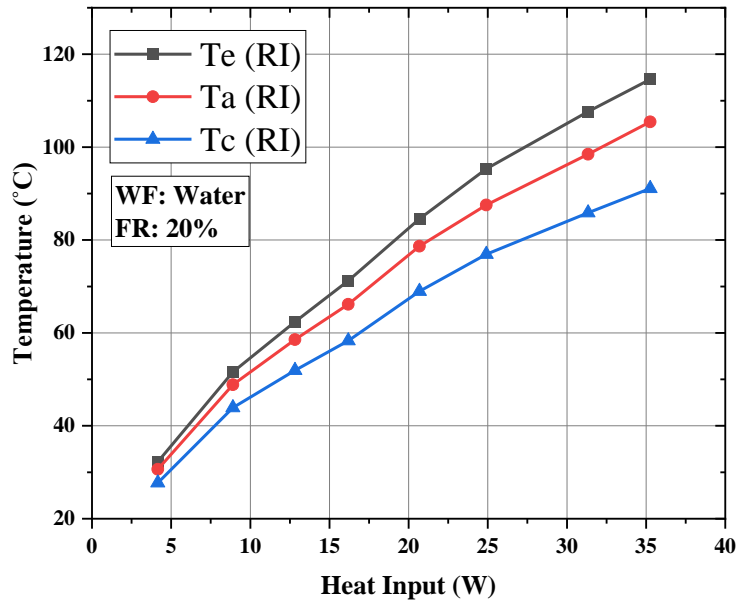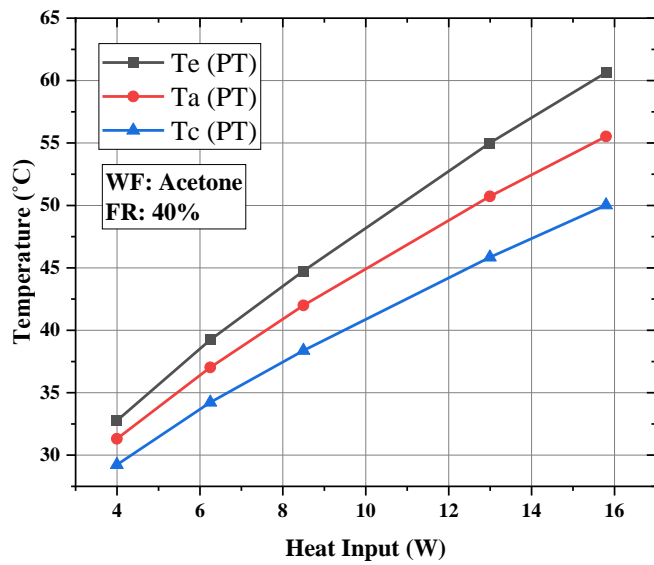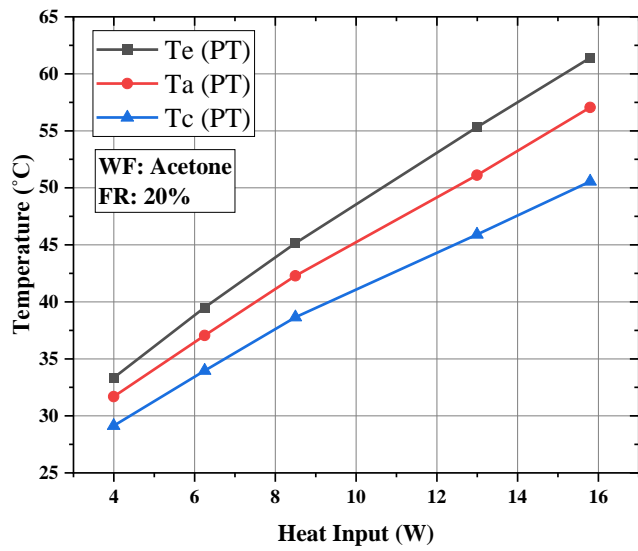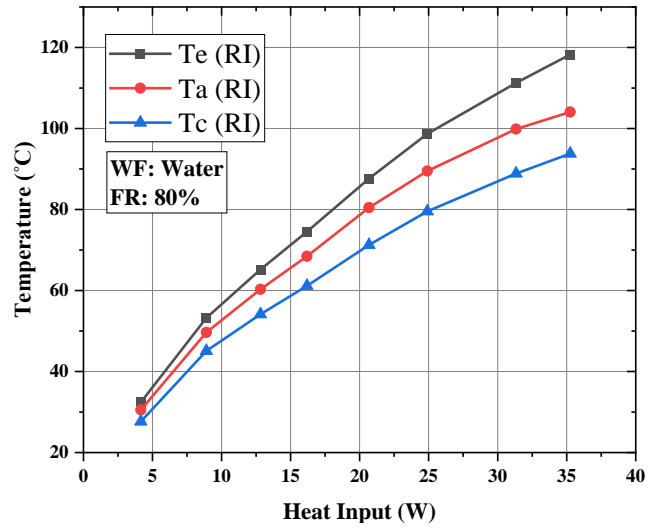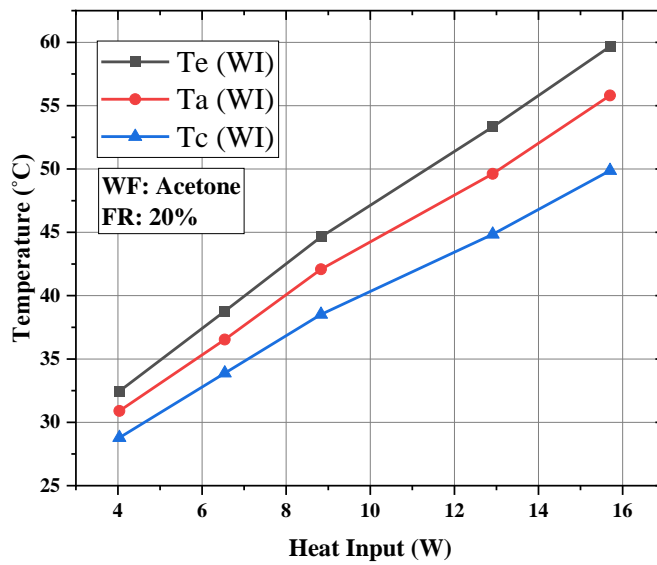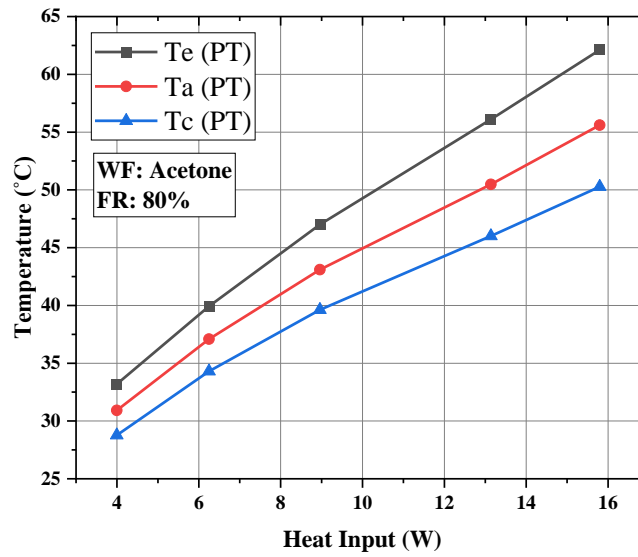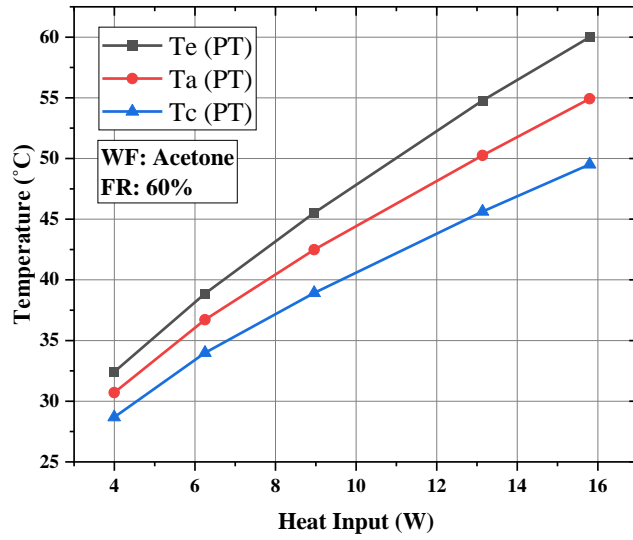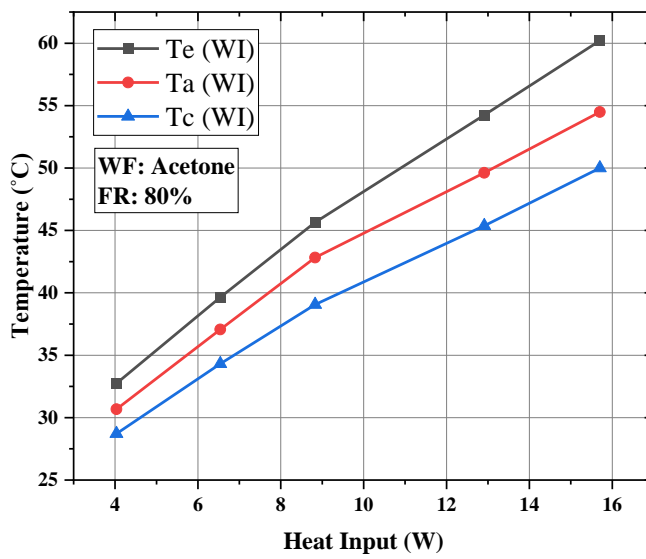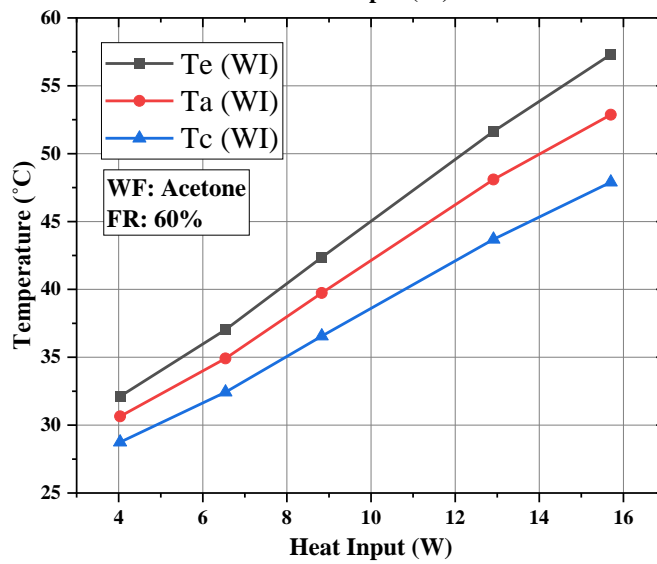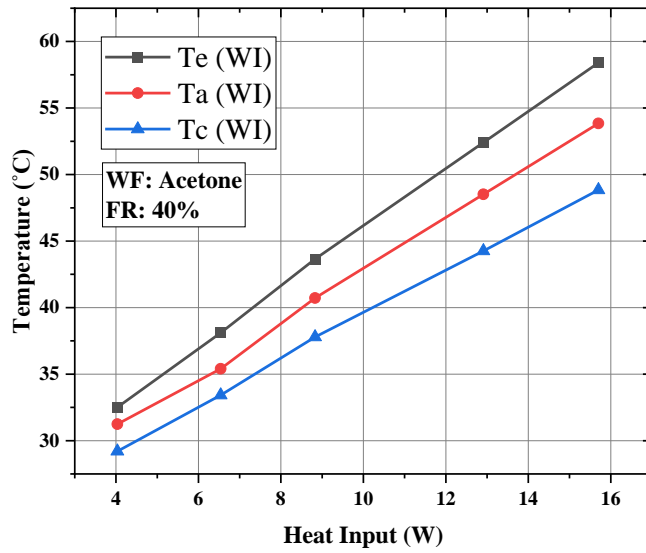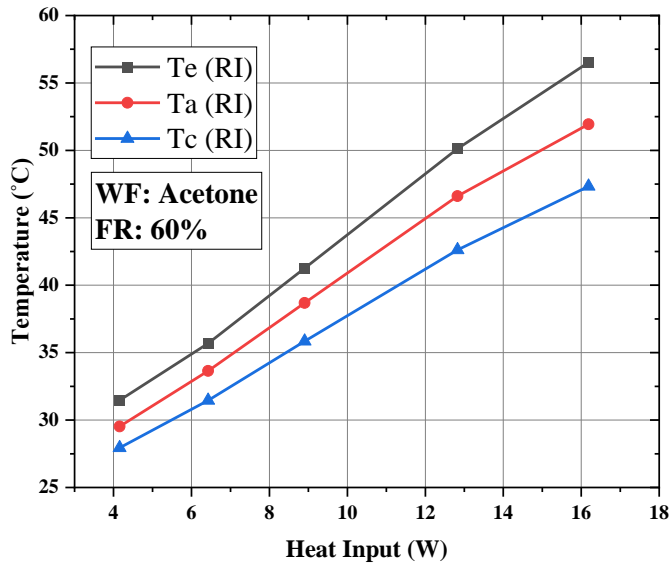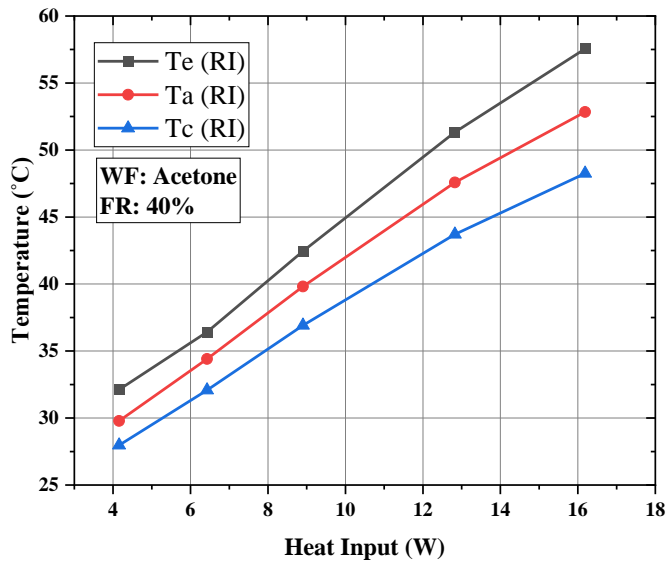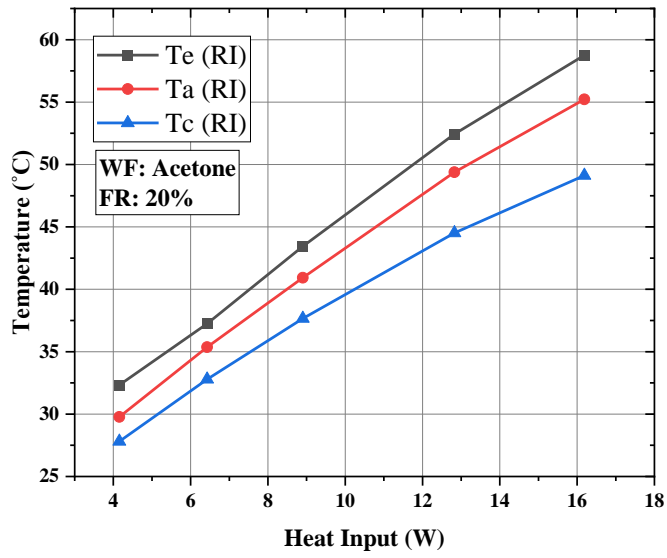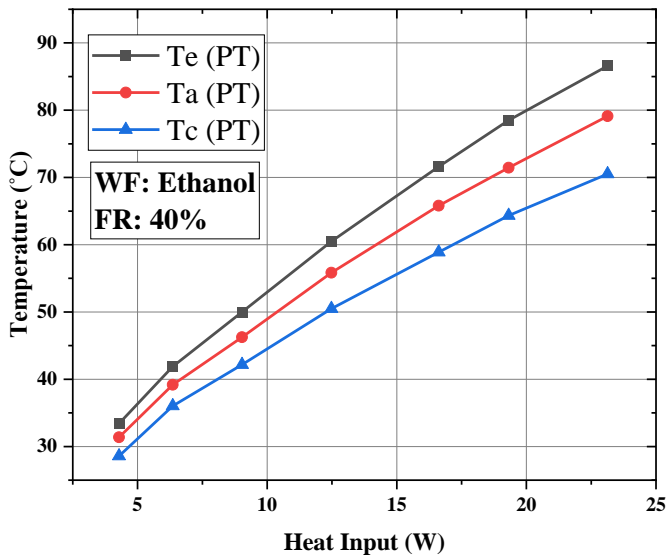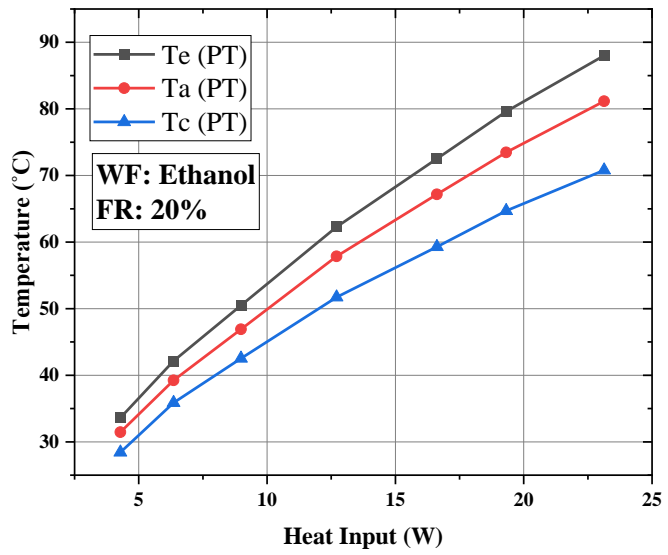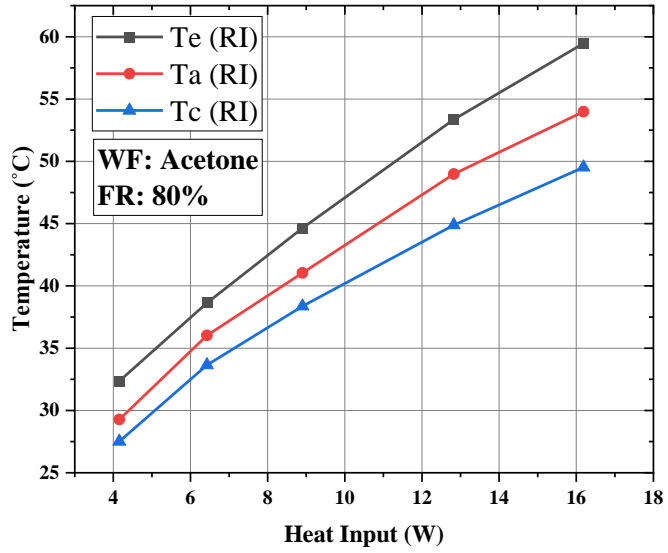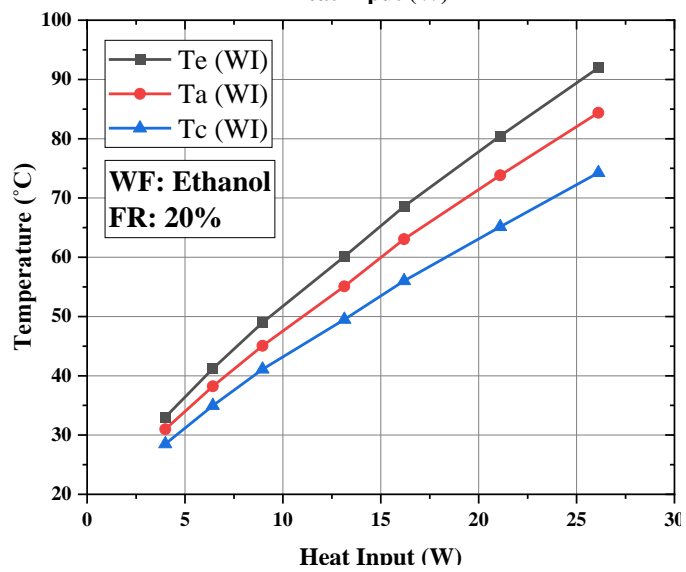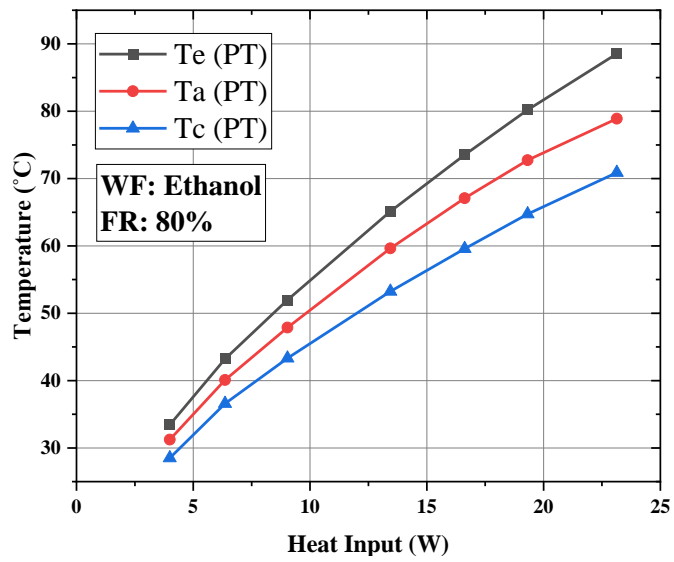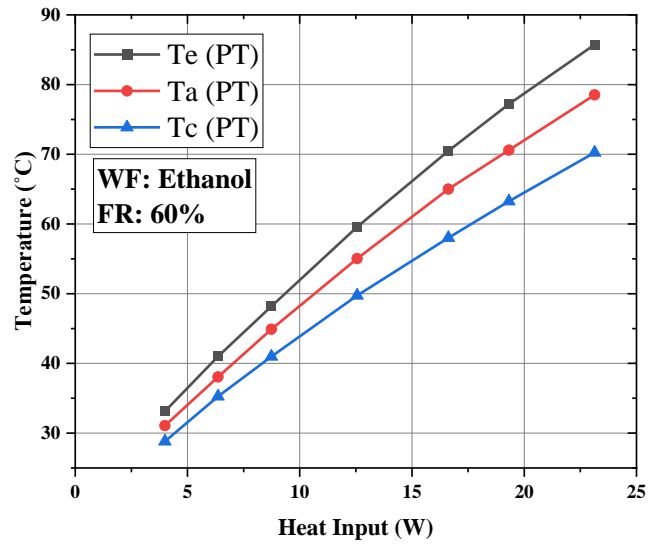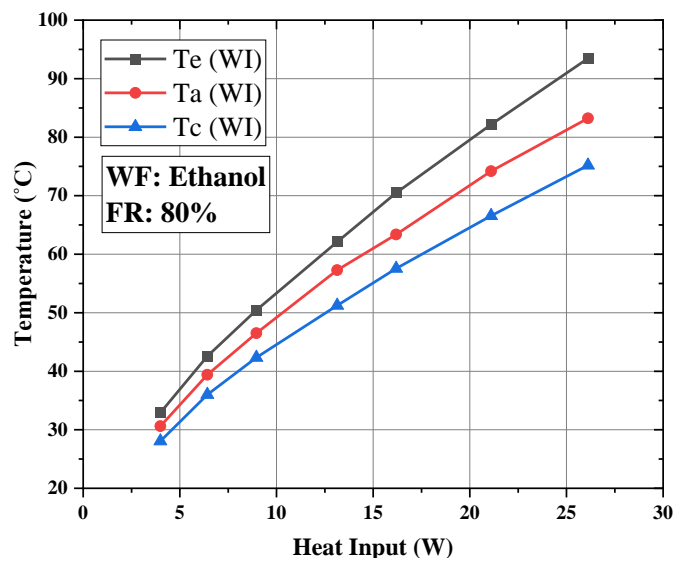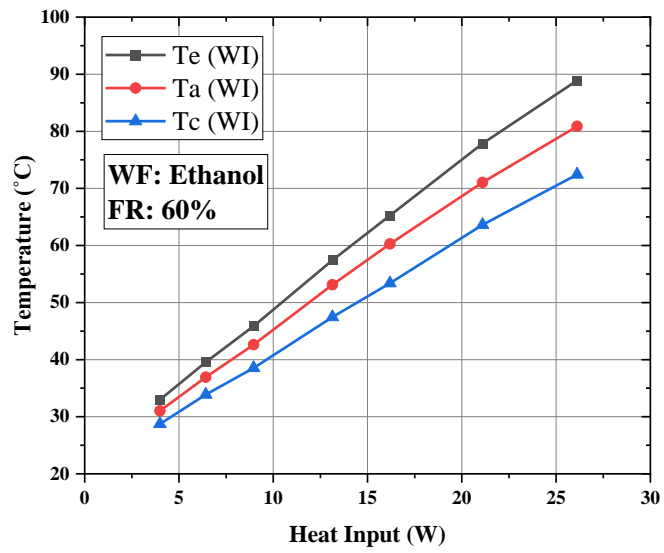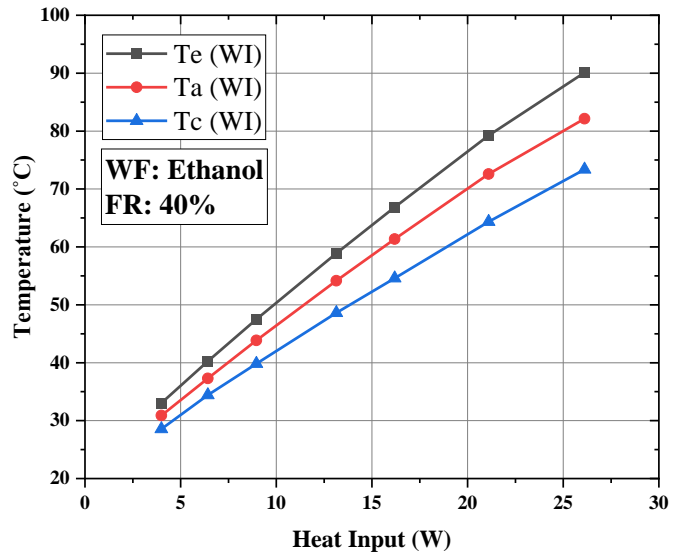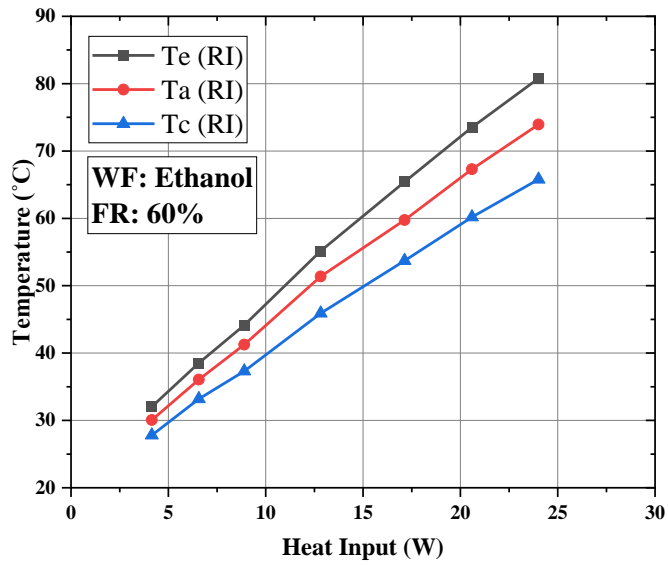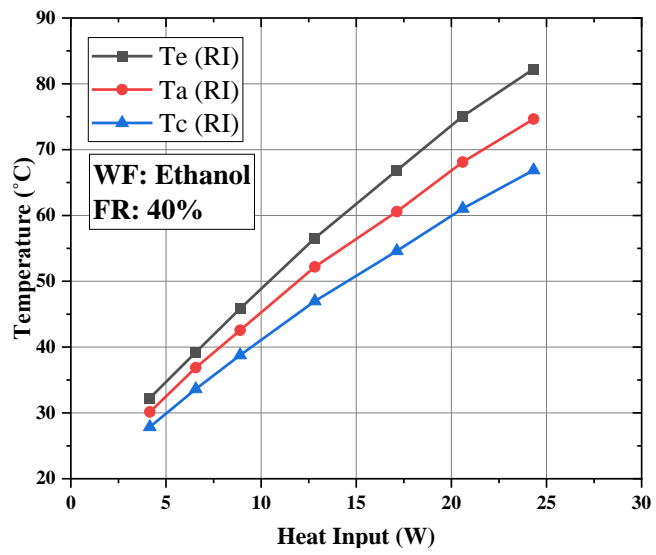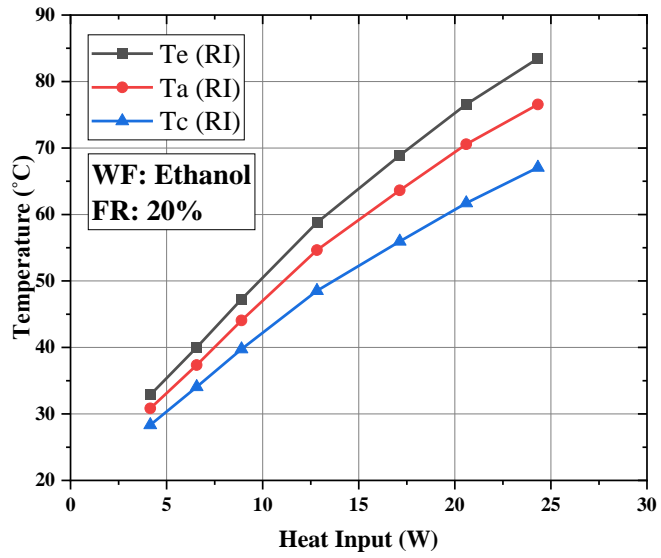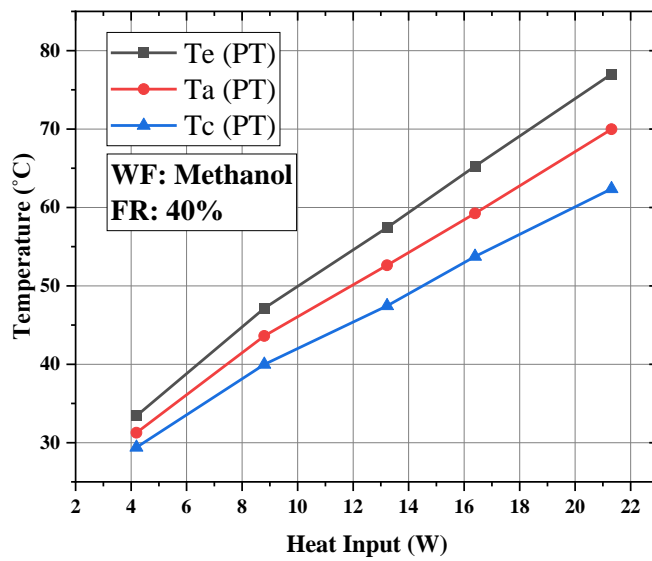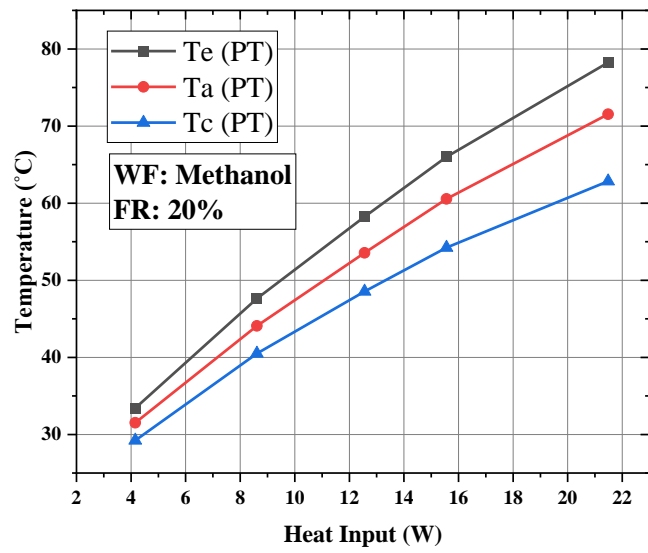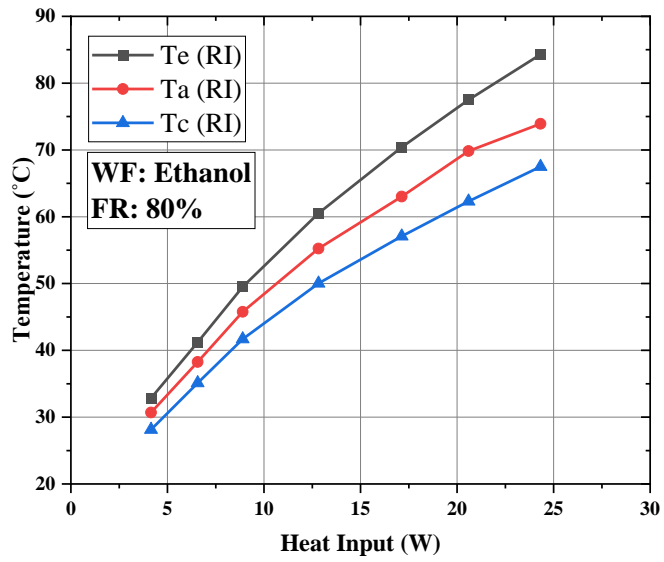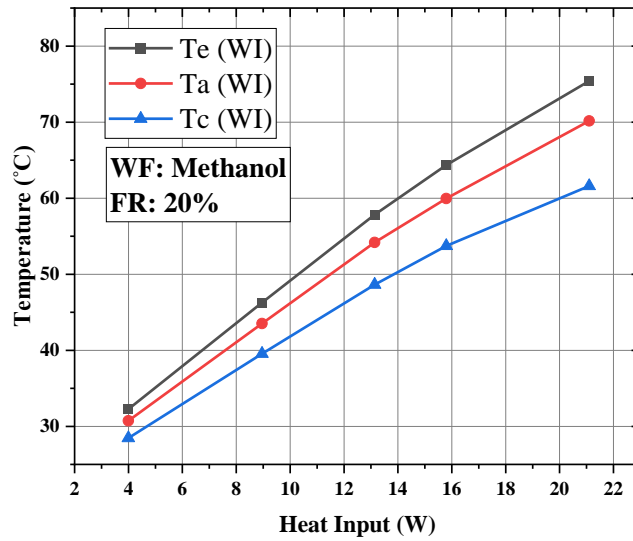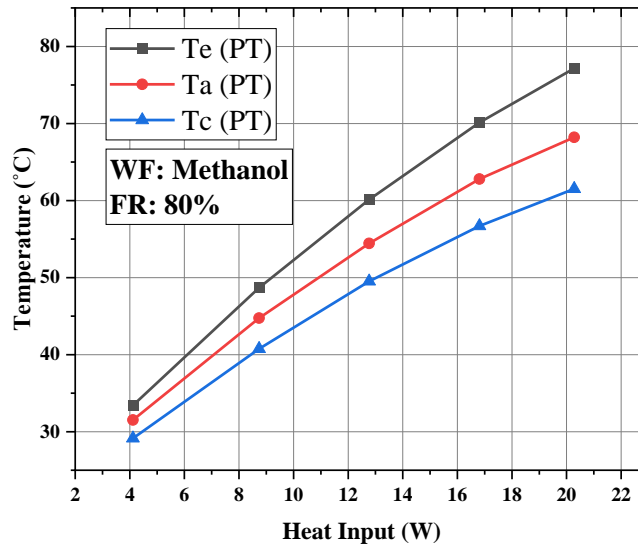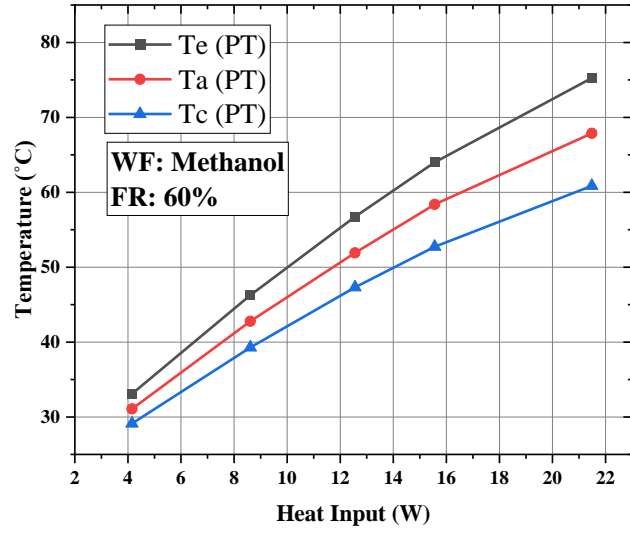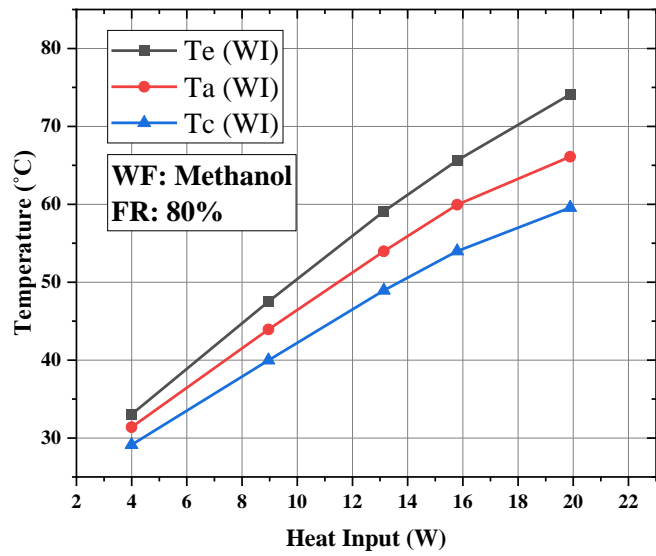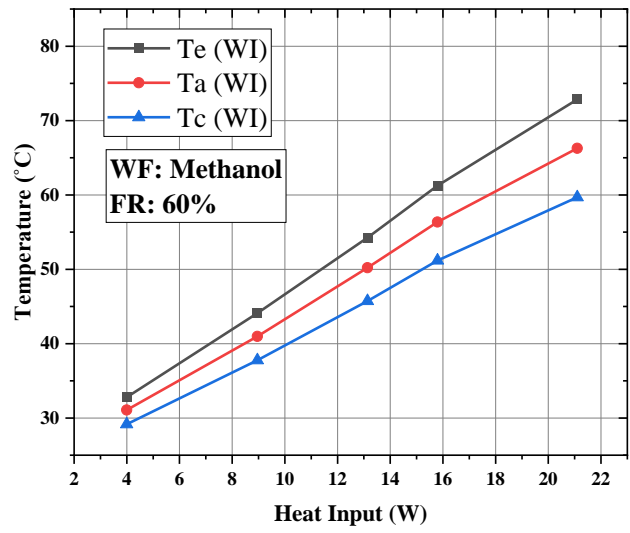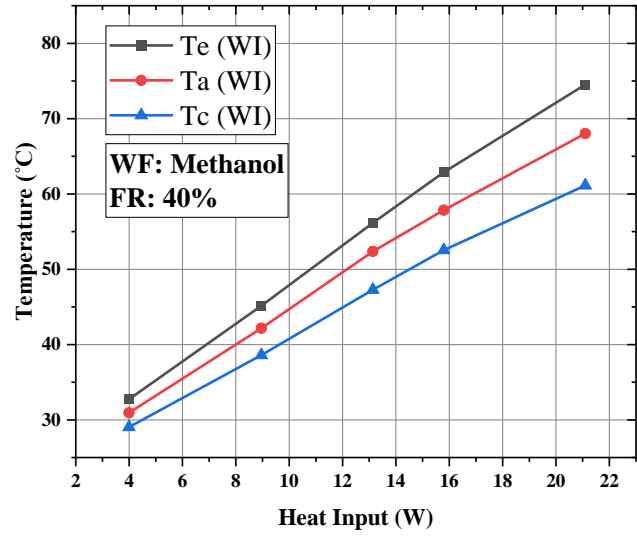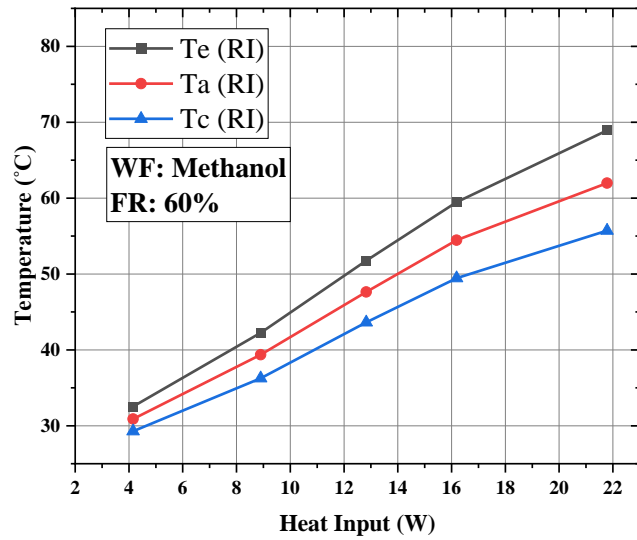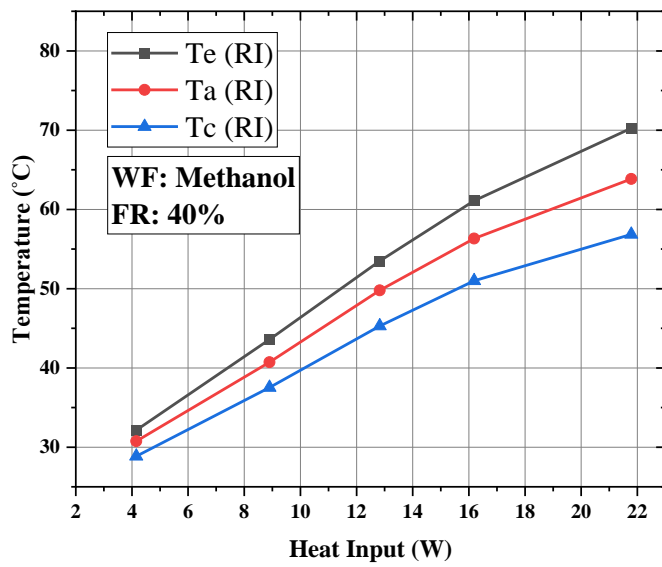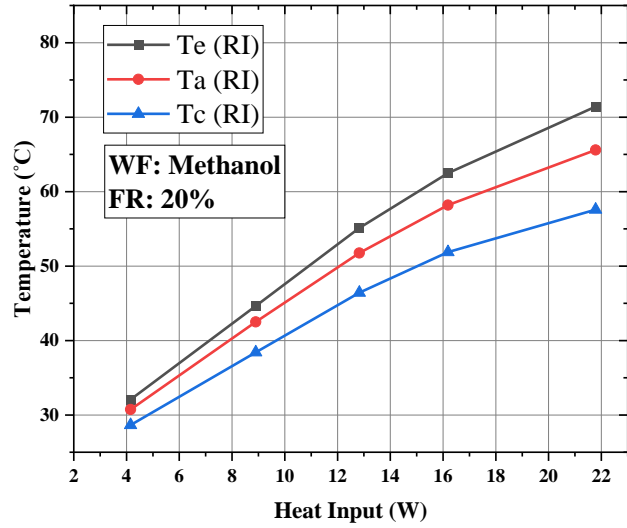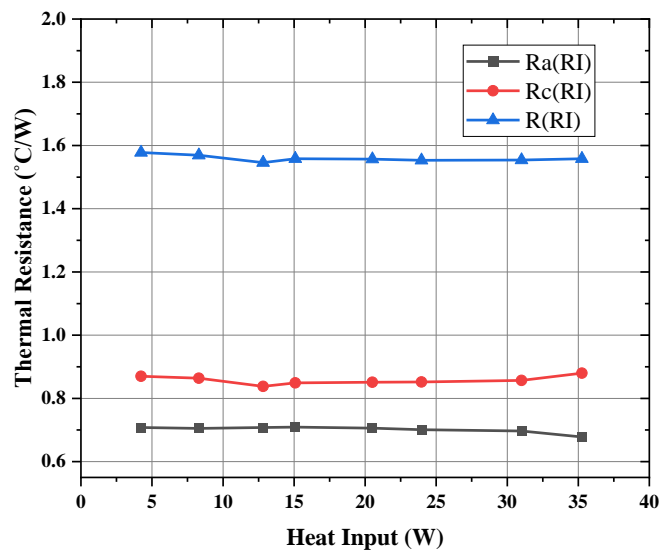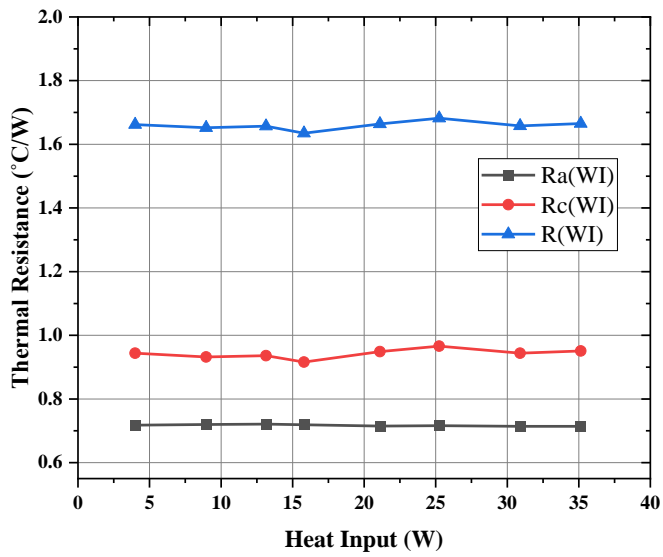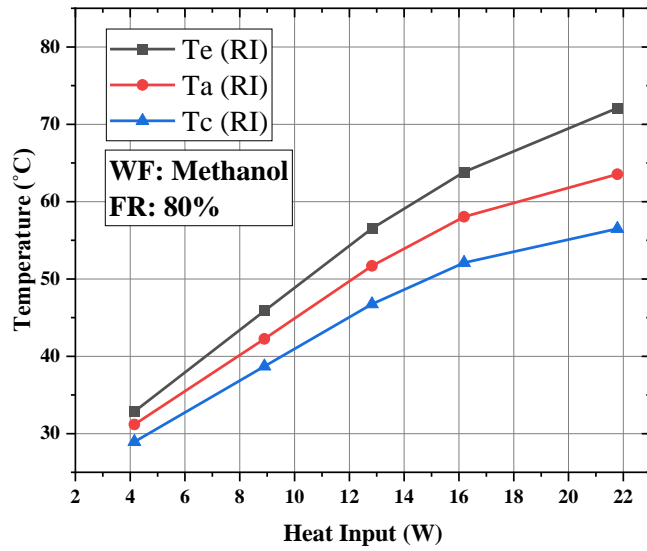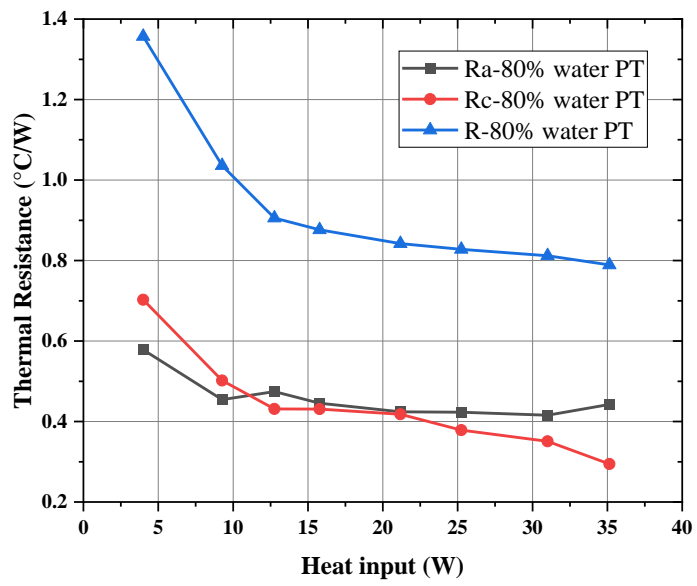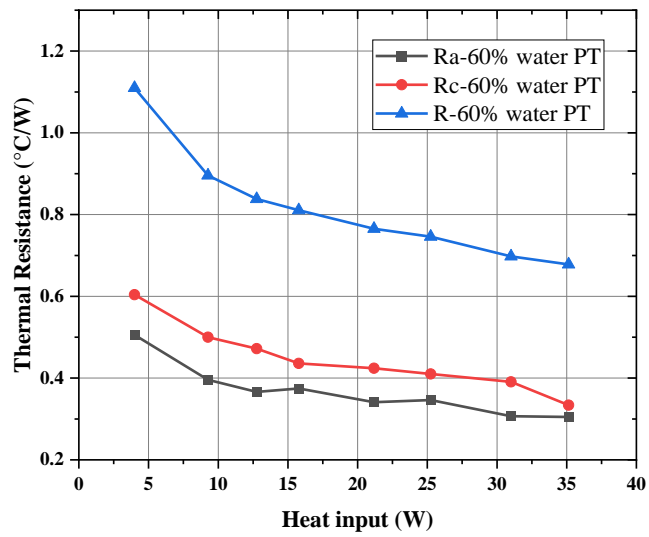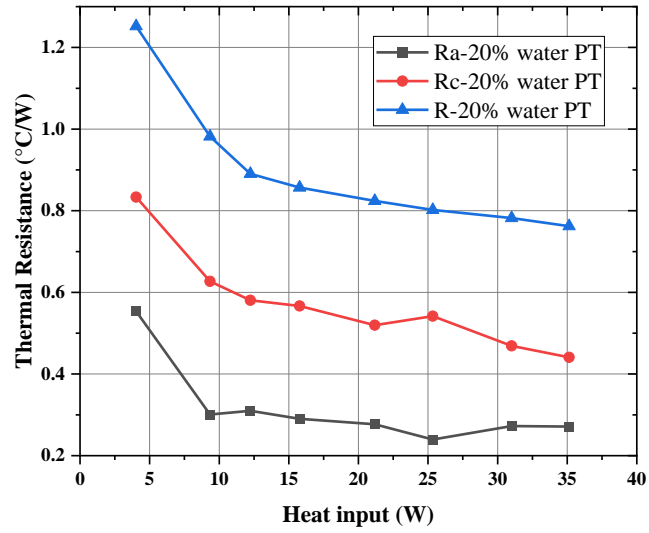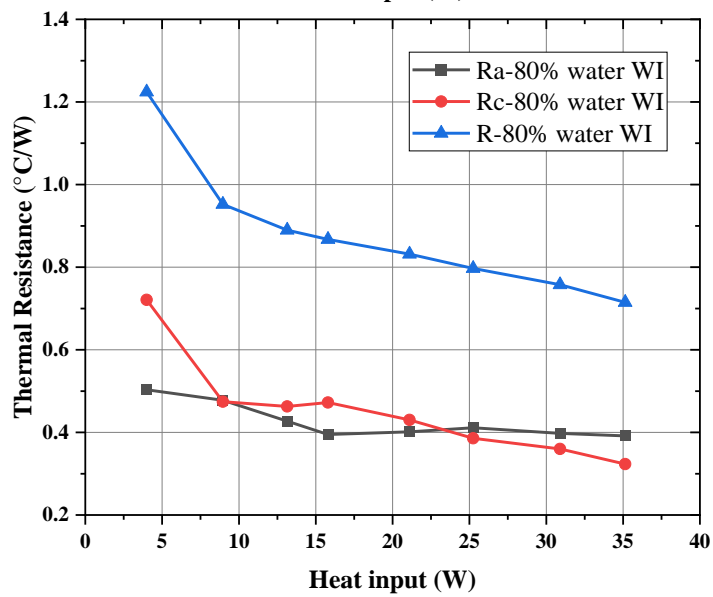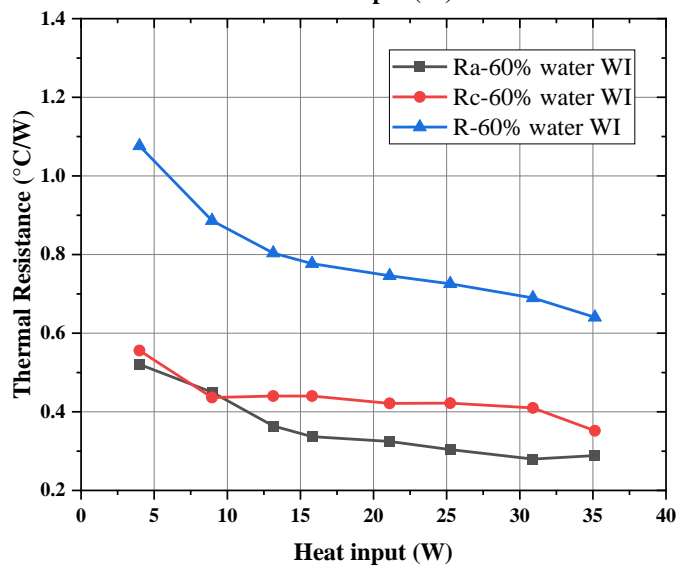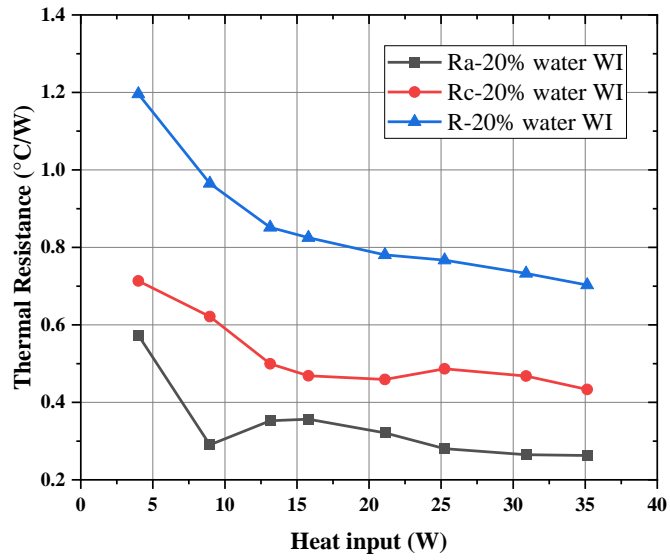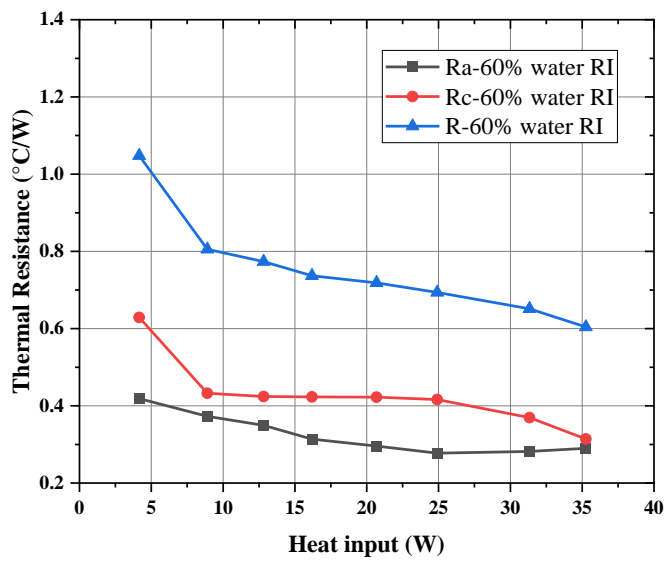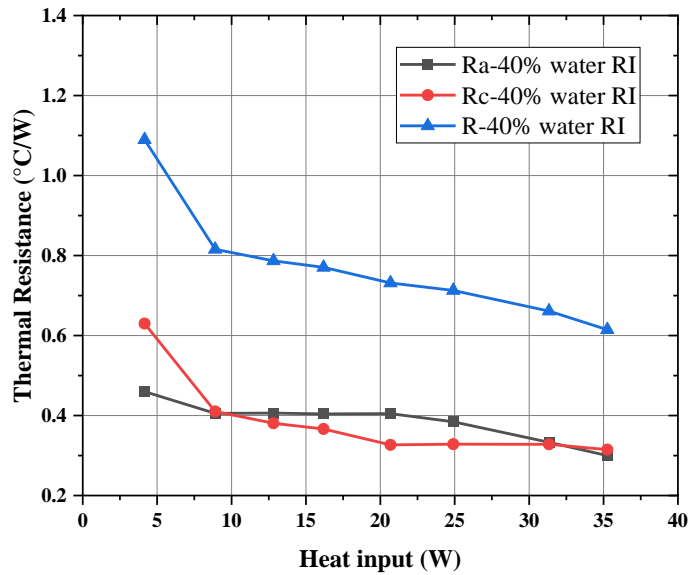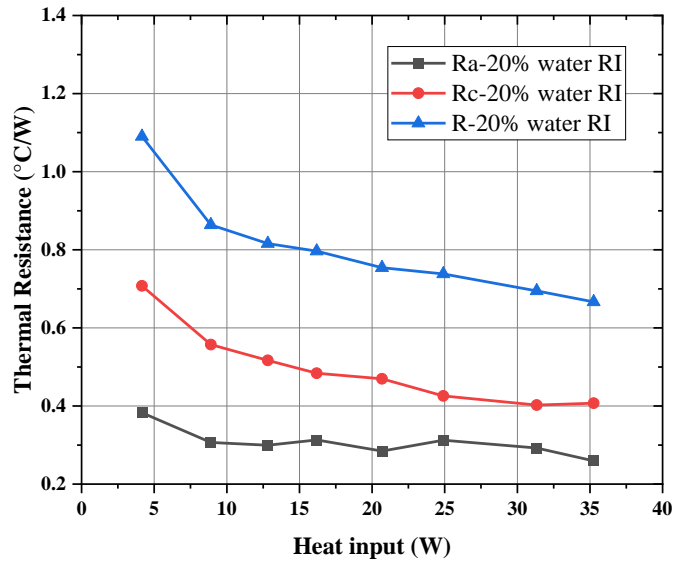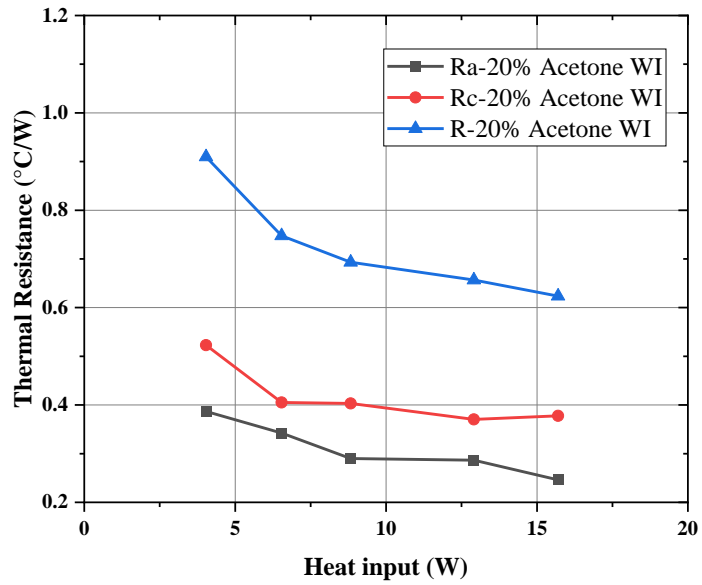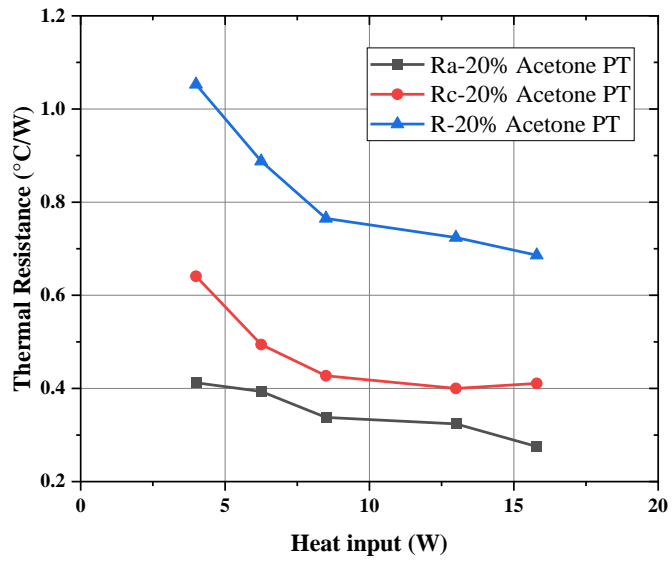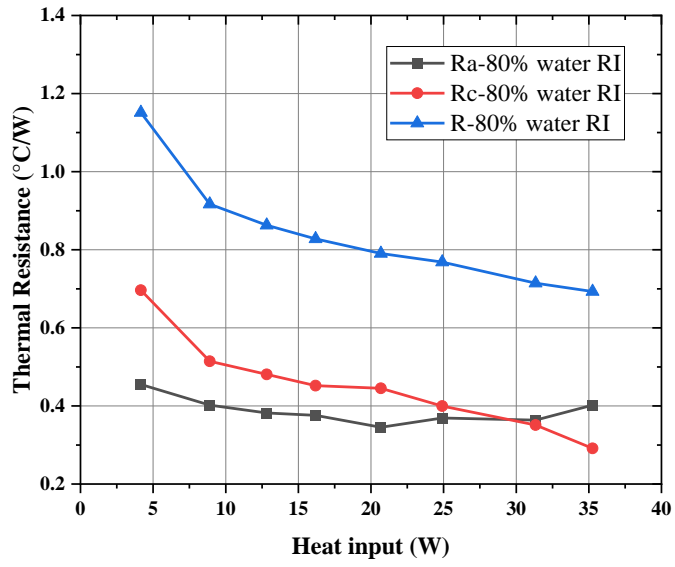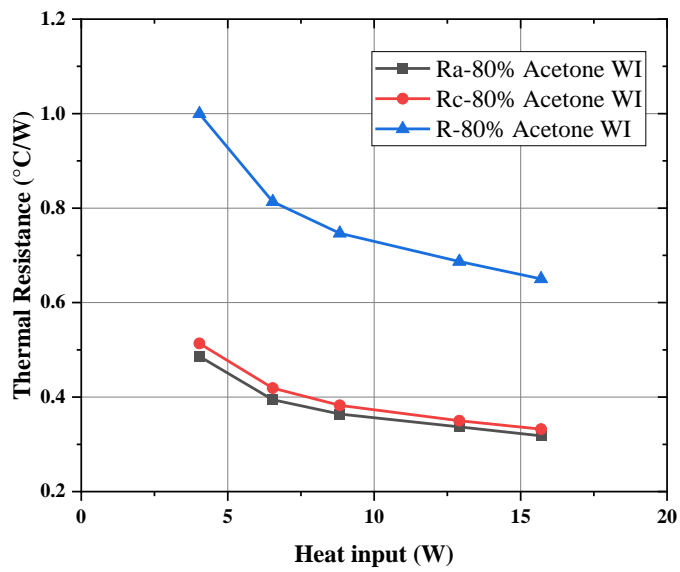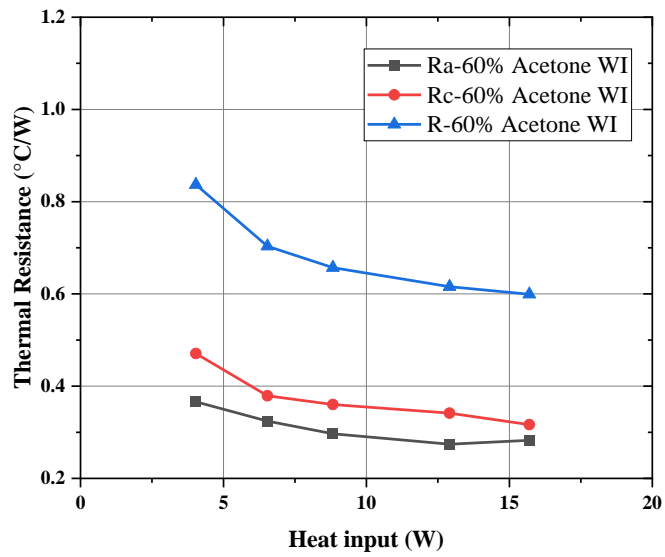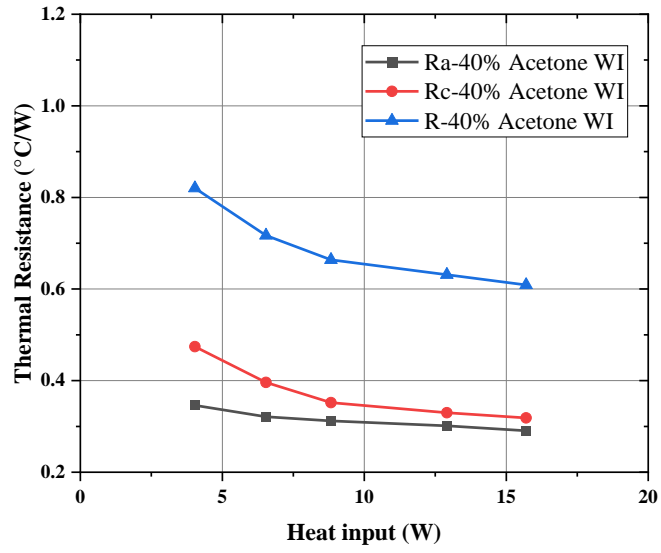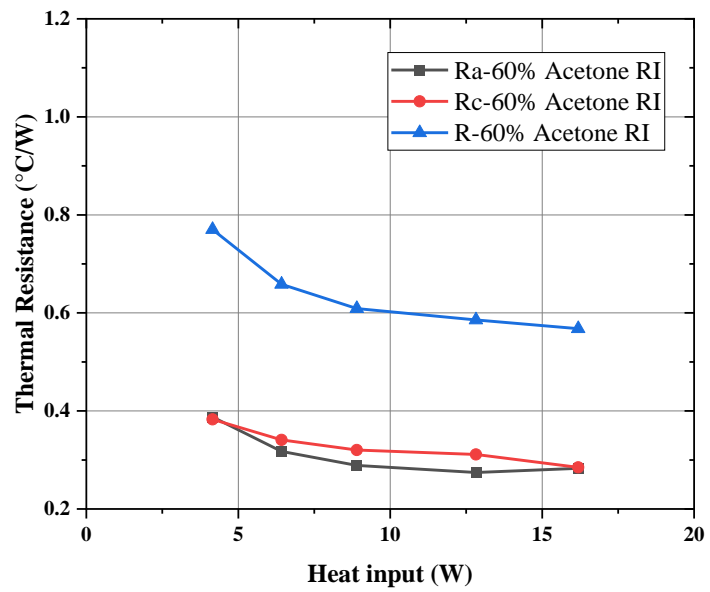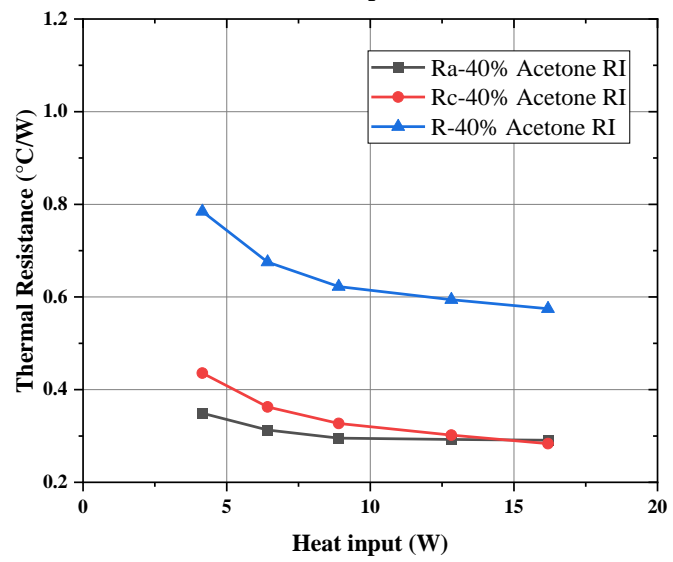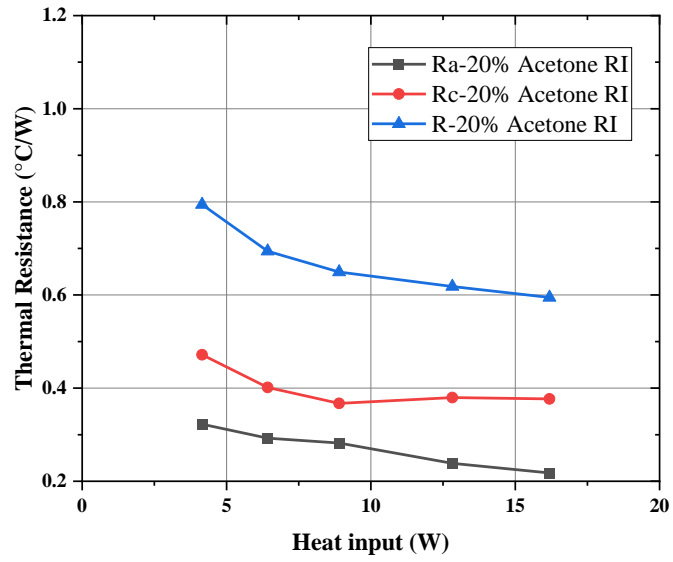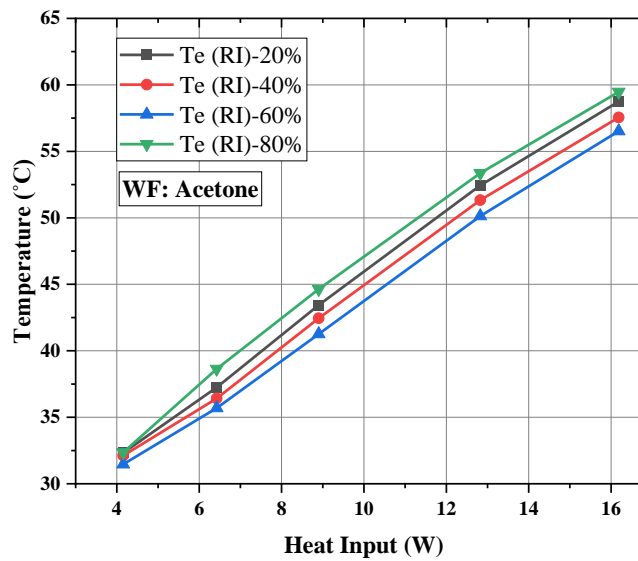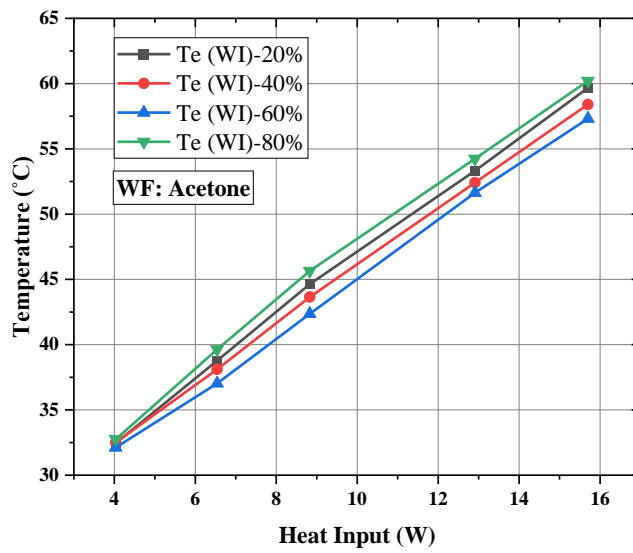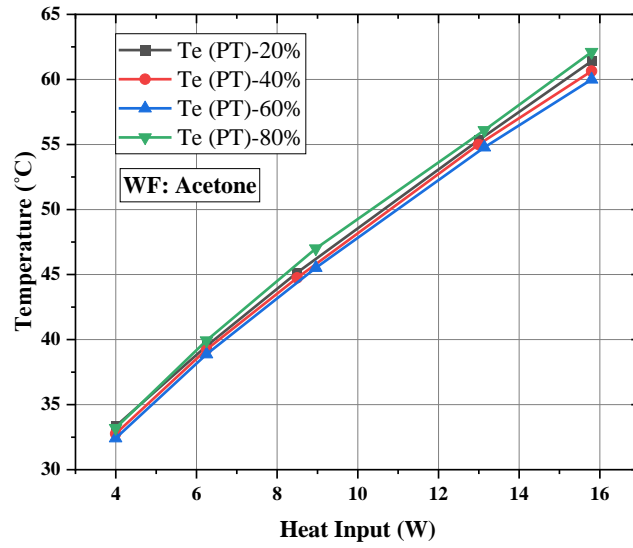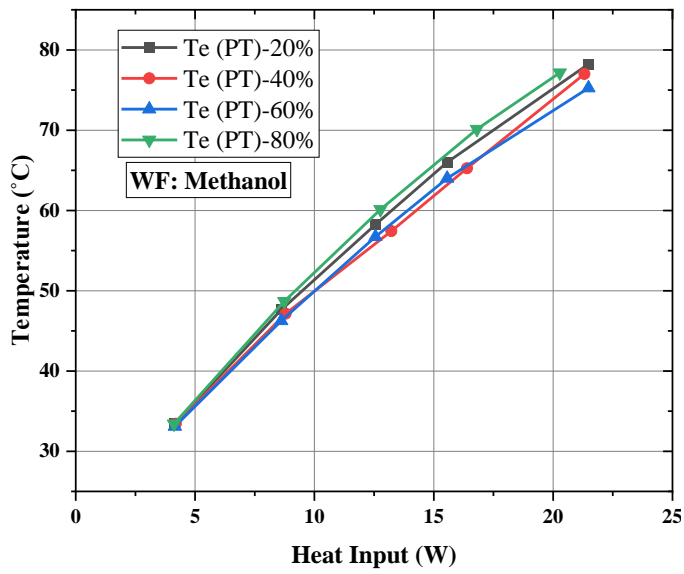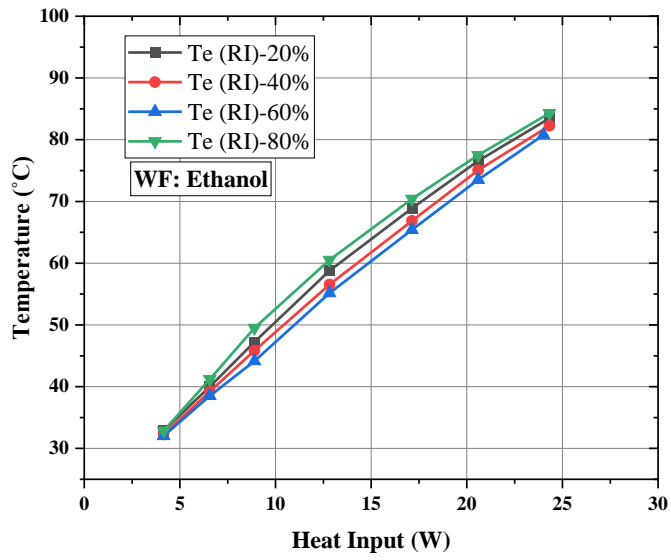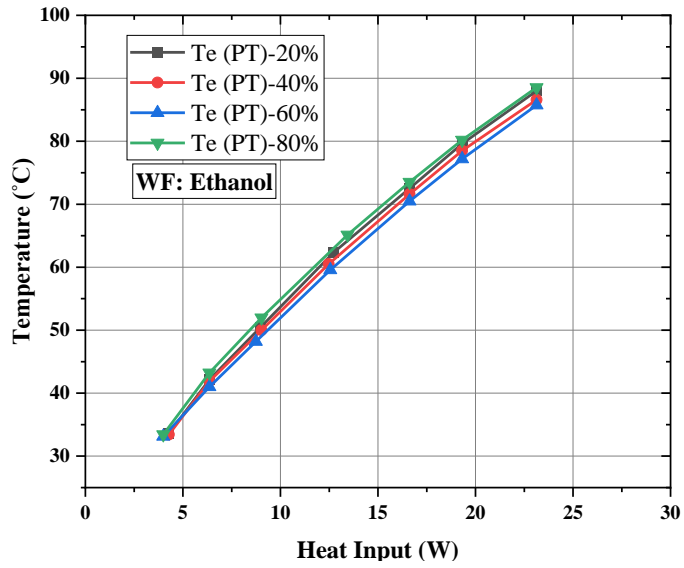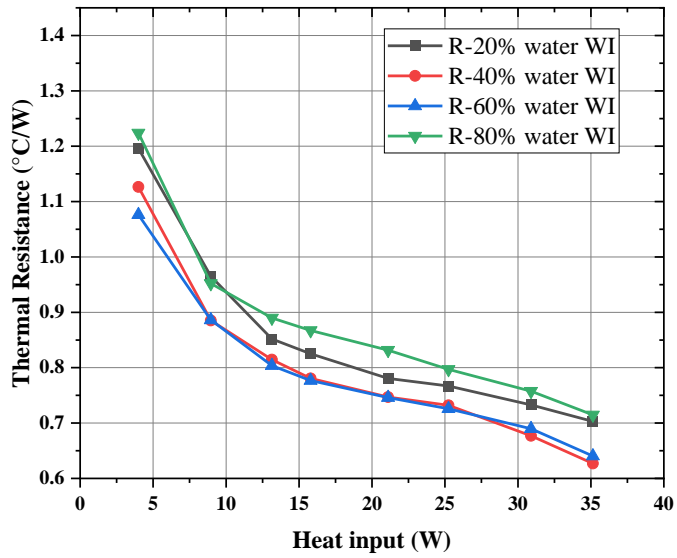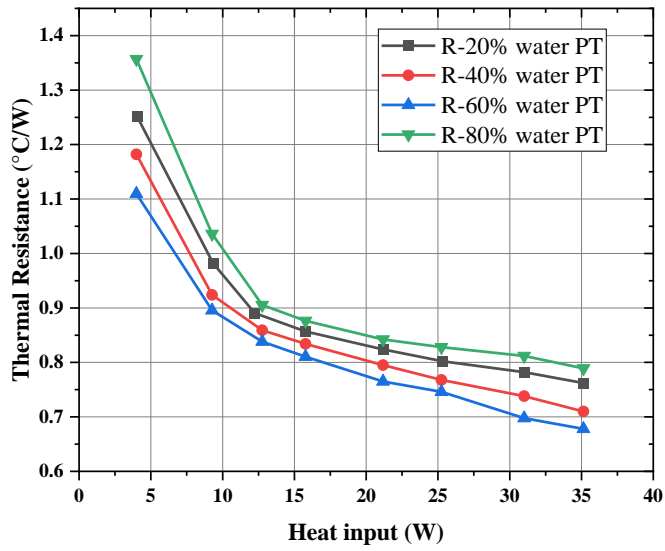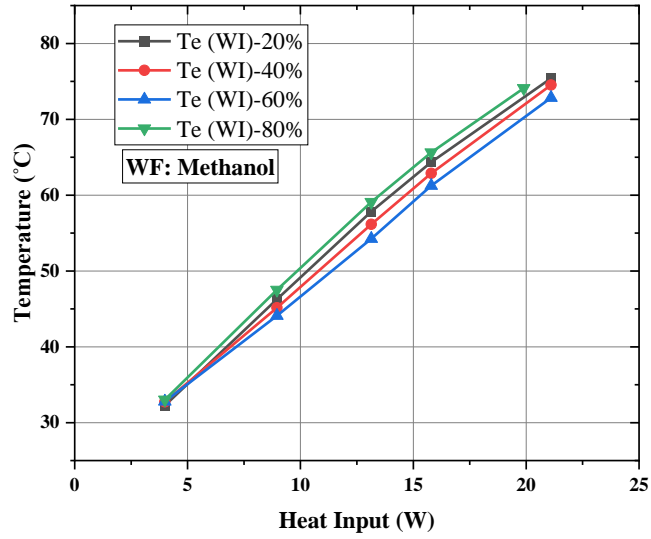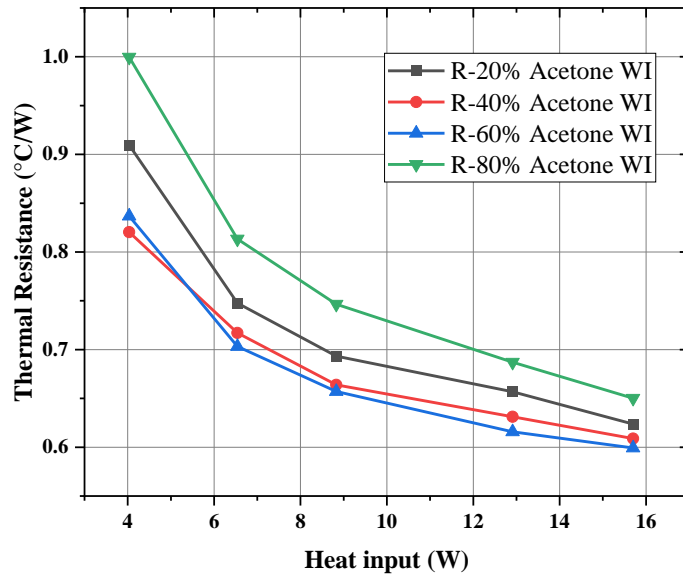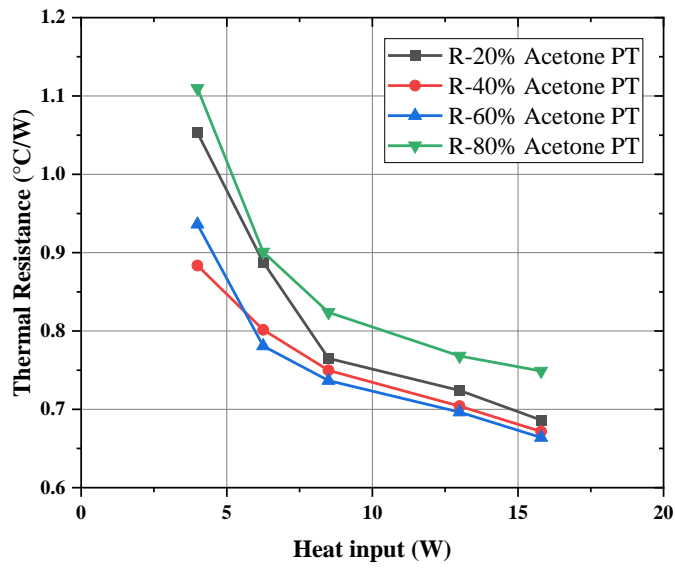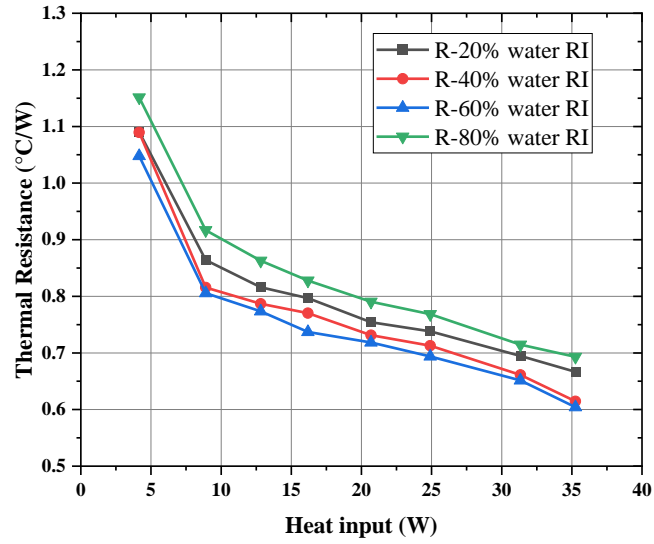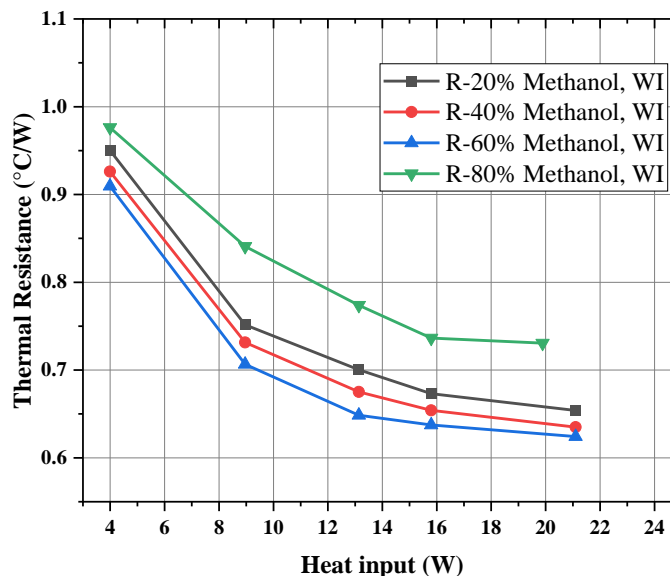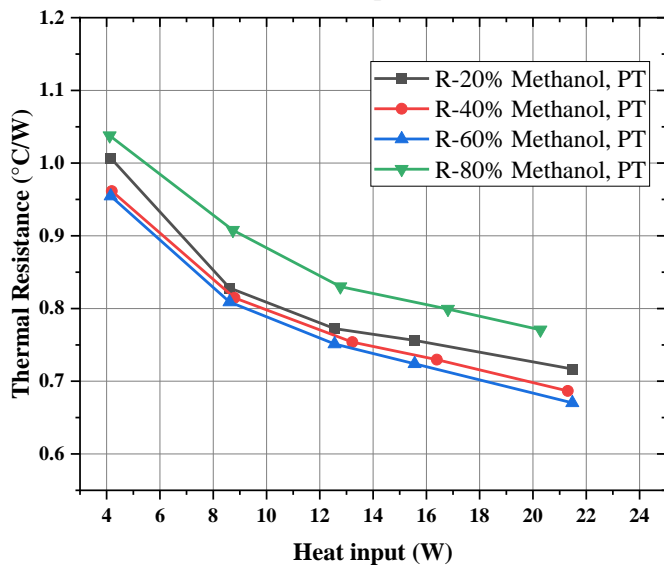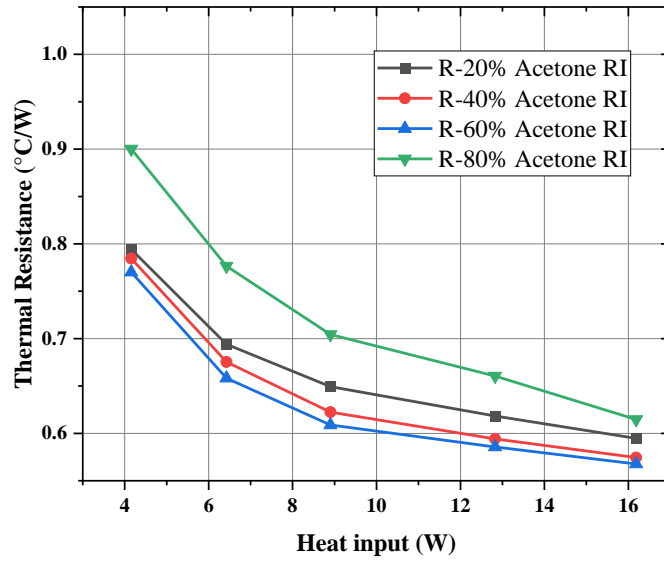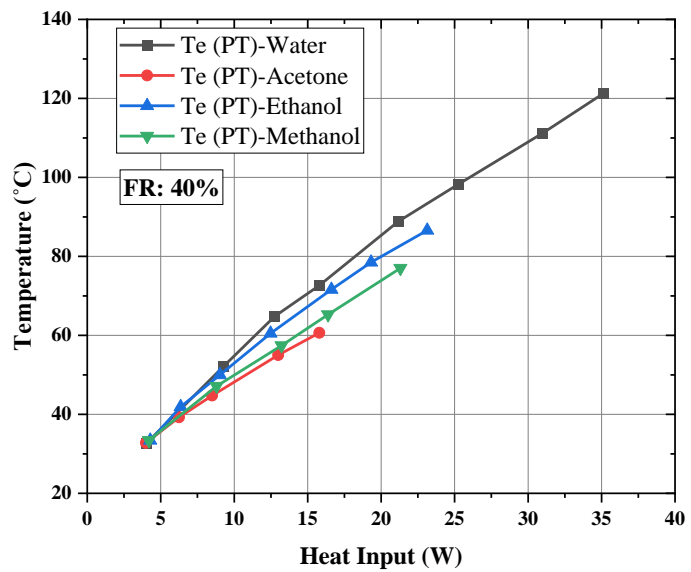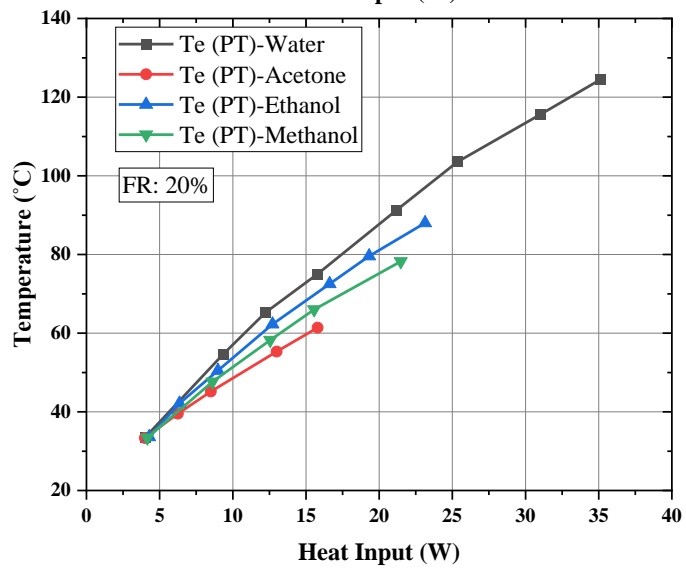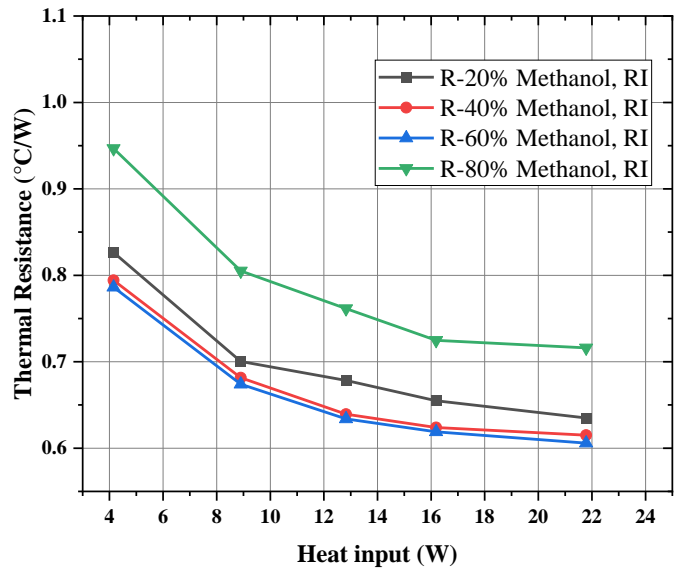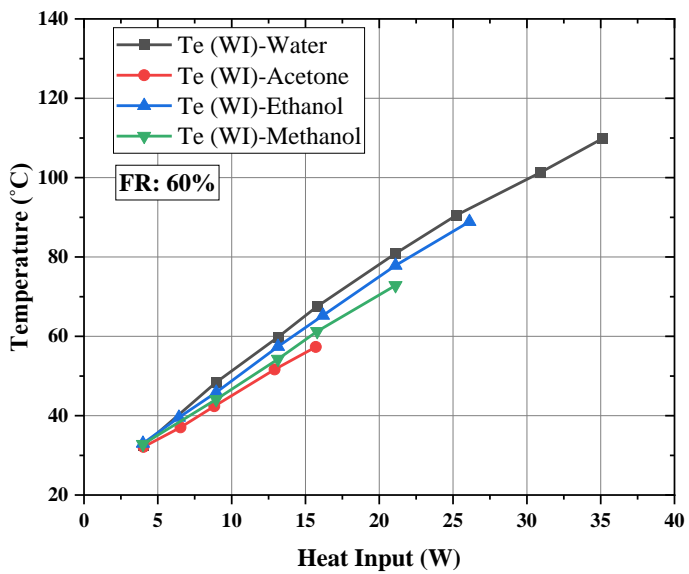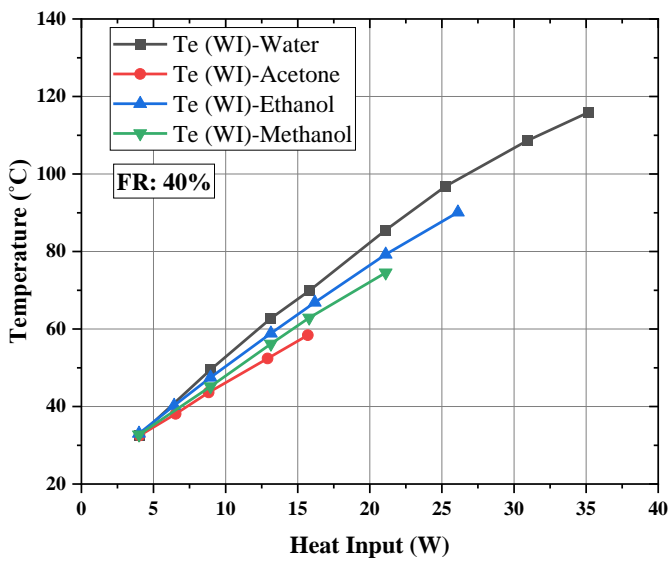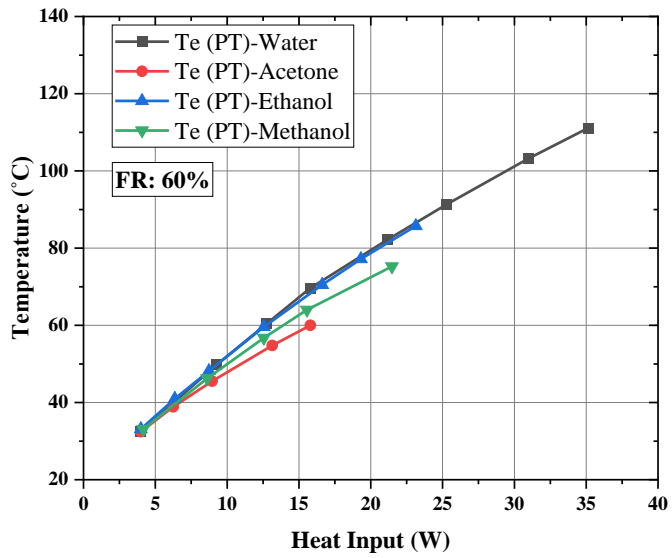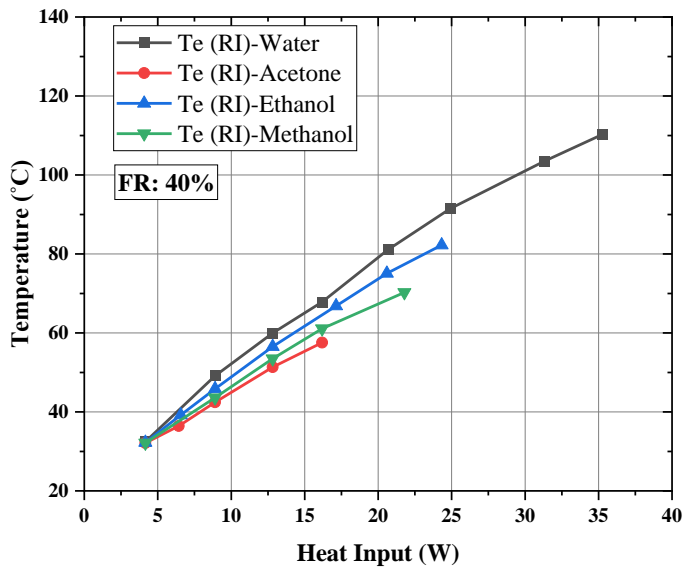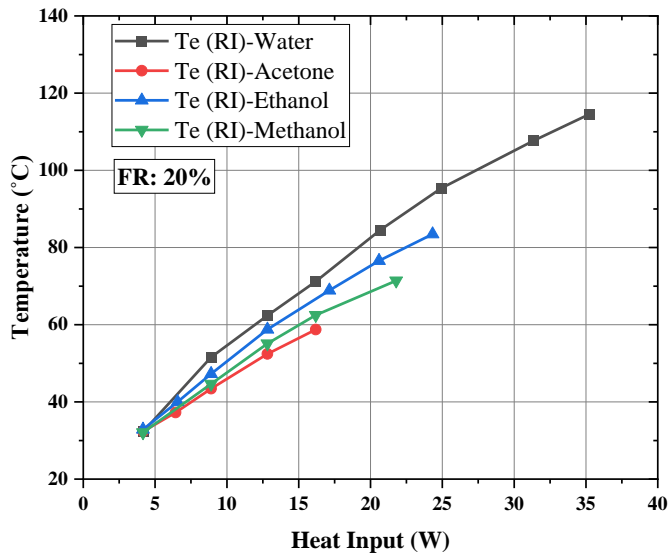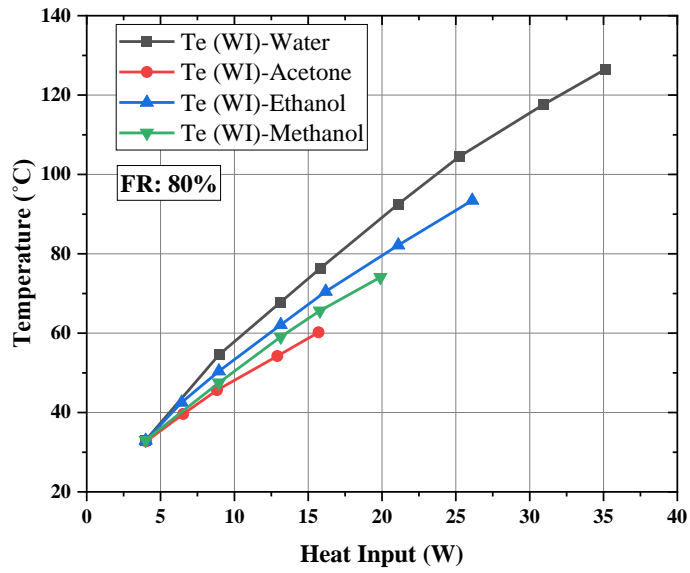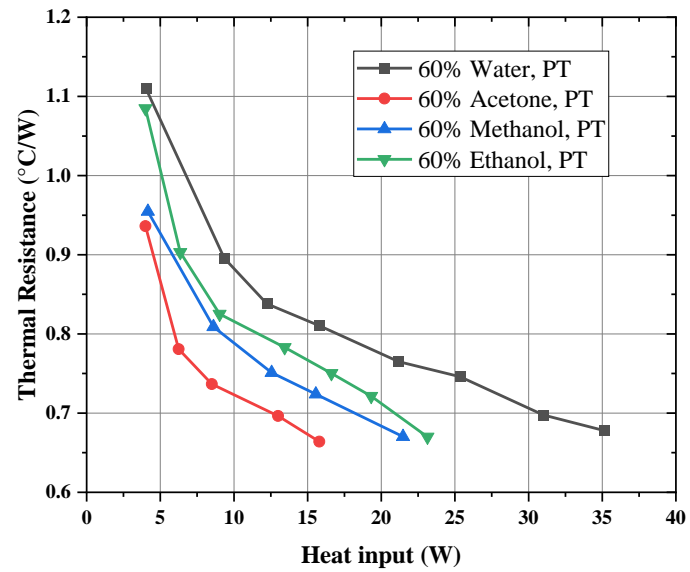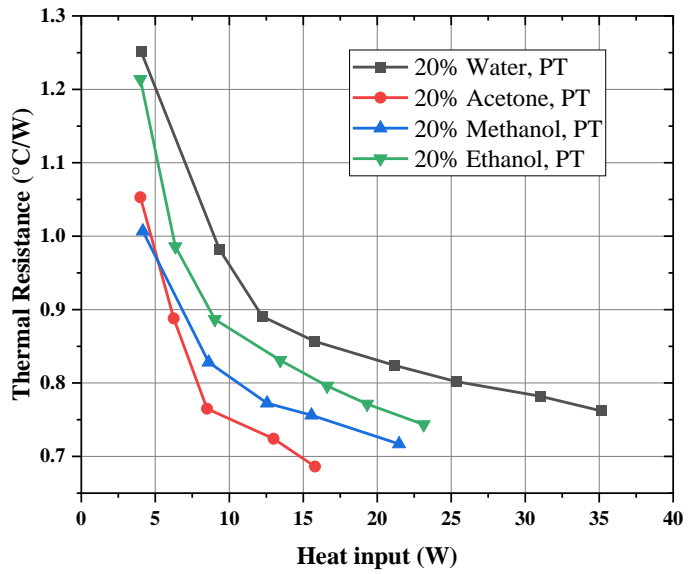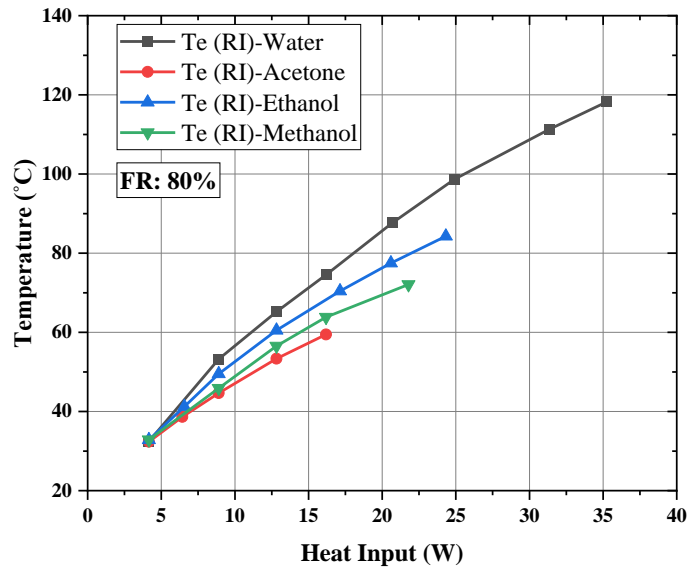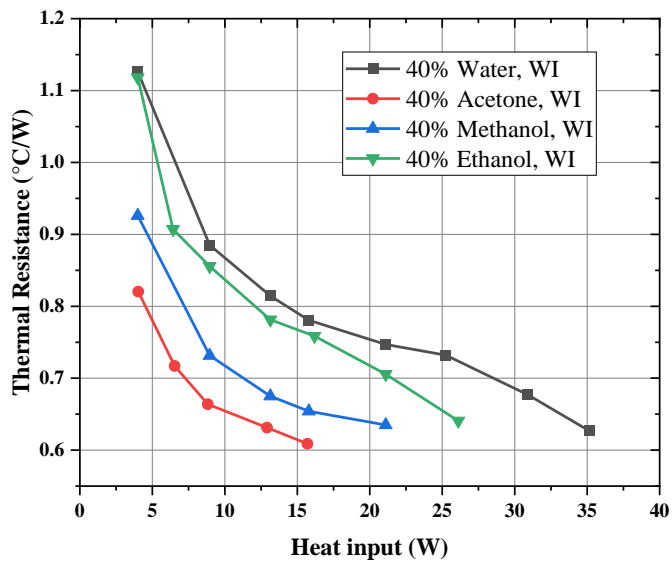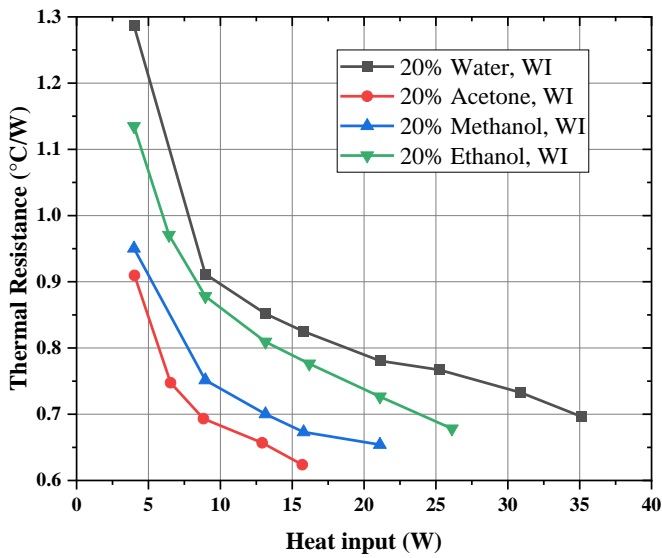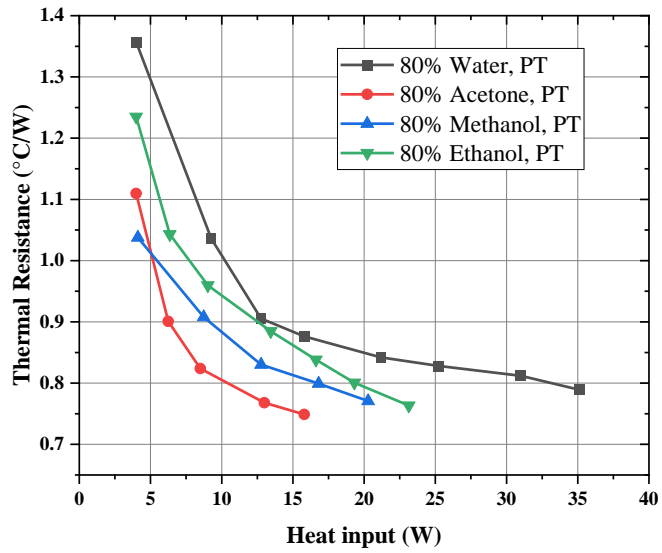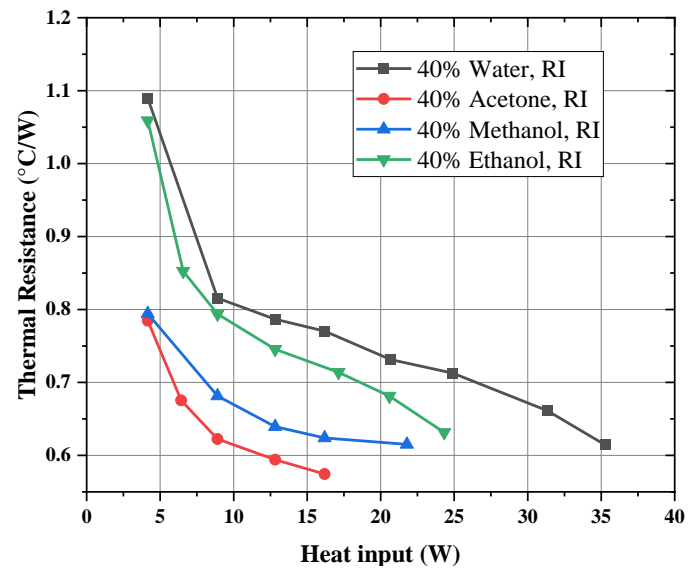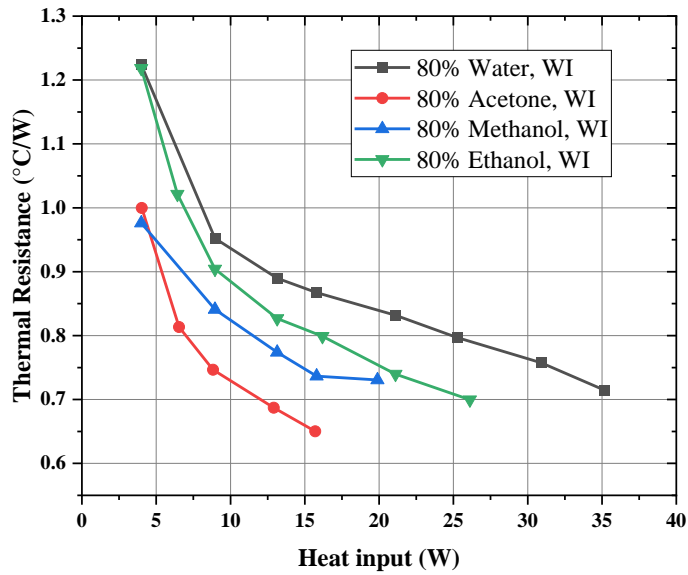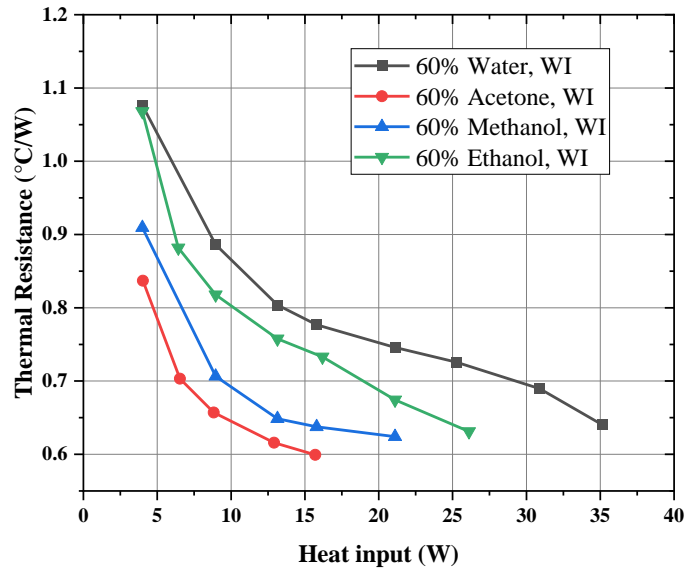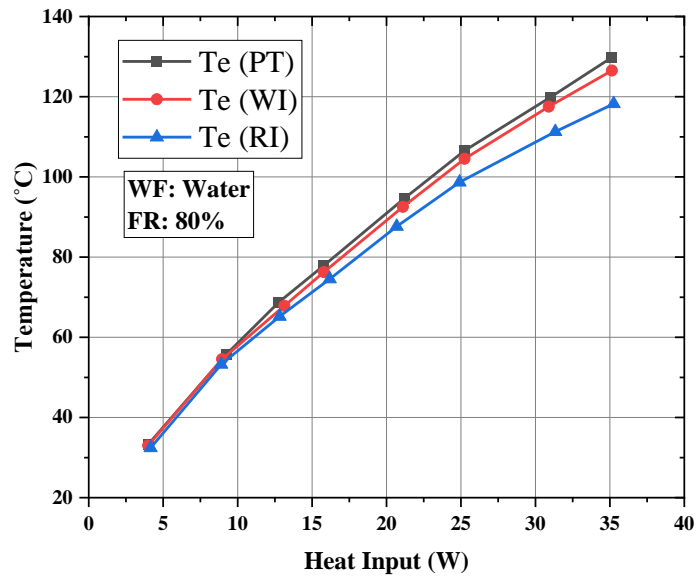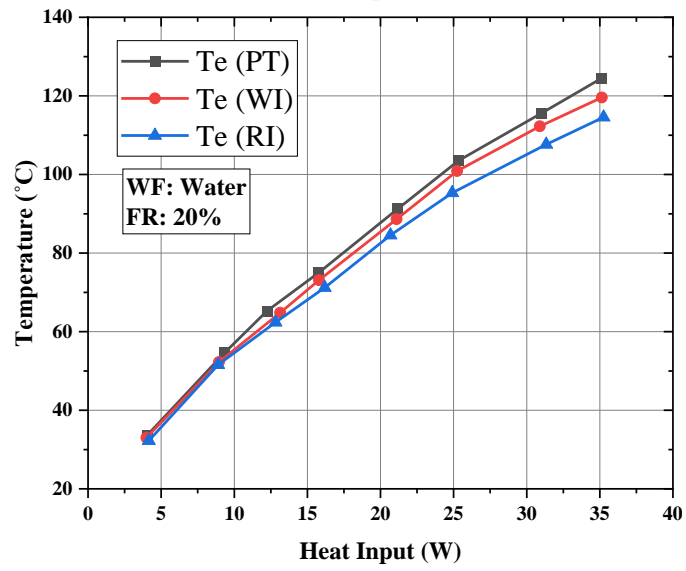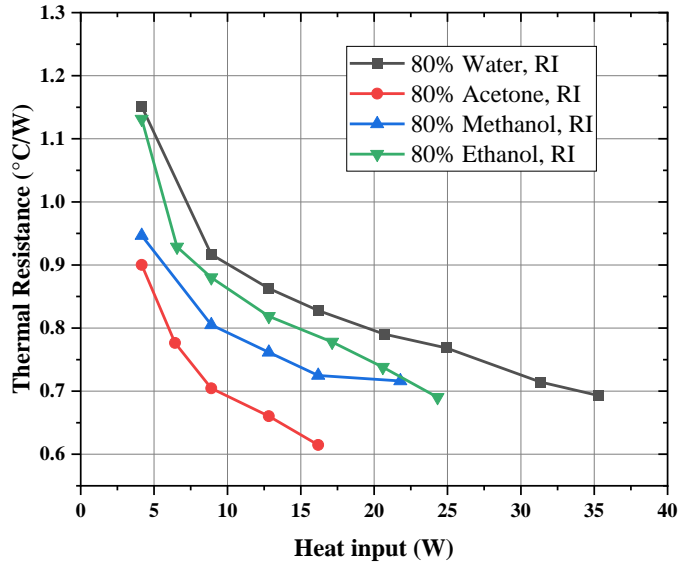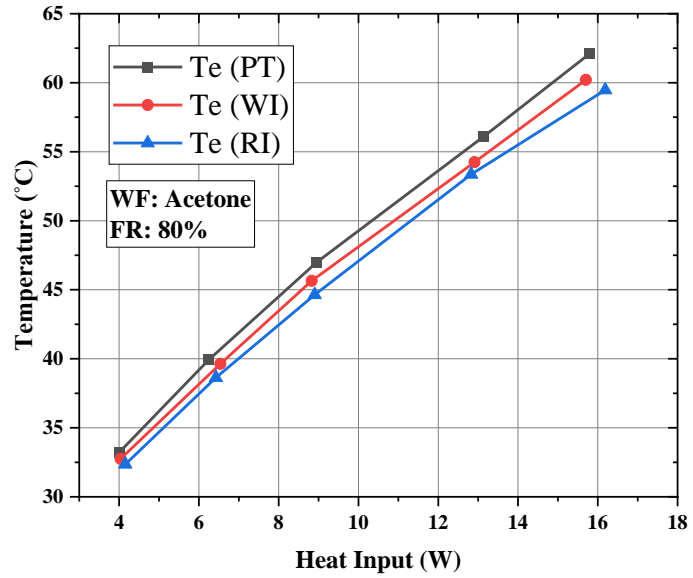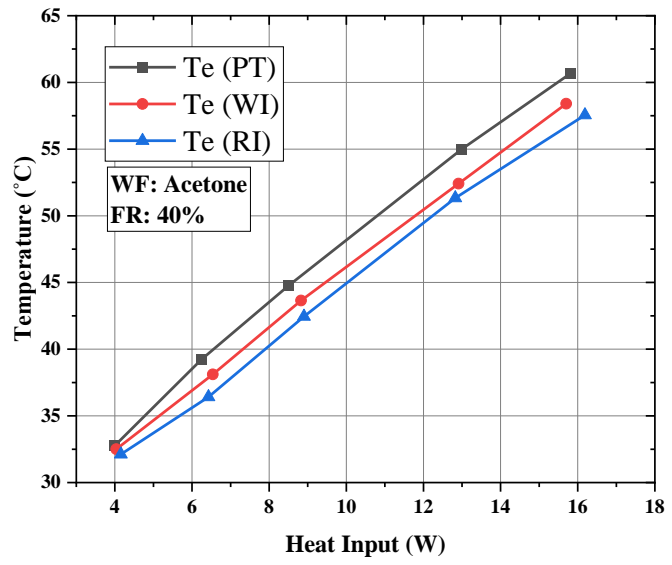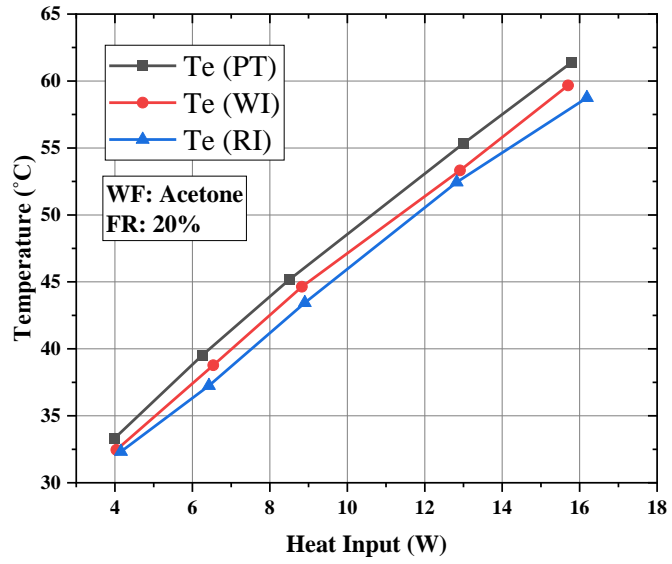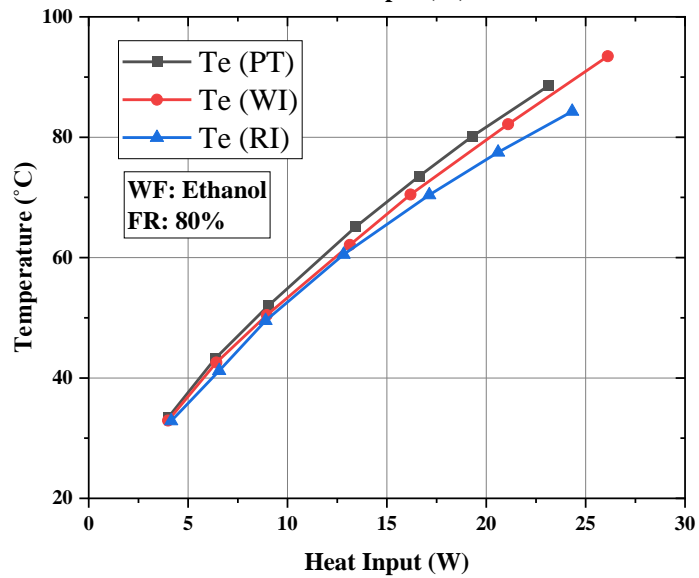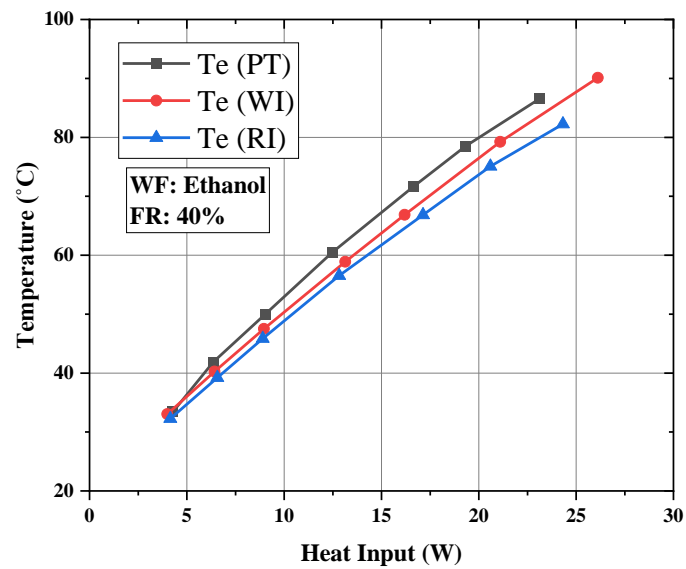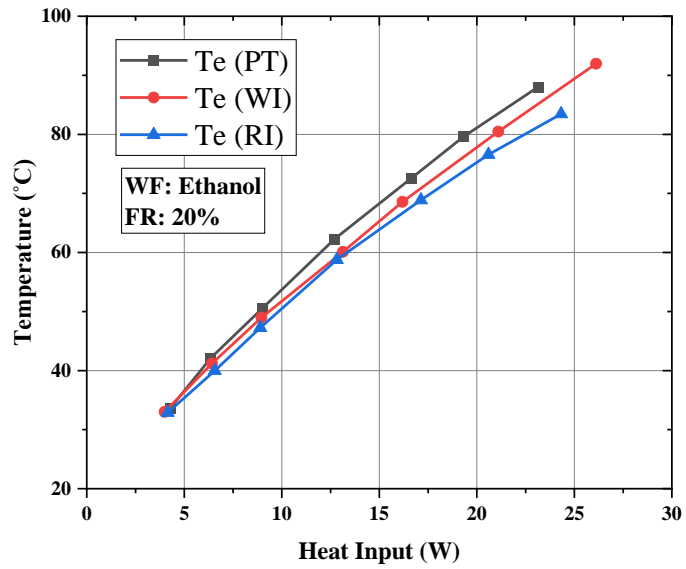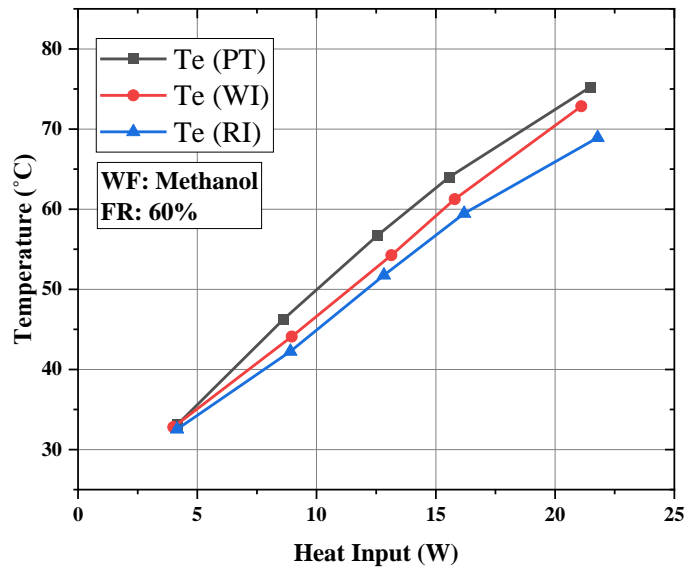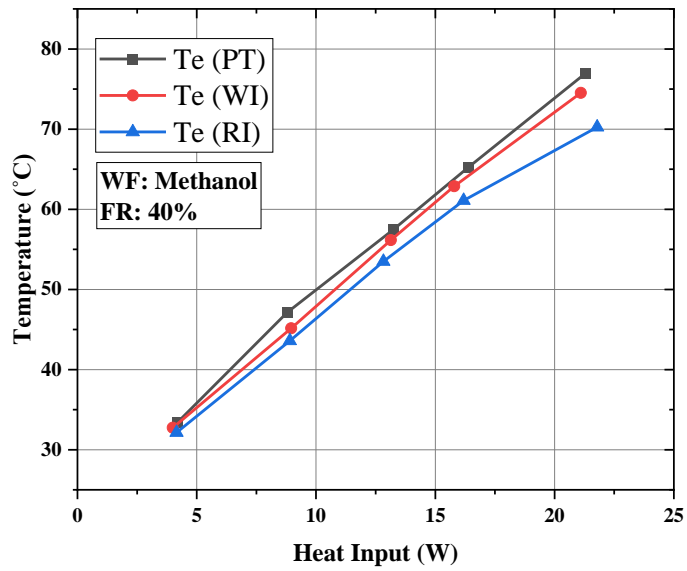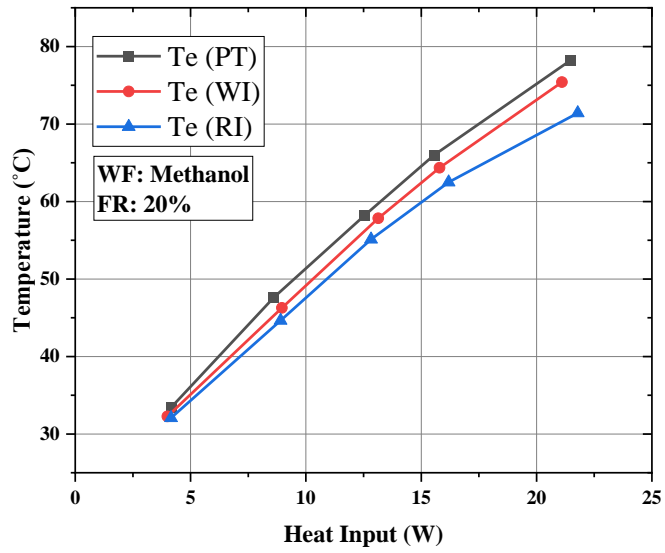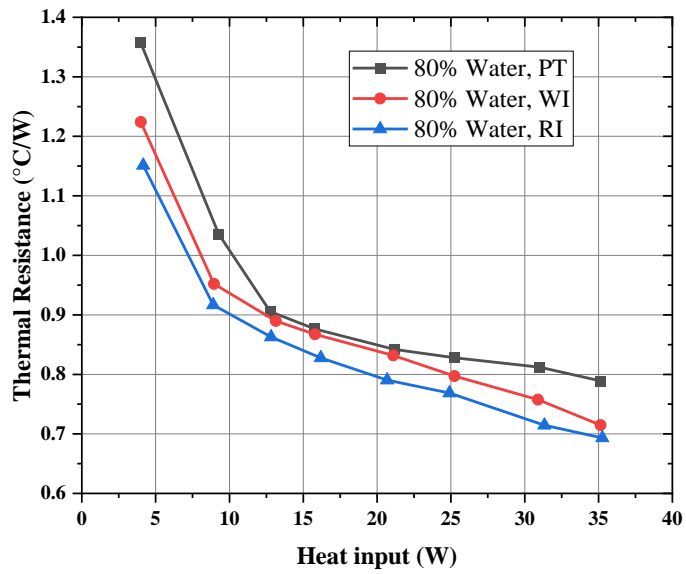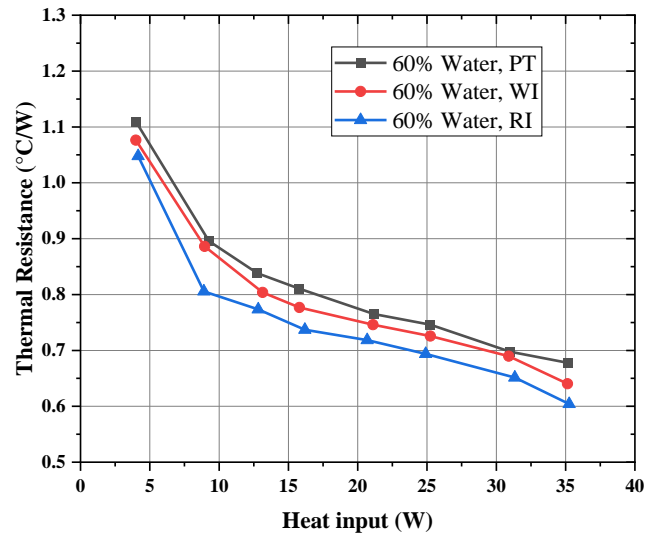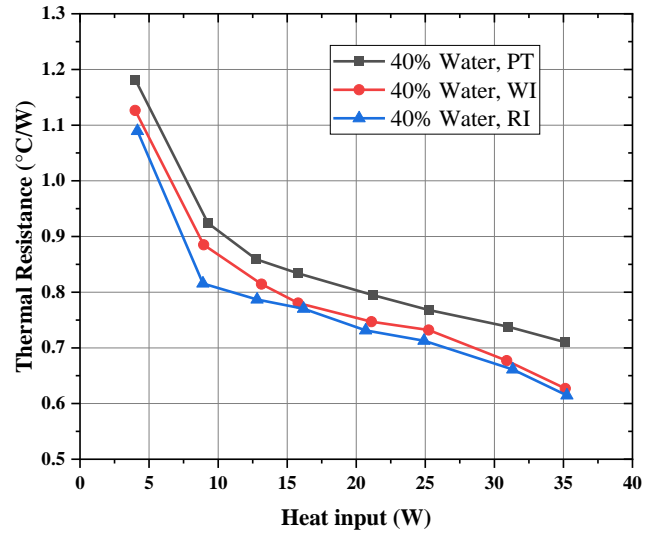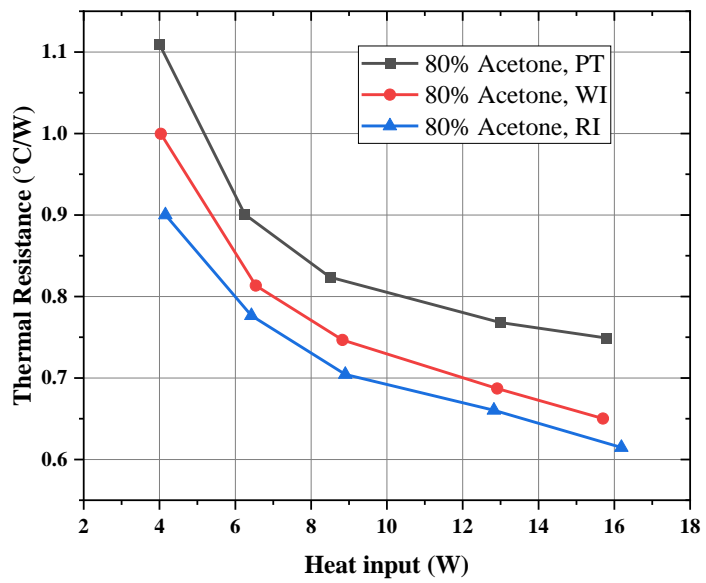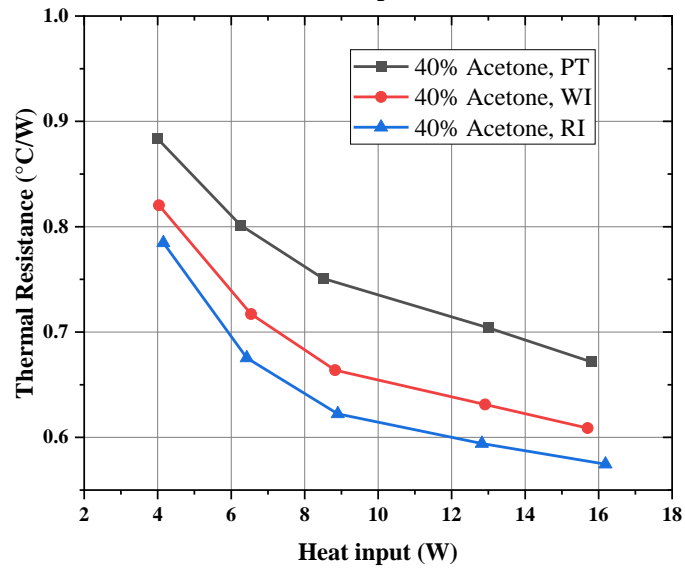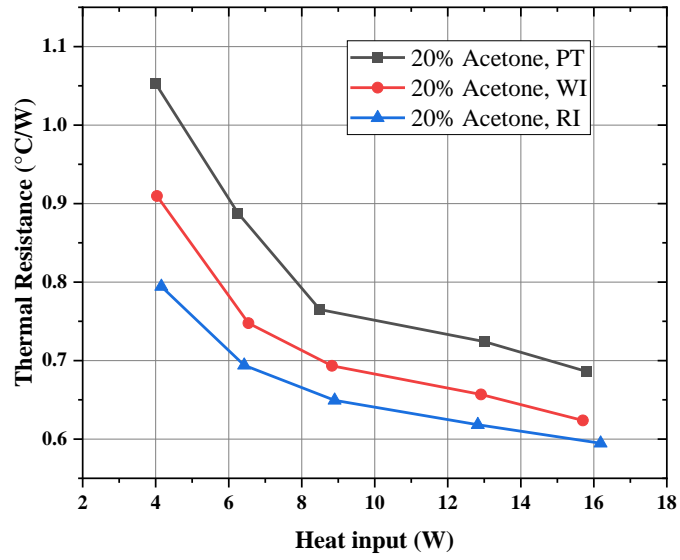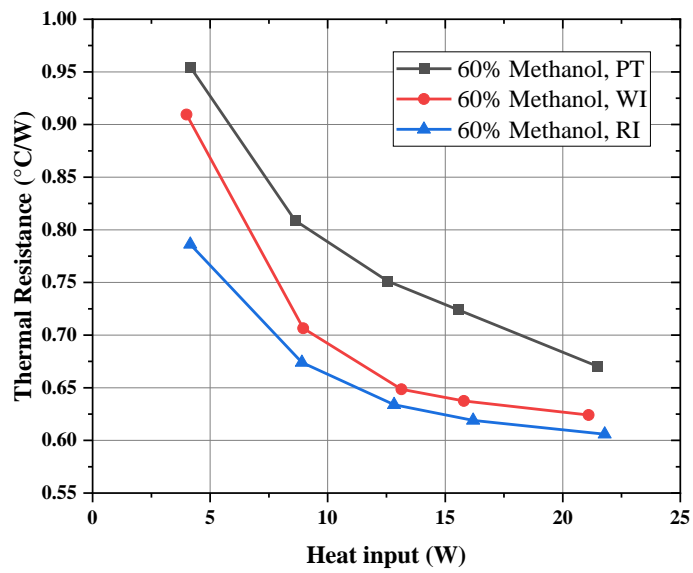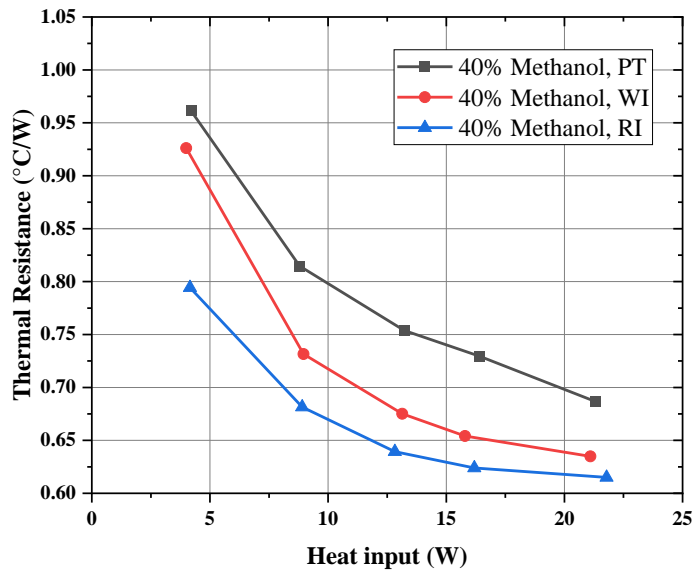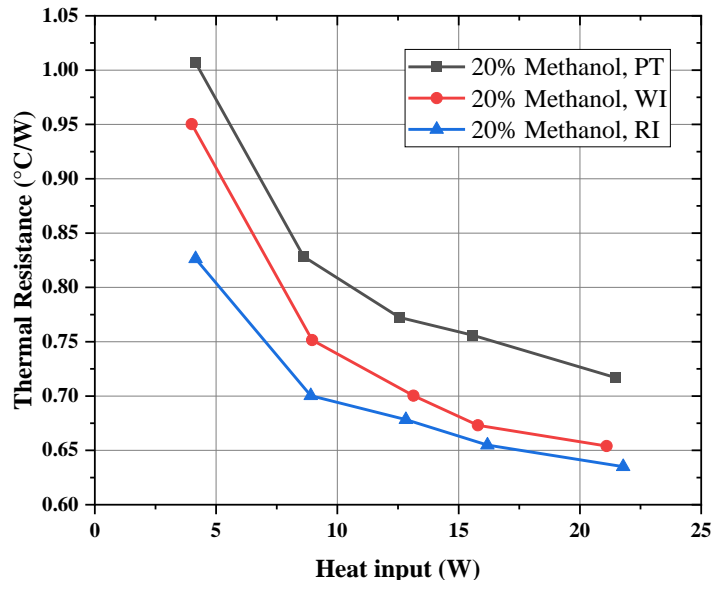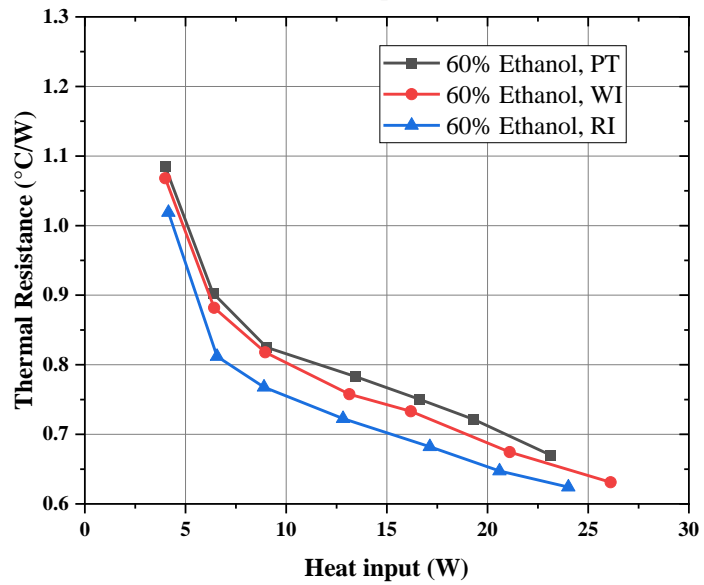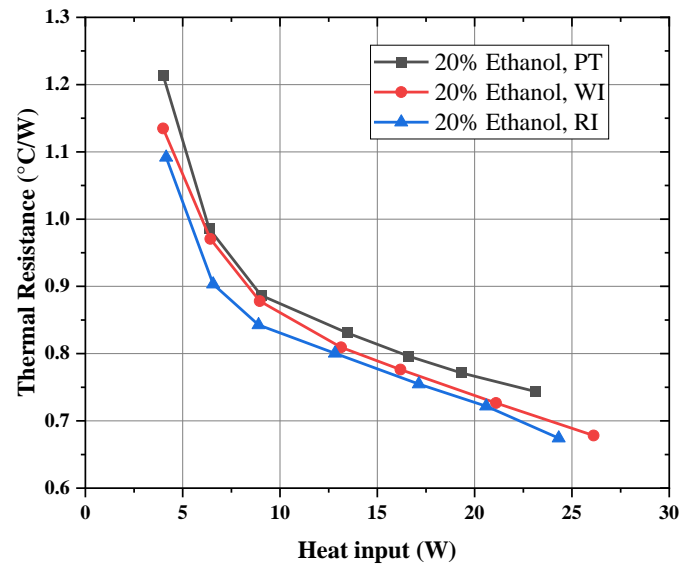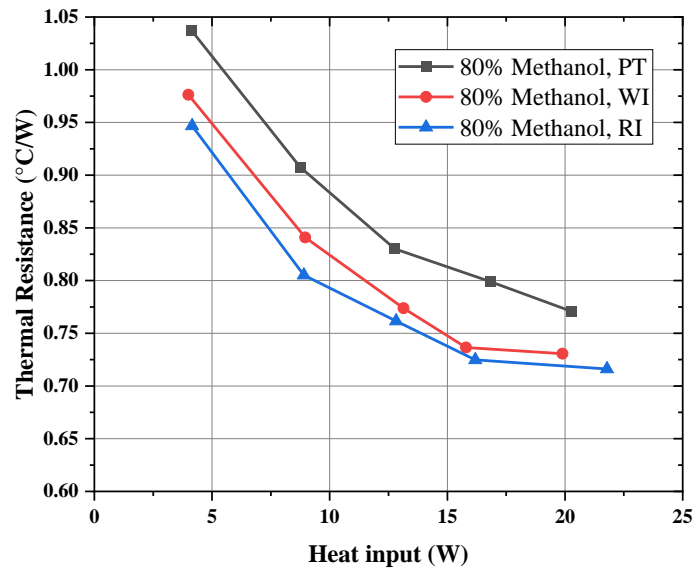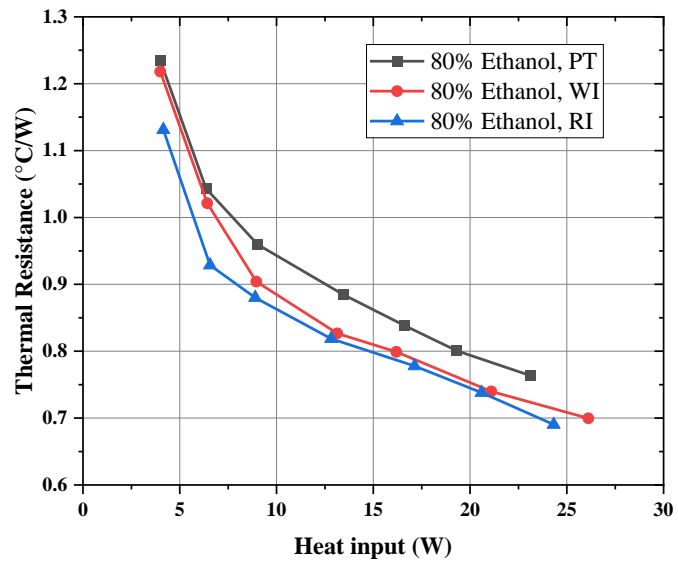
APPENDIX D

UNCERTAINITY ANALYSIS

Experimental measurements are susceptible to having a sure quantity of error. The blunder is frequently occurred by the margin of blunder of the utilized instruments and measurement techniques. Consequently, the experimental value often deviated from an actual values. Experimental uncertainty analysis provides a method for predicting the uncertainty of a variable based on its component uncertainties.

1. Uncertainty in Measured quantity:

a. Precision Limit, P: The precision limit is thus an estimate of the scatter (or lack of repeatability) caused by random error and unsteadiness. The precision limit of a measured quantity could be computed as double the standard deviation of impermanence of a set of observations measured with the apparatus in normal working condition. This element can be sampled with the available procedure and apparatus, and should be based on statistical estimates from samples whenever possible.

b. Bias Limit, B: Bias errors produce no scatter in the final result, if they are truly fixed, unchanging, and systematic. Systematic errors are often overlooked or ignored. There are several reasons available to explain this. The bias limit is an estimate of the magnitude of the fixed, constant error. The bias element cannot be exemplification (via replication) within available procedure and its extant is what edict the need of cross-checks and closures via theory.

c. Uncertainty, W: The ±5 interval about the nominal results is the band within which the experiment is 95% confident that the true value of the result lies. And it is calculated from the following:

$$W = \sqrt{[P^2 + B^2]} \tag{11}$$

2. General form of uncertainty:

Propagation method was used to examine the uncertainties of measured design parameters. The following equation is used for calculating the uncertainty of power inputs of CLPHPs.

153

$$\frac{\delta Q}{Q} = \sqrt{\left(\frac{\delta V}{V}\right)^2 + \left(\frac{\delta I}{I}\right)^2}$$

(12)

In this experimental investigation, heat power input is computed by the voltage output of variac and current having an accuracy of 0.3%. The voltage and a current having a range of 0-220 V and 0-8 A respectively.

3. Uncertainty in the present experiments:

The uncertainty of individual measurement tools used in the test is listed below:

Instrument	Uncertainty
Voltage Controller (variac)	±0.2 V
Digital A-meter	±.02A
Digital thermometer (K-type)	±0.1℃

4. Uncertainty Calculation:

A. Uncertainty of Input Heat Measurement:

Heat input, Q=V*I*CosΘ

Where, V=Variac outer voltage,

I= Electric current

CosΘ= Power factor

In this experiment, heat input power is calculated by the current and voltage having an accuracy of 0.2%. The voltage and current have ranged between 0-220 V and 0-8 A respectively. For heat input of 18 W, the minimum current and voltage were 0.92 A and 20.2 V. Hence, the uncertainty of heat input power can be calculated as:

$$\frac{\delta Q}{Q} = \sqrt{\left(\frac{\delta V}{V}\right)^2 + \left(\frac{\delta I}{I}\right)^2}$$

$$or, \quad \frac{\delta Q}{Q} = \sqrt{\left(\frac{220 \times 0.2}{20.2}\right)^2 + \left(\frac{8 \times 0.2}{0.92}\right)^2} = 2.787\%$$

The uncertainty of 18W heat input power was computed as 2.787%.

The maximum uncertainty of heat input power calculated was 5.4% for heat input power of 4.7 W and the value was seen to reduce as the heat input was increased. The maximum uncertainty 5.4% was only found in 4% of total data which is situated on permissible limit. The minimum uncertainty calculated was 1.88% for heat input of 40 W.

B. Uncertainty of Thermal resistance Calculation

Uncertainty of the Thermal Resistance: The calibrated accuracy of the thermal resistance is 1˚C. Thus, the absolute uncertainty for the temperature measurement is

$$\delta T_e = \delta T_c = \sqrt{1^2} = 1$$

For acetone as working fluid heating power at 15 W, the minimum temperature difference between the evaporation region and condensation region was $(T_e - T_c)_{min} = 4.58$ ˚C.

$$\frac{\delta \bar{R}}{\bar{R}} = \sqrt{\left(\frac{\delta T_e}{T_e - T_c}\right)^2 + \left(\frac{\delta T_c}{T_e - T_c}\right)^2 + \left(\frac{\delta Q}{Q}\right)^2}$$

$$\frac{\delta \bar{R}}{\bar{R}} = \sqrt{\left(\frac{1}{4.58}\right)^2 + \left(\frac{1}{4.58}\right)^2 + (2.787)^2}$$

$$or, \quad \frac{\delta \bar{R}}{\bar{R}} = \sqrt{(0.22)^2 + (0.22)^2 + (2.787)^2} \approx 2.80$$

The thermal resistance uncertainty was obtained with a value of 2.80%.

The maximum uncertainty of measurement carried out during the experiment is listed below:

Parameter	Uncertainty
Heat input	±2.78%
Thermal resistance	±2.80%

DIMENSIONAL ANALYSIS CALCULATION

The functional equation for the thermal resistance R may be expressed as

$$R = f\left(\sigma, \mu_l, k_l, \rho_l, \rho_v, \Delta T, D_{e,} C_{pl}, h_{fg}\right) \dots \dots \dots \dots \dots \dots \dots \dots \dots \dots (i)$$

$$or, \quad f\left(R, \sigma, \mu_l, k_l, \rho_l, \rho_v, \Delta T, D_{e,} C_{pl}, h_{fg}\right) = C \dots \dots \dots \dots \dots \dots \dots \dots \dots (ii)$$

For finding the dimensionless parameters Buckingham π-theorem will be applied. However, number of variables are 10 and all these variables may be completely described by the three fundamental dimensions of (M, L, T, θ). Hence, dimensionless π-terms will be 6.

$$f(\pi_1, \pi_2, \pi_3, \pi_4, \pi_5, \pi_6) = \acute{C} \dots \dots \dots \dots \dots \dots \dots \dots \dots \dots \dots \dots \dots (iii)$$

Here C and $\acute{C}$ are taken as constant. In order to form these π-terms, four repeating variables are considered which are mentioned in form of π-terms equation.

$$\pi_1 = \rho_l{}^{a1} \Delta T^{b1} D_e{}^{c1} \sigma^{d1} R \dots \dots \dots \dots \dots \dots \dots \dots \dots \dots \dots (iv)$$

$$\pi_2 = \rho_l{}^{a2} \Delta T^{b2} D_e{}^{c2} \sigma^{d2} \mu_l \dots \dots \dots \dots \dots \dots \dots \dots \dots \dots \dots (v)$$

$$\pi_3 = \rho_l{}^{a3} \Delta T^{b3} D_e{}^{c3} \sigma^{d3} k_l \dots \dots \dots \dots \dots \dots \dots \dots \dots \dots \dots (vi)$$

$$\pi_4 = \rho_l{}^{a4} \Delta T^{b4} D_e{}^{c4} \sigma^{d4} \rho_v \dots \dots \dots \dots \dots \dots \dots \dots \dots \dots \dots (vii)$$

$$\pi_5 = \rho_l{}^{a5} \Delta T^{b5} D_e{}^{c5} \sigma^{d5} Cp_l \dots \dots \dots \dots \dots \dots \dots \dots \dots \dots \dots (viii)$$

$$\pi_6 = \rho_l{}^{a6} \Delta T^{b6} D_e{}^{c6} \sigma^{d6} h_{fg} \dots \dots \dots \dots \dots \dots \dots \dots \dots \dots \dots (ix)$$

For π_1 term, applying dimensions of the respective variables in Eq. (iv)

$$(MLT\theta)^0 = (ML^{-3})^{a1}(k)^{b1}(L)^{c1}(MT^{-2})^{d1}(M^{-1}L^{-2}T^3\theta)$$

Equating the exponents of M, L, T and θ from the above equation

$$0 = a1 + d1 - 1$$

$$0 = -3a1 + c1 - 2$$

$$0 = -2d1 + 3 \ or, d1 = \frac{3}{2};$$

$$0 = b1 + 1 \ or \ b1 = -1;$$

Solving the above equations we get, $a1 = -\frac{1}{2}$, $b1 = -1$; $c1 = \frac{1}{2}$; $d1 = \frac{3}{2}$ and π_1 term will be as follow:

$$\pi_1 = \rho_l^{-1/2}\Delta T^{-1}D_e^{1/2}\sigma^{3/2}R \ or, \pi_1 = \frac{R}{\Delta T}\sqrt{\frac{\sigma^3 D_e}{\rho_l}} \quad\text{...... ... ...}(x)$$

For π_2 term, applying dimensions of the respective variables in Eq. (v)

$$(MLT\theta)^0 = (ML^{-3})^{a2}(k)^{b2}(L)^{c2}(MT^{-2})^{d2}(ML^{-1}T^{-1})$$

Equating the exponents of M, L, T and θ from the above equation

$$0 = a2 + d2 + 1$$

$$0 = -3a2 + c2 - 1$$

$$0 = -2d2 - 1 \ or \ d2 = -\frac{1}{2}$$

$$0 = b2$$

Solving the above equations we get, $a2 = -\frac{1}{2}$, $b2 = 0$; $c2 = \frac{5}{2}$; $d2 = -\frac{1}{2}$ and π_2 term will be as follow:

$$\pi_2 = \rho_l^{-1/2}\Delta T^0 D_e^{5/2}\sigma^{-1/2}\mu_l \ or \ \pi_2 = \mu_l\sqrt{\frac{D_e^5}{\sigma\rho_l}} \quad\text{...... ... ...}(xi)$$

For π_3 term, applying dimensions of the respective variables in Eq. (vi)

$$(MLT\theta)^0 = (ML^{-3})^{a3}(k)^{b3}(L)^{c3}(MT^{-2})^{d3}(MLT^{-3}\theta^{-1})$$

Equating the exponents of M, L, T and θ from the above equation

$$0 = a3 + d3 + 1$$

$$0 = -3a3 + c3 + 1$$

$$0 = -2d3 - 3 \ or \ d3 = -\frac{3}{2}$$

$$0 = b3 - 1 \ or \ b3 = 1$$

Solving the above equations we get, $a3 = \frac{1}{2}$, $b3 = 1$; $c3 = \frac{1}{2}$; $d3 = -\frac{3}{2}$ and π_3 term will be as follow:

$$\pi_3 = \rho_l^{1/2} \Delta T^1 D_e^{1/2} \sigma^{-3/2} k_l \ or \ \pi_3 = \Delta T k_l \sqrt{\frac{\rho_l D_e}{\sigma^3}} \ \dots\dots\dots\dots\dots\dots\dots\dots\dots\dots\dots\dots . (xii)$$

For π_4 term, applying dimensions of the respective variables in Eq. (vii)

$$(MLT\theta)^0 = (ML^{-3})^{a4}(k)^{b4}(L)^{c4}(MT^{-2})^{d4}(ML^{-3})$$

Equating the exponents of M, L, T and θ from the above equation

$$0 = a4 + d4 + 1$$

$$0 = -3a4 + c4 - 3$$

$$0 = 2d4 \ or \ d4 = 0$$

$$0 = b4$$

Solving the above equations we get, $a4 = -1$, $b4 = 0$; $c4 = 0$; $d4 = 0$ and π_4 term will be as follow:

$$\pi_4 = \rho_l^{-1} \Delta T^0 D_e^{\ 0} \sigma^0 \rho_v \ or \ \pi_4 = \frac{\rho_v}{\rho_l} \ \dots\dots\dots\dots\dots\dots\dots\dots\dots\dots\dots . (xiii)$$

For π_5 term, applying dimensions of the respective variables in Eq. (viii)

$$(MLT\theta)^0 = (ML^{-3})^{a5}(k)^{b5}(L)^{c5}(MT^{-2})^{d5}(L^2 T^{-2}\theta^{-1})$$

Equating the exponents of M, L, T and θ from the above equation

$$0 = a5 + d5$$

$$0 = -3a5 + c5 + 2$$

$$0 = 2d5 - 2 \ or, d5 = -1$$

$$b5 = 1$$

Solving the above equations we get, $a5 = -1$, $b5 = 0$; $c5 = 0$; $d5 = 0$ and π_5 term will be as follow:

$$\pi_5 = \rho_l{}^{-1}\Delta T^0 D_e{}^0 \sigma^0 \rho_v \ or \ \pi_5 = \frac{\rho_l \Delta T C_{pl} D_e}{\sigma} \dots\dots\dots\dots\dots\dots\dots\dots\dots\dots\dots. (xiv)$$

For π_5 term, applying dimensions of the respective variables in Eq. (ix)

$$(MLT\theta)^0 = (ML^{-3})^{a6}(k)^{b6}(L)^{c6}(MT^{-2})^{d6}(ML^2T^{-2})$$

Equating the exponents of M, L, T and θ from the above equation

$$0 = a6 + d6 + 1$$

$$0 = -3a6 + c6 + 2$$

$$0 = -2d6 - 2 \ or, d6 = -1$$

$$0 = b6$$

Solving the above equations we get, $a6 = 0$, $b6 = 0$; $c6 = -2$; $d6 = -1$ and π_6 term will be as follow:

$$\pi_6 = \rho_l{}^0 \Delta T^0 D_e{}^{-2}\sigma^{-1}h_{fg} \ or \ \pi_6 = \frac{h_{fg}}{\sigma D_e{}^2} \dots\dots\dots\dots\dots\dots\dots\dots\dots. (xv)$$

Now, substituting all the π-terms to Eq. (iii),

$$f\left(\frac{R}{\Delta T}\sqrt{\frac{\sigma^3 D_e}{\rho_l}}, \mu_l\sqrt{\frac{D_e{}^5}{\sigma\rho_l}}, \Delta T k_l\sqrt{\frac{\rho_l D_e}{\sigma^3}}, \frac{\rho_v}{\rho_l}, \frac{\rho_l \Delta T C_{pl} D_e}{\sigma}, \frac{h_{fg}}{\sigma D_e{}^2}\right) = \acute{C}$$

or,

$$\frac{R}{\Delta T}\sqrt{\frac{\sigma^3 D_e}{\rho_l}} = f\left(\mu_l\sqrt{\frac{D_e{}^5}{\sigma\rho_l}}, \Delta T k_l\sqrt{\frac{\rho_l D_e}{\sigma^3}}, \frac{\rho_v}{\rho_l}, \frac{\rho_l \Delta T C_{pl} D_e}{\sigma}, \frac{h_{fg}}{\sigma D_e{}^2}\right) \dots\dots\dots\dots\dots (xvi)$$

from which the expression in its usual form may be obtained.

-End-